

Experimental and Theoretical Physics

Part II

Soft Condensed Matter

Lectures 1-11

Version 1.8

Last updated on 9th January 2023

Tuomas Knowles
tpjk2@cam.ac.uk

Lent Term 2023

Foreword

Acknowledgements

These lecture notes summarise the material from the first eleven lectures on *Soft Condensed Matter*. I am grateful to Thomas Michaels, Quentin Peter and Ulrich Keyser for many useful discussions, and to Pietro Cicuta and Eugene Terentjev for providing an abundance of material on which these notes are based. Thank you also to the students who have worked through previous iterations of these notes and highlighted mistakes.

How to use this handout

The lecture will follow this handout closely. Lecture overheads will illustrate the material with practical examples and give further context to the material. Some derivations will be written out with more intermediate steps in the lectures. By the end of the course, you will be expected to have understood the concepts, methods and derivations presented in the lectures and the handout, and to be able to reproduce the results from the lecture and be able to approach yourself variations thereof using the same methods. There are few sections typeset in a smaller font size which contain material which is not examinable.

The lecture course is accompanied by supervision questions which are ordered according to the progress of the lecture. You should attempt to answer all of them, and discuss the material with your supervisor.

The notes, supervision questions and lecture overheads contain the material for the course. You will, however, also benefit by reading some of the suggested literature for a different angle to the material and additional explanations. The notes are highly unlikely to be completely error-free; please do let me know if you find mistakes, and the notes will improve!

Contents

1	Introduction	6
1.1	What is soft matter?	6
1.2	Relation to courses before and after this one	8
1.3	Structure of the course	9
1.4	Bibliography	9
2	Elements of fluid dynamics	11
2.1	General considerations	11
2.2	Governing equations	12
2.2.1	Mass flux and the continuity equation	12
2.2.2	Momentum flux and the equation of motion	13
2.3	Navier-Stokes equation	16
2.4	Material derivative	17
2.5	The Reynolds number and Stokes Flow	18
2.6	Properties of Stokes flow and locomotion of microorganisms and nanomachines	20
2.7	Vorticity	22
2.8	Fluid in mechanical equilibrium	23
2.9	Couette flow	24
2.10	Oscillatory flow near a surface	24
2.11	Diffusion of momentum	25
2.12	Stokes drag force on a spherical particle	26
2.12.1	Scaling argument	26
2.12.2	Full analysis	27
2.13	Hydrodynamic interaction between colloidal particles	30
2.14	Flow and micro- and nano channels	31
2.15	Poiseuille flow	31
2.15.1	Parallel plate channel	32
2.15.2	Channel with circular cross-section	32
2.16	Hydraulic resistance	33
2.17	Compliance	33

3 Viscoelasticity and Brownian motion	35
3.1 Basic concepts in elasticity	35
3.1.1 Strain	35
3.1.2 Stress	37
3.2 Linear elasticity and Hooke's law	38
3.2.1 Poisson's ratio	38
3.2.2 Bulk modulus	40
3.2.3 Shear deformation	41
3.2.4 Physical constraints	42
3.3 Viscoelasticity	43
3.4 Linear viscoelastic materials	44
3.5 Time translation invariance	44
3.6 Complex modulus	46
3.7 Simple models of viscoelastic materials	47
3.7.1 Maxwell fluid	47
3.7.2 Kelvin-Voigt solid	48
3.7.3 Zener standard linear solid	48
3.8 Stochastic forces and Brownian motion	49
3.9 Brownian motion	49
3.10 Langevin equation	50
3.10.1 White noise	50
3.10.2 Solution of the Langevin equation and the fluctuation-dissipation theorem	51
3.10.3 Mean square displacement and the diffusion equation	52
3.10.4 Particle flux	54
3.10.5 Diffusion controlled processes	54
3.10.6 Velocity relaxation	55
3.10.7 Overdamped limit	56
3.10.8 Confined Brownian motion	56
3.10.9 Diffusion in external potentials	57
3.11 Escape over a potential barrier	58
3.11.1 Reaction controlled processes	59
3.11.2 Microrheology	61
4 Polymers	65
4.1 Definitions and examples	65
4.2 Polydispersity	66
4.3 The ideal chain	67
4.4 Lattice polymer and freely jointed chain	67
4.5 Freely rotating chain	68
4.5.1 Bead spring model and Gaussian statistics	70

4.5.2 Segment correlation function in the ideal Gaussian chain	70
4.6 Kuhn length	71
4.7 Semi-flexible polymers	71
4.8 Entropy of an ideal chain	74
4.9 Real chains: excluded volume	76
4.10 Coil-globule transition	78
4.11 Flory Huggins free energy	80
4.12 Osmotic pressure and chemical potential of polymer solutions	82
4.13 Polymer melt	83
4.14 Semi-dilute solutions	83
4.15 Phase diagram for polymer solutions	84
4.15.1 The critical point	85
4.16 Polymers at surfaces	86
4.16.1 Grafting density	86
4.17 Rubber elasticity	87
4.18 Dynamics	89
4.18.1 Viscoelastic behaviour	90
4.19 Helix to coil transition	91
4.19.1 Non-cooperative model	91
4.19.2 Fully cooperative model	92
4.19.3 Nearest neighbour cooperative Zimm-Bragg model	92
5 Self-assembly: Part I molecular self-assembly	95
5.1 Self-assembly	95
5.2 Driving forces for molecular self-assembly	95
5.2.1 Hydrogen bonding	95
5.2.2 Hydrophobic effect	96
5.2.3 Electrostatics	97
5.3 Free energy of monomers and clusters	98
5.4 Self-assembly of amphiphiles into micelles	99
5.5 Micellar shape and packing parameter	101
5.6 Self-assembly of protein filaments	103
6 Problems	105

Chapter 1

Introduction

1.1 What is soft matter?

Soft matter is an area of condensed matter physics that focuses on systems which are readily deformed by thermal fluctuations or mechanical stresses. Many of the objects and materials in the world around us deform when squashed, can flow or are sensitive to temperature changes. These types of materials, including paint, yoghurt, shampoo, rubber and foam are all thus soft materials, and as such, soft matter physics is in many ways the “the physics of everyday life”. However, soft matter physics is also the formalism which underpins quantitative models in many areas of chemistry and biology; living matter is for the large part soft matter. As such the study of soft matter is an area with a rich set of interdisciplinary connections.

The properties of soft matter systems are not used just in nature. Mankind also exploits them extensively for technological applications, including in engineering everyday products such as plastics, foods, creams and gels.

Soft matter physics is a relatively young field of physics. As a subject, soft matter has its roots in physical chemistry, statistical mechanics and colloid science in the 1930s, but its development as a subfield of physics was largely initiated in the 1960s with physical models describing accurately the behaviour of polymers. So soft matter physics is younger than quantum mechanics, for instance.

We consider briefly what it means for a material to be easily deformable. The elastic modulus E measures how much force must be applied per unit area to deform a material by a fraction ϵ

$$p = E\epsilon \tag{1.1}$$

where $p = F/A$ is the pressure applied to an area A . A representative pressure for deforming everyday materials is the atmospheric pressure 1 bar = 10^5 N/m². The elastic modulus of diamond is $E = 1.2 \cdot 10^{11}$ Pa, and thus the fractional

deformation is $\epsilon = 8.3 \cdot 10^{-7}$ which corresponds to 8.3 nm for an object with the size of 1 cm - only a few atomic diameters. This material is hard. Now if we exert the same pressure on rubber with a modulus $E = 10^7$ Pa, we obtain $\epsilon = 10^{-2}$, a deformation of 1%. For a gelatin hydrogel (e.g. Jell-O dessert), $E = 10^3$ Pa and $\epsilon = 10000\%$; this is a very soft material. What can we learn from the fact that a material is “hard” or “soft”? Crucially, the elastic modulus has units of pressure

$$[E] = \frac{\text{force}}{(\text{length})^2} = \frac{\text{force} \cdot \text{length}}{(\text{length})^3} = \frac{\text{energy}}{\text{volume}} = \frac{u}{v} \quad (1.2)$$

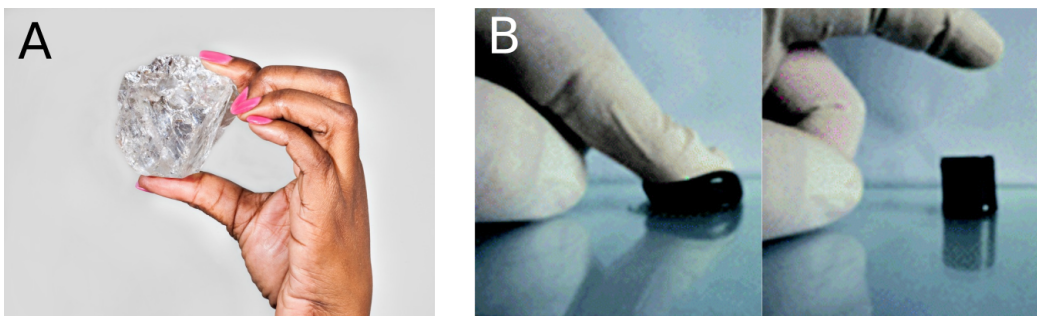


Figure 1.1: A: hard material (e.g. diamond), B: soft material (e.g. hydrogel). Covalent materials are characterised by the energy scale of the cohesive inter-atomic energy and an atomic length-scale; soft materials by contrast are characterised by the energy scale $k_B T$ and an elementary length scale larger than atomic length scales.

What are the characteristic energy and length scales? For diamond, the characteristic energy is the cohesive energy per atom from the covalent bonding network, $u = 1.2 \cdot 10^{-18}$ J (= 7.5 eV). The characteristic volume is the volume per carbon atom, $v = 6 \cdot 10^{-30}$ m³. Therefore on dimensionality grounds, we estimate the modulus of diamond to be $E \approx u/v = 2 \cdot 10^{11}$ Pa, which is of the same order of magnitude as the experimental value ($1.2 \cdot 10^{11}$ Pa). For soft materials, clearly the energy scale is smaller; the smallest physical energy scale at thermal equilibrium is the thermal energy $u = k_B T = 4.5 \cdot 10^{-21}$ J; with this energy scale, the characteristic length scale is $(u/E)^{1/3} \approx 20$ nm for a material which has an elastic modulus of $E = 10^3$ Pa. The relevant length scale is thus much larger than the size of an atom. In general, the fundamental building blocks of soft materials are larger than atomic length scales and the de Broglie wavelength is much smaller than all other relevant distances. Therefore in discussing soft materials, we can neglect quantum effects, and all fluctuations are thermal.

Soft materials are therefore materials that are in between the atomic or molecular crystals which are hard, on one hand, and gasses and simple liquids, which don’t resist shear deformations, on the other. Because the characteristic length scale that gives rise to their properties is larger than the atomic or molecular length

scale, soft materials typically contain more than one component (for instance colloids are micrometer-size particles dispersed in solvent) and they are characterized by mechanical response much softer and much slower than ordinary solids. This gives rise to behavior not encountered in simple crystalline materials crystals such as viscoelasticity.

Soft materials have a range of distinctive features:

Characteristic length scale. Soft materials are composed of supra-molecular building blocks such as polymers and colloids. Their size is larger than the size of an atom yet small enough that thermal fluctuations are excited (in practice 1nm-1000nm).

Universality and scaling. Many aspects of the behaviour of soft matter do not depend on the specific chemistry of the building blocks but are general. For instance we will see that under many conditions the size of a polymer is largely determined by its linear architecture rather than the chemical nature of its component monomers. As in other areas, this general behaviour manifests itself often in scaling laws.

Thermal fluctuations. The characteristic energy scale in soft matter is the thermal energy. This implies that the building blocks of such materials undergo thermal fluctuations and brownian motion.

Viscoelasticity. Soft materials commonly have both viscous and elastic properties, and thus combine features from simple fluids and simple solids.

Self-assembly. The building blocks of soft materials often have the propensity to assemble into intricate structures without external input. This principle is exploited extensively by biology where much of the microscopic machinery of the cell is formed through self-assembly from protein molecules.

1.2 Relation to courses before and after this one

This course builds on much Part 1A and 1B material, in particular the Dynamics course in 1B. However, there are also close connections between this course and the Statistical and Thermal Physics Part II course, and the soft matter field in general uses extensively tools from statistical physics. The area of soft matter is further developed at Part III level and in particular there are two courses which build on this material

- Major option “Soft Matter” which examines some of the themes introduced in the current lecture in more detail.

- Minor option “Biological Physics” which focuses on the applications of soft matter physics and statistical physics to biological systems

1.3 Structure of the course

The first 11 lectures of this course provide an introduction to the basic concepts in simple fluids and elasticity and then examine in more detail one of the main classes of soft systems, polymers. The second 11 lectures of this course focus in large part on the second important class of soft matter, colloids.

Chapter 2: Elements of fluid dynamics. Many soft materials can flow. This chapter summarises briefly the concepts and formalism of simple fluids that will be used in the lecture, with a specific focus on the behaviour of fluids on small scales and slow flow rates which are situations characteristic of soft matter systems.

Chapter 3: Viscoelasticity. Soft materials combine features of simple liquids (viscosity) and simple solids (elasticity). Here we first summarise the basic formalism of elasticity and then examine how materials can exhibit both types of behaviours simultaneously.

Chapter 4: Polymers. Polymers are one of the major classes of soft materials. We explore how thermal fluctuations govern their shapes and sizes, and the viscoelastic behaviour of polymer solutions and networks, including the entropic elasticity of rubber.

Chapter 5: Molecular self-assembly. The elementary building blocks of soft matter are structures on a mesoscopic scale, intermediate between atomic dimensions and the macroscopic world. Such structures can form spontaneously as clusters from molecular elements through self-assembly. We explore the driving forces for molecular self-assembly and study the equilibrium behaviour of molecular clusters.

1.4 Bibliography

Introductory textbooks

- Jones, R. A. L. (2002). *Soft Condensed Matter*. Oxford University Press
- Doi, M. (2013). *Soft Matter Physics*. Oxford University Press

- Rubinstein, M. and Colby, R. H. (2003). *Polymer physics*. Oxford University Press

More advanced references

- de Gennes, P.-G. (1979). *Scaling Concepts in Polymer Physics*. Cornell University Press
- Doi, M. and Edwards, S. F. (1986). *The Theory of Polymer Dynamics*. Oxford University Press
- Landau, L. D. and Lifshitz, E. M. (1987). *Fluid Mechanics*, Pergamon Press

Chapter 2

Elements of fluid dynamics

2.1 General considerations

This chapter discusses the dynamics of fluids, with a particular focus on flows that occur slowly or on small length scales, situations characteristic of soft matter systems as we will see. In addition to fluid-like behaviour, soft materials also exhibit elastic characteristics - these aspects will be discussed in Chapter 4. Specifically, in this chapter we will be concerned with the motion of liquids and introduce the general formalism and framework of fluid dynamics. Generally, a fluid, either a liquid or a gas, has the property that it deforms readily under the action of external forces. In particular, the shape of a fluid, unlike that of a solid, is governed by the shape of the container which holds it. As such, the presence of even small shear forces can result in large changes in the positions of the microscopic components of the liquid. The two main classes of fluids, liquids and gases, are distinguished principally by their densities and the level of interactions between the constituent atoms or molecules. In particular, in a liquid, each molecule or atom is surrounded by a number of other species within atomic distances, while in a gas, the inter-particle separation is typically much larger. As a consequence of this fact, liquids cohere, i.e. liquid can be contained in an open vessel where it meets only its own vapour on one side (e.g. water in a beaker) or even as a drop with its whole surface free, whereas a gas expands until it is surrounded by the walls of a container.

Although liquids are quantised on the atomic or molecular level, most simple liquids appear continuous on the micro to macro scale. We treat such systems therefore as a continuum. Moreover, we will initially assume that the properties of the liquid we study are isotropic¹.

As such, we will describe the fluid with quantities that are averaged over the

¹In the second part of the course we will encounter anisotropic liquids such as liquid crystals.

microscopic components of the fluid. The density field of the fluid at time t and at a position \vec{r} in space is defined as the average over a fluid element of volume ΔV :

$$\rho(\vec{x}, t) = \frac{1}{\Delta V} \sum_{i \in \Delta V} m_i \quad (2.1)$$

where m_i is the mass of a microscopic constituent of the fluid. Similarly, the fluid flow velocity field can be defined as:

$$\vec{v}(\vec{x}, t) = \frac{1}{\rho(\vec{r}, t)\Delta V} \sum_{i \in \Delta V} m_i \vec{v}_i \quad (2.2)$$

where \vec{v}_i are the velocities of the microscopic components of the fluid. To describe the motion of the fluid, we are looking to find Eq. (2.2) in different situations.².

2.2 Governing equations

2.2.1 Mass flux and the continuity equation

We consider the general case of a compressible fluid where the density ρ can vary with space \vec{r} and time t . The total mass inside a fixed region with an arbitrary shape in the fluid is given by:

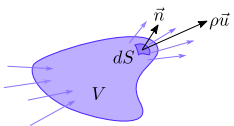


Figure 2.1: Schema showing the mass current density field $\rho\vec{v}$ flowing through a fixed volume V . The current flowing through the area dS is given by the projection $\rho\vec{v} \cdot \vec{n}dS$.

$$M(V, t) = \int_V d^3 r \rho(\vec{r}, t) \quad (2.3)$$

Since mass is conserved, m can only vary through a flux of mass through the surface $S := \partial V$ in or out of the volume V . To find out the flux, we consider a fluid of mass density ρ occupying a volume $\Delta V = \Delta x \Delta y \Delta z$. If the fluid is moving along the x axis with the speed v_x , the entire volume has passed through the cross-sectional area $\Delta S = \Delta y \Delta z$ in the time $\Delta t = \Delta x / v_x$. The mass current density J is the mass per unit time that has crossed a unit area and hence $J_x = (\rho \Delta V) / (\Delta S) / \Delta t = \rho \Delta x / \Delta t = \rho v_x$. More generally:

$$\vec{J}(\vec{r}, t) = \rho(\vec{r}, t) \vec{v}(\vec{r}, t) \quad (2.4)$$

Since the region V is fixed in time, the rate of change of M can be evaluated as:

$$\partial_t M(V, t) = \partial_t \int_V d^3 r \rho(\vec{r}, t) = \int_V d^3 r \partial_t \rho(\vec{r}, t) \quad (2.5)$$

²The complete description of a moving fluid is given by the knowledge of $\vec{v}(\vec{x}, t)$ and two of the thermodynamic variables of the fluid, for example the density field $\rho\vec{r}, t$ from Eq. (2.1) and the pressure field. Other thermodynamic quantities can be derived from these three fields by using the equation of state of the fluid

But due to conservation of mass, this rate of change has to equal the net flux of mass flowing in and out of the volume V as described by the surface integral:

$$\partial_t M(V, t) = - \int_S dS \vec{n} \cdot [\rho(\vec{r}, t) \vec{v}(\vec{r}, t)] = - \int_V d^3 r \vec{\nabla} \cdot [\rho(\vec{r}, t) \vec{v}(\vec{r}, t)] \quad (2.6)$$

where the second equality originates from Gauss's divergence theorem, and \vec{n} is the outward pointing normal vector to the surface S . The minus sign originates from the fact that the mass inside the volume V decreases if the mass flux $\rho\vec{v}$ is parallel to \vec{n} (flowing out). Equations (2.5) and (2.6) are valid for arbitrary fixed shapes with volume V and surface S and hence the integrands in both equations are identical, yielding the continuity equation:

$$\partial_t \rho = -\vec{\nabla} \cdot (\rho \vec{v}) = -\vec{\nabla} \cdot \vec{J} \quad (2.7)$$

For incompressible fluids, ρ is constant, and the continuity equation Eq. (2.7) can be simplified to:

$$\vec{\nabla} \cdot \vec{v} = 0 \quad (2.8)$$

2.2.2 Momentum flux and the equation of motion

To obtain the equation of motion for a fluid, we repeat the analysis of the type discussed in section 2.2.1 but for the momentum density $\vec{P} = \rho\vec{v}$ rather than the mass density ρ . We note that momentum density is the same as mass current density. We thus consider the rate of change of the (i th component of the) total momentum $P_i(V, t)$ inside a fixed shape of volume V :

$$\partial_t P_i(V, t) = \partial_t \int_V d^3 r \rho(\vec{r}, t) v_i(\vec{r}, t) = \int_V d^3 r ((\partial_t \rho)v_i + \rho \partial_t v_i) \quad (2.9)$$

The total momentum P_i can change either by convection $\partial_t P_i^{\text{conv}}$, with momentum flowing in or out of the volume V , or through the action of forces F_i as described by Newton's second law $\dot{P}_i = F_i$. These forces can be either contact forces, which act on the surface $S = \partial V$ (pressure and viscosity, given by $\partial_t P_i^{\text{press}}$ and $\partial_t P_i^{\text{visc}}$, respectively) or body forces, $\partial_t P_i^{\text{body}}$ which act on the interior of V (gravity). Taking explicitly into account these four contributions we can write the rate of change of the momentum as:

$$\partial_t P_i = \partial_t P_i^{\text{conv}} + \partial_t P_i^{\text{press}} + \partial_t P_i^{\text{visc}} + \partial_t P_i^{\text{body}} \quad (2.10)$$

We analyse each contribution in turn below.

Convection of momentum

In Eq.(2.6), we saw that the convection of the mass density scalar field ρ is described by the vector field $\rho\vec{v}$ and that the amount of mass entering or leaving the volume V through an infinitesimal surface element was given by $dM = \rho\vec{v} \cdot \vec{n}dS$. Similarly, the amount of the i th component of the momentum that enters or leaves the volume V through an infinitesimal area dS is given by $dP_i = (\rho v_i)\vec{v} \cdot \vec{n}dS$, where the advecting quantity is now ρv_i rather than simply ρ as was the case for the change in mass. This motivates the definition of the momentum flux density tensor Π' as:

$$\Pi'_{ij} = \rho v_i v_j \quad (2.11)$$

We can now write the rate of change of P_i as a result of convection of momentum into and out of the volume V as the surface integral³:

$$\partial_t P_i^{\text{conv}}(V, t) = - \int_S dS \vec{n} \cdot (\rho v_i \vec{v}) = - \int_S dS n_j \rho v_i v_j = - \int_S dS n_j \Pi'_{ij} \quad (2.12)$$

And again as in Eq. (2.6) the negative sign originates from the convention that \vec{n} is the outward pointing normal vector to S .

Pressure forces

The normal force dF_\perp on an area dS is given as a function of the pressure p as:

$$dF_\perp = dS \vec{n} p \quad (2.13)$$

Hence the change in momentum in the volume V due to pressure forces is given as the surface integral of Eq.(2.13):

$$\partial_t P_i^{\text{press}} = - \int_S dS \vec{n} \cdot (p \vec{e}_i) = - \int_S dS n_j p \delta_{ij}. \quad (2.14)$$

Eq. (2.14) and Eq. (2.12) are of the same form and we can thus extend the definition of the momentum flux density tensor from Eq. (2.11) to:

$$\Pi_{ij} = \Pi'_{ij} + p \delta_{ij} = \rho v_i v_j + p \delta_{ij} \quad (2.15)$$

where Π'_{ij} is the momentum flux density tensor without the pressure forces.

³We will often make use of index notation. A vector \vec{v} is written in terms of its components as $\vec{v} = \sum_{i=x,y,z} v_i \vec{e}_i = v_i \vec{e}_i$. By definition repeated indices, here i , imply summation over that index (Einstein convention), and \vec{e}_i are basis vectors in Cartesian coordinates (x, y, z) . In this notation the scalar product $\vec{v} \cdot \vec{v}$ is written as $v_i v_i$, and a matrix product $\vec{v} = M \vec{v}$ is $v_i = M_{ij} v_j$. The Nabla operator in Cartesian coordinates is given by $\vec{\nabla} = \vec{e}_x \partial_x + \vec{e}_y \partial_y + \vec{e}_z \partial_z$

Viscous forces

In general, adjacent fluid elements can exert tangential forces in addition to the normal forces discussed above. As such, if tangential stresses are present, the force dF_i through a small surface dS is no longer parallel to the surface normal vector n_i , and we need to replace the earlier expression $d\vec{F} = p \vec{n} dS$ with:

$$dF_i = \sigma_{ij} n_j dS \quad (2.16)$$

where σ_{ij} is stress tensor giving the force dF_i per unit area dS in the i direction transmitted across the plane normal to the j direction, where $i, j \in [x, y, z]$.

For shear flow between two flat plates, for Newtonian fluids⁴, the shear stress originating from purely viscous forces without the contribution from pressure forces $\sigma'_{ij} = F_i/S_j$ is proportional to the gradient of the fluid flow velocity:

$$\sigma'_{ij} = \eta \partial_j v_i \quad (2.17)$$

where η is a property of the fluid, the viscosity⁵. More generally, for an arbitrary geometry, we can write the shear stress tensor as:

$$\sigma'_{ij} = \eta (\partial_i v_j + \partial_j v_i) \quad (2.18)$$

and hence the change of momentum within the volume V is given as:

$$\partial_t P_i^{\text{visc}} = \int_S dS n_j \sigma'_{ij} \quad (2.19)$$

Many real fluids, including water, satisfy Eq. (2.17) to a good approximation over a range of conditions. Many complex fluids, which will be the focus of the following chapters, are however governed by a more complex relationship, but as the basis for the following discussion, we first summarise here the key features of Newtonian fluids. We note that similarly to Eq. (2.15) it is possible to combine the contributions from viscous and pressure forces to give an overall stress tensor:

$$\sigma_{ij} = \sigma'_{ij} - p \delta_{ij} \quad (2.20)$$

⁴In the second book of *Philosophiae Naturalis Principia Mathematica* ‘The circular motion of fluids’ Newton proposed that “The resistance arising from the want of lubricity in the parts of a fluid, is [...] proportional to the velocity with which the parts of the fluid are separated from one another.”, in modern terminology that the shear stress is proportional to the shear rate, with “lubricity” being the viscosity.

⁵It is also common to define $\nu = \eta/\rho$ as the kinematic viscosity.

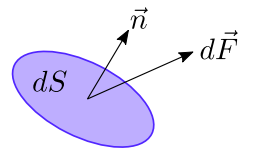


Figure 2.2: Illustration of the force $d\vec{F}$ through a surface dS with normal vector in a system with both normal and tangential forces.

Body forces

External forces, such as gravity and electrostatic forces, act throughout the body of the fluid. The change in momentum within a volume V due to the action of gravity is:

$$\partial_t P_i^{\text{body}} = \int_V d^3r \rho g_i \quad (2.21)$$

where \vec{g} is the gravitational acceleration.

2.3 Navier-Stokes equation

In the above sections, we have computed in turn the individual contributions to the change of momentum Eq. (2.10). By equating the sum of these contributions from Eqs.(2.12), (2.14), (2.19) and (2.21) to the change of momentum from Eq. (2.9) we obtain:

$$\int_V d^3r [(\partial_t \rho)v_i + \rho \partial_t v_i] = \int_S dS n_j (-\rho v_i v_j - p \delta_{ij} + \sigma'_{ij}) + \int_V d^3r \rho g_i \quad (2.22)$$

Using Gauss' divergence theorem, we can rewrite the surface integrals on the right hand side of Eq.(2.22) over $S = \partial V$ involving the surface normal vector n_j as a volume integral over V of the divergence ∂_j of the integrand:

$$\int_V d^3r [(\partial_t \rho)v_i + \rho \partial_t v_i] = \int_V d^3r [-\partial_j(\rho v_i v_j) - \partial_j(p \delta_{ij}) + \partial_j \sigma'_{ij} + \rho g_i] \quad (2.23)$$

Since this equality holds for an arbitrary shape V , we can equate the integrands to yield:

$$(\partial_t \rho)v_i + \rho \partial_t v_i = -\partial_j(\rho v_i v_j) - \partial_j(p \delta_{ij}) + \partial_j \sigma'_{ij} + \rho g_i \quad (2.24)$$

We note that expanding the derivative of the product $\partial_j(\rho v_j v_i)$ yields the terms $-\partial_j(\rho v_j v_i) = -\partial_j(\rho v_j)v_i - \rho v_j \partial_j v_i$. Due to the continuity equation $\partial_t \rho = -\partial_j(\rho v_j)$ from Eq. (2.7), we have $-\partial_j(\rho v_j)v_i = (\partial_t \rho)v_i$; the last term of this expression is the first term on the left hand side of Eq.(2.24). Using this observation, and by regrouping the pressure term $p \delta_{ij}$ together with the viscous stress tensor σ'_{ij} into the full stress tensor $\sigma_{ij} = \sigma'_{ij} - p \delta_{ij}$, we can simplify Eq. (2.24) to:

$$\rho \partial_t v_i + \rho v_j \partial_j v_i = \partial_j \sigma_{ij} + \rho g_i \quad (2.25)$$

This expression is the general equation of motion for the (Eulerian) velocity field \vec{v} of a viscous fluid. For a Newtonian fluid, we can use the expression for the viscous stress tensor σ' from Eq. (2.18) and evaluate the derivative:

$$\begin{aligned} \partial_j \sigma_{ij} &= \underbrace{\partial_j \sigma'_{ij}}_{=\eta \partial_j \partial_i v_j + \eta \partial_j \partial_j v_i} - \underbrace{\partial_j p \delta_{ij}}_{=\partial_i p} \end{aligned} \quad (2.26)$$

For incompressible fluids, the divergence of the velocity field $\partial_j v_j$ vanishes, and the term $\eta \partial_j \partial_i v_j = 0$. Therefore for incompressible Newtonian fluids we can rewrite Eq. (2.25) as:

$$\rho(\partial_t v_i + v_j \partial_j v_i) = -\partial_i p + \eta \partial_j^2 v_i + \rho g_i \quad (2.27)$$

This equation is the Navier-Stokes equation. For completeness, in vector notation the equation reads:

$$\rho \left[\partial_t \vec{v} + (\vec{v} \cdot \vec{\nabla}) \vec{v} \right] = -\vec{\nabla} p + \eta \nabla^2 \vec{v} + \rho \vec{g} \quad (2.28)$$

The left hand side of the Navier-Stokes equation relates to inertial force densities and the right hand side encompasses intrinsic (viscosity) and applied force densities (pressure gradient and gravity). For conservative external forces $\vec{f}_i = -\vec{\nabla} V$, including gravity, the external force term can be absorbed into the pressure term by writing $-\vec{\nabla} p + \rho \vec{g} = -\vec{\nabla} \bar{p}$ with $\bar{p} = p + V$ with $\rho \vec{g} = \vec{\nabla} V$.

2.4 Material derivative

So far to describe the motion of a fluid, we have used the Eulerian picture, in which coordinates \vec{r} are fixed in space and the velocity field $\vec{v}(\vec{r}, t)$ is given as a function of these coordinates in the laboratory frame. There is a different mathematical representation of fluid flow, the Lagrangian picture, in which the locations of the individual fluid particles are tracked. The latter representation is less straightforward to use when fluid elements exchange momentum and energy, but is useful for obtaining a qualitative picture of fluid flow as will be discussed below.

A helpful concept for analysing fluid motion is that of a streamline⁶, defined as a curve which at a given time t has the same direction as $\vec{v}(\vec{r}, t)$. Even in steady state flows, \vec{v} , ρ or any general field $f(x, y, z, t)$ can change when we follow a particular fluid element. This motivates the definition of the *material derivative* or the rate of change of f following the fluid⁷:

$$\frac{Df}{Dt} = D_t f = \frac{d}{dt} f(r_x(t), r_y(t), r_z(t), t) \quad (2.29)$$

where $r_x(t)$, $r_y(t)$ and $r_z(t)$ are (the Lagrangian) position coordinates changing with time at the local flow velocity \vec{v} :

$$\frac{d}{dt}(r_x, r_y, r_z) = \vec{v} \quad (2.30)$$

⁶Also referred to as flowlines or lines of flow

⁷Also known as the advective derivative, or the convective derivative (convection is used for phenomena which involve both advection and diffusion, and advection indicates movement with the flow).

Applying the chain rule to Eq. (2.29) yields⁸:

$$\underbrace{\frac{Df}{Dt}}_{\text{Lagrangian rate of change}} = \underbrace{\frac{\partial f}{\partial t}}_{\text{Eulerian rate of change}} + \underbrace{(\vec{v} \cdot \vec{\nabla})f}_{\text{Convective rate of change}} \quad (2.31)$$

In particular the acceleration of a fluid element is:

$$\frac{D\vec{v}}{Dt} = \frac{\partial \vec{v}}{\partial t} + (\vec{v} \cdot \vec{\nabla})\vec{v} \quad (2.32)$$

In a steady state flow, the rate of change of f following a fluid element is $(\vec{v} \cdot \vec{\nabla})f$. This expression has a simple qualitative interpretation: let \vec{e} be a unit vector which is always parallel to the streamlines and pointing in the sense of the flow. Then:

$$(\vec{v} \cdot \vec{\nabla})f = |\vec{v}| \vec{e} \vec{\nabla} f = |\vec{v}| \frac{\partial f}{\partial s} \quad (2.33)$$

where s is the distance along a streamline, and $\frac{\partial f}{\partial s}$ is the rate of change of f along a streamline, and therefore as expected $|\vec{v}| \frac{\partial f}{\partial s}$ gives the rate of change of f when following the flow.

We can now understand the Navier-Stokes equation as a consequence of Newton's second law. For a particle with mass m that evolves under the action of external forces $\sum_j F_j$, Newton's second law gives $mdv/dt = \sum_j F_j$. To work with a fluid, we require not the mass but the mass density ρ and the force density f_j . Moreover, we note that the Eulerian time derivative $\partial_t u$ in Eq. (2.27) is not the velocity of any particular fluid particle, as would be required for the application of Newton's second law. Rather, to obtain a physically correct equation of motion, we need to consider the acceleration of a given fluid element, described by the convective acceleration Eq. (2.32), yielding:

$$\rho D_t \vec{v} = \rho \left[\partial_t \vec{v} + (\vec{v} \cdot \vec{\nabla})\vec{v} \right] = \sum_j f_j \quad (2.34)$$

The force densities are the pressure, viscosity and body force densities discussed earlier, and therefore Eq. (2.34) reduces to Eq.(2.27).

2.5 The Reynolds number and Stokes Flow

The Navier-Stokes equation generates an astonishing variety and richness of phenomena, and is used to understand systems as diverse as oceanic currents, atmospheric phenomena and weather and blood flow in the body. This richness

⁸The parenthesis around $(\vec{v} \cdot \vec{\nabla})$ are not required when operating on a scalar field f but are required in the case of a vector field \vec{f} as the operator then acts on each component (and not e.g. on $\vec{\nabla} \cdot \vec{f}$).

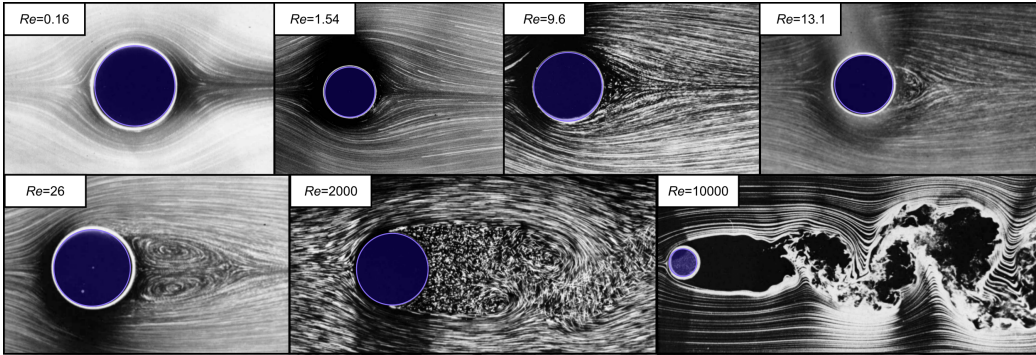


Figure 2.3: Flow around a sphere at increasing Reynolds numbers (From: *An album of fluid motion*, Milton Van Dyke.)

originates largely from the presence of the non-linear term $\rho(\vec{v} \cdot \vec{\nabla})\vec{v}$ in the equation; this non-linearity also makes the Navier-Stokes equation very challenging to solve in the general case⁹.

In the limit of low flow velocities, or small sizes, which are typically relevant for soft condensed matter, the non-linear term can commonly be neglected. To explore this idea further, we make the Navier-Stokes equation dimensionless. To this effect, we express all physical variables in terms of a characteristic length scale L_0 and velocity v_0 to give $\vec{r} = L_0 \tilde{\vec{r}}$ and $\vec{v} = v_0 \tilde{\vec{v}}$, where the dimensionless quantities are indicated with a tilde. Similarly, time and pressure can be made dimensionless: $t = (L_0/v_0)\tilde{t}$ and $p = (\eta v_0/L_0)\tilde{p}$. In many cases a quantity can be made dimensionless in more than one way; for instance for the pressure we can choose $P_0 = \eta v_0/L_0$ or $P_0 = \rho v_0^2$ – we work here with the former expression, but the latter expression is useful at high velocities (see Problem Q1 in the written work). Finally, we can convert the derivatives: $\partial_t = (1/T_0)\tilde{\partial}_t$ and $\vec{\nabla} = (1/L_0)\tilde{\vec{\nabla}}$. Using these rescaled quantities and the Navier-Stokes equation Eq. (2.27) reads:

$$\rho \left[\frac{v_0}{T_0} \tilde{\partial}_t \tilde{\vec{v}} + \frac{v_0^2}{L_0} (\tilde{\vec{v}} \cdot \tilde{\vec{\nabla}}) \tilde{\vec{v}} \right] = -\frac{P_0}{L_0} \tilde{\vec{\nabla}} \tilde{p} + \frac{\eta v_0}{L_0^2} \tilde{\vec{\nabla}}^2 \tilde{\vec{v}} \quad (2.35)$$

where we assumed $T_0 = L_0/v_0$ in the RHS. This can be simplified to:

$$Re \left[\tilde{\partial}_t \tilde{\vec{v}} + (\tilde{\vec{v}} \cdot \tilde{\vec{\nabla}}) \tilde{\vec{v}} \right] = -\tilde{\vec{\nabla}} \tilde{p} + \tilde{\vec{\nabla}}^2 \tilde{\vec{v}} \quad (2.36)$$

⁹For instance it has not been proven that in three dimensions solutions to the Navier-Stokes equation always exist, or that if they do exist, they don't contain singularities. A proof (or a counter example) of this statement is one of the Millennium Problems, a collection of the seven most important open problems in mathematics, and for the solution of which the Clay Mathematics Institute has offered a \$1000000 prize.

where:

$$Re = \frac{\rho v_0 L_0}{\eta} \quad (2.37)$$

is the dimensionless Reynolds number.

We see from Eq. (2.36) that when $Re \ll 1$, the viscous term $\vec{\nabla}^2 \vec{v}$ dominates over the inertia term $(\vec{v} \cdot \vec{\nabla}) \vec{v}$, while for $Re \gg 1$, the inertia term dominates on the left hand side of the dimensionless Navier-Stokes equation Eq. (2.36).

At low Reynolds numbers $Re \ll 1$, the non-linear Navier-Stokes equation is reduced to the linear Stokes equation:

$$0 = -\vec{\nabla} p + \eta \nabla^2 \vec{v} \quad (2.38)$$

In deriving the Stokes equation, we have assumed that the time derivative $\partial_t \vec{v}$ is given by the intrinsic timescale $T_0 = L_0/v_0$. However, if an external driving force is applied, for instance an oscillating boundary, the time derivative is given by the external driving force and is not necessarily negligible. Under such conditions we use the time-dependent Stokes equation:

$$\rho \partial_t \vec{v} = -\vec{\nabla} p + \eta \nabla^2 \vec{v} \quad (2.39)$$

2.6 Properties of Stokes flow and locomotion of microorganisms and nanomachines

We have seen that at low Reynolds numbers, a situation corresponding to small length scales or slow flows, fluid motion is governed by the Stokes equation Eq. (2.38). We discuss here a few properties of this equation.

Due to the absence of the time derivative, Stokes flows are instantaneous; this is expected since we have neglected inertial terms.

Since time doesn't enter explicitly the Stokes equation and it is linear, the flow pattern is unchanged when the pressure is increased, only the flow velocity is changed.

If we reverse spatial directions, the pressure gradient $\vec{\nabla} p \rightarrow -\vec{\nabla} p$ changes sign, the Laplacian $\eta \nabla^2 \rightarrow \eta \nabla^2$ keeps its sign, but the flow velocity changes sign $\vec{v} \rightarrow -\vec{v}$. As such the Stokes equation is unchanged under reversal of spatial coordinates.

Therefore before and after streamlines around an object are unchanged. It is not possible from inspecting the flow lines for flows at low Reynolds numbers to deduce the direction of flow. This leads to kinematic reversibility: if the driving force (e.g. pressure) is inverted, the flow field is inverted, and as such the fluid flow

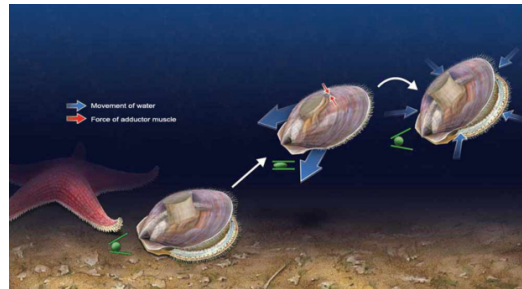


Figure 2.4: A scallop is able to use its single hinged shell to swim by avoiding kinematic reversibility through use of high Reynolds number flows. (Illustration from: *Natural History Magazine*)

appears fully reversible. Note that this is not true thermodynamic reversibility since a viscous fluid always dissipates energy.

This observation has interesting consequences for locomotion on small scales as is applicable to micro-organisms or artificial nanomachines. Indeed, the kinematic reversibility property of Stokes flows implies that a microorganism which attempts to swim through a reversible sequence of changes of shape, returning to its original shape by going through the sequence in reverse, will not translate, since any motion that it undergoes in the first half of the cycle will be reversed in the second part of the swimming cycle. This is known as the Scallop theorem (originally by Edward Purcell). A scallop swims to a good approximation by opening and closing a single hinge. At low Reynolds numbers, the forward movement upon opening would be exactly cancelled by the motion during the reverse stroke and thus the scallop would remain stationary. A real scallop is able to avoid this problem by closing the hinge very rapidly, escaping the low Reynolds number regime. This is made possible by its size - such an escape becomes increasingly difficult for smaller scale objects such as microorganisms and artificial nanorobots.

Table 2.1: Swimming at different scales

System	Re
Large whale swimming at 10 m/s	300000000
Crawl swimmer at 1 m/s	3000000
Large dragonfly at 7 m/s	30000
Swimmer in honey ($\eta = 1000\eta_{H_2O}$)	3000
Flapping wings of small insect	30
Invertebrate larva of size 0.3 mm at 1 mm/s	0.3
Bacterial cell of size 1 μm at 30 $\mu\text{m}/\text{s}$	0.00003

Therefore successful propulsion at low Reynolds numbers using a cyclic change

of configurations requires a sequence of configurations that breaks time-reversal symmetry. Biology has evolved a number of strategies to this effect. For instance, cilia or flagella on cells have many degrees of freedom in bending, and can propel a cell by changing its shape in a manner where the forward path is not simply an inverse of the backward path, a fact which is not possible with a single degree of freedom such as that of a scallop.

A different strategy to break time-reversal symmetry is to operate with a circular motion using rotary molecular motors which drive the rotation of a flagella. This is a strategy that has been adopted by a number of bacteria, including the common *E. coli*.

2.7 Vorticity

The local angular rate of rotation of a fluid is given by the curl of the velocity field and is known as the vorticity ω (pseudo¹⁰) vector field.

$$\vec{\omega} = \vec{\nabla} \times \vec{v} \quad (2.40)$$

It can be seen as the generalisation to fluid dynamics of angular velocity from rigid body kinematics.

We can obtain the time evolution of the vorticity for Stokes flows by taking the curl on both sides of the Stokes equation Eq. (2.39):

$$\underbrace{\vec{\nabla} \times \rho \partial_t \vec{v}}_{=\rho \partial_t \vec{\omega}} = -\underbrace{\vec{\nabla} \times \vec{\nabla} p}_{=0} + \underbrace{\vec{\nabla} \times \eta \nabla^2 \vec{v}}_{=\eta \nabla^2 \vec{\omega}} \quad (2.41)$$

where we have used the fact that the curl of the divergence of a scalar field vanishes and that $\vec{\nabla} \times \nabla^2 = \nabla^2 \vec{\nabla} \times$. Hence the time evolution of the vorticity is given as:

$$\partial_t \vec{\omega} = \frac{\eta}{\rho} \nabla^2 \vec{\omega} \quad (2.42)$$

which is a diffusion equation for ω and as such this flow behaviour at low Reynolds numbers is sometimes known as “diffusion of vorticity”. The term η/ρ acts as the effective diffusion coefficient and is known as the kinematic viscosity.

It is interesting to note that taking the divergence on both sides of the Stokes equation results in:

$$\rho \partial_t \underbrace{\vec{\nabla} \cdot \vec{v}}_{=0(\text{incomp.})} = -\vec{\nabla} \cdot \vec{\nabla} p + \underbrace{\eta \vec{\nabla} \cdot \nabla^2 \vec{v}}_{=0} \quad (2.43)$$

¹⁰ $\vec{\omega}$ transforms like a vector for all coordinate transformations except mirror transformations where its transformation rules differ in sign from those of a true vector. This distinction will not be crucial for the material covered in this lecture.

and hence the pressure obeys a simple Laplace equation at low Reynolds numbers:

$$\nabla^2 p = 0 \quad (2.44)$$

For completeness we can repeat this analysis for the full non-linear Navier-Stokes equation. Indeed, first by using the vector identity $1/2\vec{\nabla}(\vec{v} \cdot \vec{v}) = (\vec{v} \cdot \vec{\nabla})\vec{v} + \vec{v} \times (\vec{\nabla} \times \vec{v})$ we can rewrite the Navier Stokes equation Eq. (2.27) as:

$$\frac{\partial \vec{v}}{\partial t} + \frac{1}{2}\vec{\nabla}(\vec{v} \cdot \vec{v}) - \vec{v} \times (\underbrace{\vec{\nabla} \times \vec{v}}_{\vec{\omega}}) = -\frac{1}{\rho}\vec{\nabla}p + \frac{\eta}{\rho}\nabla^2\vec{v} \quad (2.45)$$

Now, by taking the curl on both sides of this equation, we find:

$$\partial_t \underbrace{\vec{\nabla} \times \vec{v}}_{\vec{\omega}} + \frac{1}{2} \underbrace{\vec{\nabla} \times \vec{\nabla}(\vec{v} \cdot \vec{v})}_{=0} - \vec{\nabla} \times (\vec{v} \times \vec{\omega}) = -\frac{1}{\rho} \underbrace{\vec{\nabla} \times \vec{\nabla}p}_{=0} + \frac{\eta}{\rho} \underbrace{\vec{\nabla} \times \nabla^2\vec{v}}_{=\nabla^2\vec{\omega}} \quad (2.46)$$

By recalling (or looking up!) the general expression for the curl of a vector product $\vec{\nabla} \times (\vec{v} \times \vec{\omega}) = (\vec{\omega} \cdot \vec{\nabla})\vec{v} - (\vec{v} \cdot \vec{\nabla})\vec{\omega} + \vec{v} \vec{\nabla} \cdot \vec{\omega} - \vec{\omega} \vec{\nabla} \cdot \vec{v}$ and noting that the last two terms vanish (the first one since the divergence of the curl vanishes and the second one since the divergence of the velocity field vanishes for an incompressible fluid) we finally obtain:

$$\underbrace{\partial_t \vec{\omega} + (\vec{v} \cdot \vec{\nabla})\vec{\omega} - (\vec{\omega} \cdot \vec{\nabla})\vec{v}}_{=D_t \vec{\omega}} = \frac{\eta}{\rho}\nabla^2\vec{\omega} \quad (2.47)$$

which is the general vorticity transport equation.

In the next sections we explore the physics of Stokes flows with the help of analytical solutions to cases of practical relevance.

2.8 Fluid in mechanical equilibrium

A viscous fluid in mechanical equilibrium has to be at rest $\vec{v} = 0$ relative to the container in which it is placed. Indeed, otherwise viscous forces within the fluid would cause the fluid to lose kinetic energy. The Stokes equation reduces therefore to:

$$0 = -\vec{\nabla}p - \rho g \vec{e}_z \quad (2.48)$$

For an incompressible fluid, we can integrate this equation to yield:

$$p(z) = p^* - \rho g z \quad (2.49)$$

where p^* is the constant of integration which represents the pressure at an arbitrarily defined zero level $z = 0$ and the z -dependent contribution to the pressure is given as the hydrostatic pressure:

$$p_{\text{hs}} := -\rho g z \quad (2.50)$$

We can therefore regroup the effects of gravity into the pressure term and write the total pressure as:

$$p_{\text{tot}} = p + p_{\text{hs}} \quad (2.51)$$

2.9 Couette flow

Couette flow is a flow induced in a liquid through the movement of one or more of the walls of a vessel containing a fluid relative to the other walls. A practically relevant example is that of two concentric cylinders rotating with respect to each other. This experimental setup is commonly used to measure the viscosity of a fluid by measuring the torque required to sustain a given constant speed of relative rotation. We discuss below Couette flow in a planar geometry where a liquid is placed between two infinite planar plates and the bottom plate at $z = 0$ is kept stationary while the top plate located at $z = h$ is moved in the x -direction with a constant speed v_0 .

Since the system is infinite in the x and y directions and as such translationally invariant in these directions, the flow field can only depend on z . Since the driving force is in the x -direction, only the x -component of the velocity field is non-zero. The hydrostatic pressure is cancelled by the gravitational body forces as discussed in Section 2.8. Therefore the stokes equation reads:

$$\eta \partial_z^2 v_x(z) = 0 \quad (2.52)$$

The boundary conditions on \vec{v} are no-slip boundary conditions at the top and bottom planes located at $z = 0$ and $z = h$, yielding $v_x(z = 0) = 0$ and $v_x(z = h) = v_0$. The solution to Eq. (2.52) under these boundary conditions is a simple linear profile:

$$v_x(z) = v_0 \frac{z}{h} \quad (2.53)$$

We can then use the viscous stress tensor σ' to determine the horizontal force required to maintain the velocity of the top plate at v_0 :

$$F_z = \sigma'_{xz} A = \eta \frac{v_0 A}{h} \quad (2.54)$$

where A is the area of the plates. This approach is used to experimental determination of the viscosity of a fluid through a measurement of the force F_x and the geometry of the system.

2.10 Oscillatory flow near a surface

If the driving force is applied in an oscillatory manner rather than in the steady state situation described above, we can obtain the time dependent flow field through

the use of the time dependent Stokes equation which in this situation reads:

$$\rho \partial_t v_x = \eta \partial_z^2 v_x \quad (2.55)$$

We consider an infinite body of fluid in contact with a single surface located at $z = 0$. We assume that the driving force applies an oscillatory motion to this surface such that its velocity is described by:

$$v_x \sim e^{i\omega t} \quad (2.56)$$

Since there is neither a pressure gradient nor any external force, the motion of the fluid is driven by the boundary conditions. Therefore Eq.(2.55) becomes with $v_x(z) = \tilde{v}_x e^{i\omega t}$:

$$i\rho \omega \tilde{v}_x = \eta \partial_z^2 \tilde{v}_x \quad (2.57)$$

This equation has a travelling wave solution of the form:

$$v_x = C e^{i(\omega t - kz)} \quad (2.58)$$

with

$$k = \pm(1 - i)\sqrt{\frac{\omega\rho}{2\eta}} = \pm\frac{1 - i}{\delta} \quad (2.59)$$

with $\delta = \sqrt{2\eta/(\omega\rho)}$. We can define the value of the constant C by requiring that $v_x = v_0 e^{i\omega t}$ at $z = 0$ (no-slip boundary condition) and that the flow decays to zero at infinite distances from the plate $\lim_{z \rightarrow \infty} v_x = 0$ to yield:

$$v_x = v_0 e^{i\omega t} e^{(-1+i)z/\delta} \quad (2.60)$$

The parameter δ gives the decay length of the wave in the fluid. The stress on the moving surface from the viscous forces imparted by the fluid is given by

$$F/A = \eta \partial_z v_x(z = 0) = (-1 + i) \frac{\eta v}{\delta} \quad (2.61)$$

This geometry is commonly used in instruments to study soft layers adsorbed onto surfaces, for instance the Quartz Crystal Microbalance (QCM) which consists of a quartz plate oscillating in plane and in contact with a liquid on one side. The instrument then measures the viscosity of the liquid and of materials adsorbed to its surface by measuring the force required to maintain oscillation.

2.11 Diffusion of momentum

We discuss now how the time-dependent Stokes equation can be seen as an equation describing the diffusion of momentum¹¹. We consider a simple geometry: an

¹¹These arguments are from Frenkel, in Poon and Andelman, 2006

infinite plane in the x, y dimensions in contact with a fluid and initially at rest. At time $t = 0$ the wall begins to move in the x direction with velocity v . Due to symmetry, the resulting flow field in the fluid will be non-zero only in the x -direction, v_x . The equation of motion for the flow field is given by the time-dependent Stokes equation:

$$\rho \partial_t v_x(z, t) = \eta \nabla^2 v_x(z, t) = \eta \partial_z^2 v_x(z, t) \quad (2.62)$$

which is a diffusion equation for the transverse flow velocity $v_T = v_x$ with a diffusion coefficient equal to $\eta/\rho = \nu$, the kinematic viscosity. The larger the kinematic viscosity, the faster the transverse momentum diffuses in the z -direction away from its source at the moving plane. Diffusion equations of this type typically emerge when we consider the transport of a quantity that is conserved, such as mass, energy, or as here, momentum.

2.12 Stokes drag force on a spherical particle

We consider a spherical body of radius a moving with a velocity \vec{v} through a fluid which is overall stationary. As the sphere moves through the fluid, it creates a temporary disturbance in the flow field which disappears again some time after the body has passed a fixed observation point. This problem was first solved exactly by Stokes (in 1851) by working in spherical polar coordinates in the rest frame of the sphere. In the low Reynolds number regime ($\text{Re} = \rho v a / \eta \ll 1$), he calculated that the drag force that the sphere experiences due to the motion of the underlying fluid is

$$\vec{F} = 6\pi\eta a \vec{v}. \quad (2.63)$$

We now discuss two different derivations of this key result.

2.12.1 Scaling argument

Before reproducing the full solution, we discuss here how we can use the concept of momentum diffusion from section 2.11 to estimate the frictional drag on a sphere using a scaling argument. Note that if kinetic gas theory would apply to the motion of colloids, the frictional force acting on a spherical colloid would be caused by independent collisions with the solvent molecules and we would find that the frictional force is proportional to the velocity of the colloid, $F \sim v$ (which is correct, see Eq. (2.39)) and the effective area of the colloid ($F \sim \pi a^2$) (which is wrong). In fact, the true frictional force is proportional to a and not a^2 in the low Reynolds number regime. We discuss below physical arguments which will make the this functional dependence qualitatively clear.

Relative to the situation with an infinite plane discussed above, we lose the translational symmetry in the x and y directions, and the transverse momentum is a vector. However, a qualitative solution exhibiting the correct functional dependencies on the system parameters can be derived by considering the diffusion of the magnitude of the transverse flow velocity v_T . In the low Reynolds number regime, assuming stationary flow and neglecting the pressure gradient term, we need to consider the following version of the Navier-Stokes equation:

$$\nabla^2 v_T = 0 \quad (2.64)$$

with no-slip boundary conditions on the surface of the moving sphere. A moving sphere acts as a source of transverse momentum in a manner similar to the moving infinite plane discussed earlier. Indeed, in order to keep moving, a constant force has to be exerted on the sphere. At steady state, the sphere does not accelerate, and all the momentum that the sphere has received from the external force pulling it is lost to the fluid. Hence the sphere acts as steady state momentum source. The solution to Eq.(2.64) in spherical polar coordinates is ¹² :

$$v_T(r) = v \frac{a}{r} \quad (2.65)$$

where a is the radius of the sphere where we have used the boundary condition that $v_T(r = a) = v$ at the surface of the sphere. The viscous stress acting on the sphere is $\sigma' \sim \eta \partial_r v_T = \eta v a / r^2$. The total force from viscous drag is then given by Eq. (2.19) as the integral over the surface S of the sphere:

$$F_{\text{approx}} = \int_S \sigma' dS = 4\pi a^2 \eta v \frac{1}{a} = 4\pi \eta a v \quad (2.66)$$

The exact solution of Eq.(2.64) is:

$$F = 6\pi \eta a v \quad (2.67)$$

and our approximate analysis results in the pre-factor of order unity being slightly different (4π in stead of 6π) but with the correct functional relationship.

2.12.2 Full analysis

We outline briefly here how the velocity field around a sphere can be determined exactly in the low Reynolds number regime. We consider an immobile sphere in

¹²To see this, we can use the r -dependent part of the Laplacian in spherical coordinates , which reads $\vec{\nabla}^2 = \frac{\partial^2}{\partial r^2} + \frac{2}{r} \frac{\partial}{\partial r}$. Using this formula, it is easy to calculate that $\vec{\nabla}^2(1/r) = 0$ for $r \neq 0$.

a fluid flowing with velocity \vec{v}_0 . The equations we wish to solve are Eq. (2.38) together with the continuity equation for an incompressible fluid

$$\eta \vec{\nabla}^2 \vec{v} = \vec{\nabla} p \quad (2.68)$$

$$\vec{\nabla} \cdot \vec{v} = 0. \quad (2.69)$$

The boundary conditions of the problem are that very far away from the sphere the flow field \vec{v} approaches \vec{v}_0 , and that no-slip boundary conditions hold on the surface of the moving sphere. These two conditions can be formulated as:

$$\vec{v} \rightarrow \vec{v}_0, \quad |\vec{x}| = r \rightarrow \infty \quad (2.70)$$

$$\vec{v} = 0, \quad |\vec{x}| = r = R. \quad (2.71)$$

Determination of velocity field

As the starting point for finding the solution to Eqs. (2.68) and (2.69), we consider the following vector field

$$\vec{w}_1 = \frac{\vec{v}_0}{r} \quad (2.72)$$

as in Eq. (2.65). As noted in the previous section, \vec{w}_1 is a solution of the Laplace equation, i.e. it satisfies

$$\vec{\nabla}^2 \vec{w}_1 = 0. \quad (2.73)$$

The divergence of \vec{w}_1 is

$$\vec{\nabla} \cdot \vec{w}_1 = -\frac{\vec{v}_0 \cdot \vec{x}}{r^3}. \quad (2.74)$$

Clearly, \vec{w}_1 does not satisfy Eqs. (2.68) and (2.69) because the Laplacian of the solution must equal a gradient and its divergence must be zero. However, we can arrive at a solution by constructing, from \vec{w}_1 , two further vector fields as follows:

$$\vec{w}_2 = \vec{\nabla}(\vec{\nabla} \cdot \vec{w}_1) = -\vec{\nabla} \left(\frac{\vec{v}_0 \cdot \vec{x}}{r^3} \right) \quad (2.75)$$

$$\vec{w}_3 = r^2 \vec{w}_2. \quad (2.76)$$

The divergence of these vector fields reads

$$\vec{\nabla} \cdot \vec{w}_2 = 0 \quad (2.77)$$

$$\vec{\nabla} \cdot \vec{w}_3 = 4 \frac{\vec{v}_0 \cdot \vec{x}}{r^3} \quad (2.78)$$

while the Laplacians read

$$\vec{\nabla}^2 \vec{w}_2 = 0 \quad (2.79)$$

$$\vec{\nabla}^2 \vec{w}_3 = -6 \vec{w}_2 = \vec{\nabla} \left(\frac{6 \vec{v}_0 \cdot \vec{x}}{r^3} \right). \quad (2.80)$$

Crucially, we note that the divergence of \vec{w}_2 is zero, while the divergence of \vec{w}_1 and \vec{w}_3 differ simply by a numerical prefactor. Moreover, \vec{w}_1 and \vec{w}_2 have zero Laplacian, while the Laplacian

of \vec{w}_2 is equal to a gradient. From these considerations, we hypothesize that the full solution is of the form

$$\vec{v} = \vec{v}_0 + A\vec{w}_1 + B\vec{w}_2 + C\vec{w}_3, \quad (2.81)$$

where A , B and C are coefficients to be determined. Note that, because \vec{w}_1 , \vec{w}_2 and \vec{w}_3 decay to zero as $r \rightarrow \infty$, the full solution tends to \vec{v} far away from the sphere. From the condition $\vec{\nabla} \cdot \vec{v} = 0$, we have

$$A - 4C = 0. \quad (2.82)$$

Finally, at $r = R$ we must have $\vec{v} = 0$. Setting $r = R$ in Eq. (2.81), we find

$$\vec{v} = \left(1 + \frac{A}{R} - \frac{B}{R^3} - \frac{C}{R}\right)\vec{v}_0 + \left(\frac{3B}{R^5} + \frac{3C}{R^3}\right)(\vec{x} \cdot \vec{v}_0)\vec{x}|_{|\vec{x}|=R} = 0. \quad (2.83)$$

Because \vec{v} and $(\vec{x} \cdot \vec{v}_0)\vec{x}$ are linearly independent, each coefficient in front of \vec{v} and $(\vec{x} \cdot \vec{v}_0)\vec{x}$ must vanish separately. This leads to the conditions:

$$1 + \frac{A}{R} - \frac{B}{R^3} - \frac{C}{R} = 0 \quad (2.84)$$

$$\frac{3B}{R^5} + \frac{3C}{R^3} = 0. \quad (2.85)$$

It follows

$$A = -R, \quad B = \frac{R^3}{4}, \quad C = -\frac{R}{4} \quad (2.86)$$

and the solution for the velocity field is therefore

$$\vec{v} = \vec{v}_0 - \frac{3R}{4r}\vec{v}_0 - \frac{R}{4r^3}[3(\vec{x} \cdot \vec{v}_0)\vec{x} + R^2\vec{v}_0] + \frac{3R^3}{4r^5}(\vec{x} \cdot \vec{v}_0)\vec{x}. \quad (2.87)$$

Note that the leading term in this equation is of the order r^{-1} , as we found in Eq. (2.65).

Calculation of the drag force on the sphere

We have calculated the velocity field. How can we now calculate the total force acting on the sphere? We recall that the total force vector can be calculated as follows

$$F_i = \int_S d^2 r n_j \sigma_{ij}, \quad (2.88)$$

where

$$\sigma_{ij} = -p\delta_{ij} + \sigma'_{ij}. \quad (2.89)$$

The pressure can be calculated from the Navier Stokes equation Eq. (2.68) if the flow field is known; similarly, σ'_{ij} is obtained as

$$\sigma'_{ij} = \eta(\partial_i v_j + \partial_j v_i). \quad (2.90)$$

Let us start with the calculation of the pressure p . Since only \vec{w}_3 has a non-vanishing Laplacian, using Eq. (2.68), we find for the pressure

$$\vec{\nabla} p = \eta \vec{\nabla}^2 \vec{v} = \eta C \vec{\nabla} \left(\frac{6\vec{v}_0 \cdot \vec{x}}{r^3} \right) = -\frac{3\eta R}{2} \vec{\nabla} \left(\frac{\vec{v}_0 \cdot \vec{x}}{r^3} \right). \quad (2.91)$$

Hence,

$$p = -\frac{3\eta R}{2} \frac{\vec{v}_0 \cdot \vec{x}}{r^3}. \quad (2.92)$$

Integrating over the surface of the sphere, we find

$$\vec{F}_{\text{pressure}} = - \int d^2 r \vec{r} p = 2\pi\eta a \vec{v}_0. \quad (2.93)$$

Next, we calculate the contribution to the force from σ'_{ij} . We note that the leading contributions to σ'_{ij} come from the second and third terms in Eq. (2.87), which are both of the order r^{-1} . Using Eq. (2.90), we find

$$\sigma'_{ij} = -\frac{3\eta R}{2} \vec{v} \cdot \vec{x} \left(\frac{\delta_{ij}}{r^3} - \frac{3x_i x_j}{r^5} \right) + \mathcal{O}(r^{-4}). \quad (2.94)$$

Integrating over the surface of the sphere, we find

$$\vec{F}_{\text{viscous}} = 4\pi\eta a \vec{v}_0. \quad (2.95)$$

It is interesting to note that this result equals the one we have obtained using the scaling argument. This makes perfect sense, because in that calculation we have used the solution to $\vec{\nabla}^2 \vec{v} = 0$, Eq. (2.67), which is obtained from the Navier-Stokes equation for the problem when neglecting the pressure gradient term.

Finally, adding the two contributions together, we find the final result

$$\vec{F} = \vec{F}_{\text{pressure}} + \vec{F}_{\text{viscous}} = 6\pi\eta a \vec{v}_0. \quad (2.96)$$

2.13 Hydrodynamic interaction between colloidal particles

An interesting consequence of Eq.(2.65) is that the flow velocity at a distance r from a moving colloid, decays as $1/r$. Through this velocity field, one colloid can exert a drag force on another colloid. Such hydrodynamic interactions between colloidal particles are very long-ranged as they decay slowly as the inverse of the particle separation. These interactions can be expressed formally by extending Stokes' relation to multiple particles:

$$\vec{v}_n = \underline{\underline{H}}_{nm} \vec{F}_m \quad (2.97)$$

where \vec{F}_m is the force applied to the m th particle and \vec{v}_n is the velocity of the n th particle. The matrix H_{nm} is the mobility matrix and is in general challenging to compute. However, under dilute conditions where we only expect interactions

with one particle, Eq.(2.97) should reduce to Eq. (2.67) when $m = n$ and we expect a pairwise interaction decaying as $1/r$ for $n \neq m$:

$$H_{nm,ij} = \begin{cases} \frac{\delta_{ij}}{\frac{6\pi\eta a}{8\pi\eta|\vec{r}_{nm}|}(r_{nm,i}/|\vec{r}_{nm}|)(r_{nm,j}/|\vec{r}_{nm}|)} & \text{if } n = m \\ \frac{\delta_{ij}}{8\pi\eta|\vec{r}_{nm}|} & \text{otherwise} \end{cases} \quad (2.98)$$

where \vec{r}_{nm} is the separation of the two colloids m and n .

2.14 Flow and micro- and nano channels

2.15 Poiseuille flow

We consider pressure-driven steady state flow through small channels. This class of systems is technologically important and occurs in a number of areas, including micro and nanofluidic systems which through miniaturisation are transforming chemical and biological research as well as medical diagnostics. To analyse such systems, we seek solutions to the Navier Stokes equation under low Reynolds number flow conditions for a channel parallel to the x -axis with an arbitrary cross section \mathcal{C} in the yz plane. The flow is driven by a constant pressure difference Δp maintained over a segment of length L of the channel: $p(x = 0) = \Delta p$ and $p(x = L) = 0$. Due to the translational invariance of the channel in the x -direction, the flow velocity field $\vec{v} = v_x(y, z)\vec{e}_x$ will have a non-vanishing component only in the x -direction and is invariant under translations along the channel length. To obtain the flow profile, we solve the Stokes equation:

$$0 = \eta \nabla^2 [v_x(y, z)\vec{e}_x] - \vec{\nabla}p \quad (2.99)$$

This equation implies $\partial_y p = \partial_z p = 0$ and hence we can simplify the Stokes equation to:

$$\eta[\partial_y^2 + \partial_z^2]v_x(y, z) = \partial_x p(x) \quad (2.100)$$

The left hand side of Eq. (2.100) is a function of y and z while the right hand side is a function of x only. The only way that the left and right hand sides can be equal therefore is if they equal the same constant. We thus immediately find out that the pressure varies linearly along the length of the channel:

$$p(x, y, z) = \frac{\Delta p}{L}(L - x) + p^* \quad (2.101)$$

where Δp is the pressure difference over the channel length and p^* is the hydrostatic pressure. We assume no-slip boundary conditions at the walls of the

channel, $\partial\mathcal{C}$ and therefore:

$$[\partial_y^2 + \partial_z^2]v_x(y, z) = -\frac{\Delta p}{\eta L} \quad \text{for } (y, z) \in \mathcal{C} \quad (2.102)$$

$$v_x(y, z) = 0 \quad \text{for } (y, z) \in \partial\mathcal{C} \quad (2.103)$$

where \mathcal{C} is the cross section of the channel. We now examine two specific geometries of practical interest.

2.15.1 Parallel plate channel

A very high aspect ratio channel can be approximated by two infinite parallel plates. The planar symmetry implies identical behaviour in both y and z directions and thus Eq. (2.103) simplifies to

$$\partial_z^2 v_x(z) = -\frac{\Delta p}{\eta L} \quad (2.104)$$

$$v_x(z = 0) = 0 \quad (2.105)$$

$$v_x(z = h) = 0 \quad (2.106)$$

The solution is a parabolic flow profile

$$v_x(z) = \frac{\Delta p}{2\eta L}(h - z)z \quad (2.107)$$

The overall flow is characterised by the volumetric flow rate, Q :

$$Q := \int_{\mathcal{C}} dy dz v_x(y, z) \quad (2.108)$$

The flow rate through a section of width w is

$$Q = \int_0^w dy \int_0^h dz \frac{\Delta p}{2\eta L}(h - z)z = \frac{h^3 w}{12\eta L} \Delta p \quad (2.109)$$

2.15.2 Channel with circular cross-section

This geometry leads itself to the use of cylindrical coordinates for which we have:

$$(x, y, z) = (x, r \cos \varphi, r \sin \varphi) \quad (2.110)$$

$$\vec{e}_x = \vec{e}_x \quad (2.111)$$

$$\vec{e}_r = \cos \varphi \vec{e}_y + \sin \varphi \vec{e}_z \quad (2.112)$$

$$\vec{e}_{\varphi} = -\sin \varphi \vec{e}_y + \cos \varphi \vec{e}_y \quad (2.113)$$

and the Laplace operator is $\nabla^2 = \partial_x^2 + \partial_r^2 + \frac{1}{r}\partial_r + \frac{1}{r^2}\partial_\varphi^2$. As discussed in section 2.15, the velocity field is parallel to the long axis of the channel, $\vec{v} = v(r)\vec{e}_x$ and $\partial_\varphi \vec{v} = 0$ and hence the Navier-Stokes equation becomes

$$\left[\partial_r^2 + \frac{1}{r} \frac{\partial}{\partial r} \right] v_x(r) = -\frac{\Delta p}{\eta L} \quad (2.114)$$

The general solution to the homogeneous equation $\partial_r^2 v_x + r^{-1} \partial_r v_x = 0$ is $v_x(r) = A + B \ln r$; in this situation $B = 0$ since there is no divergence at $r = 0$ in the physical system. A particular inhomogeneous solution is $v_x(r) = -\frac{\Delta p}{4\eta L} r^2$ and the general solution is obtained as a sum of the particular solution to the inhomogeneous equation and the general solution to the homogeneous equation. Considering the no-slip boundary condition $v_x(r = a) = 0$ and the condition $\partial_r v_x(r = 0) = 0$ from symmetry around $r = 0$ yields the solution

$$v_x(r) = \frac{\Delta p}{4\eta L} (a^2 - r^2) \quad (2.115)$$

For this situation the volumetric flow rate is

$$Q = \int_0^{2\pi} d\varphi \int_0^a dr r \frac{\Delta p}{4\eta L} (a^2 - r^2) = \frac{\pi a^4}{8\eta L} \Delta p \quad (2.116)$$

2.16 Hydraulic resistance

We have seen in Eqs. (2.116) and (2.109) for different geometries that the flow rate, Q , in a straight channel at steady state is proportional to the pressure difference at its ends Δp :

$$\Delta p = R_{\text{hydr}} Q \quad (2.117)$$

where we have introduced the proportionality constant R_{hydr} , the hydraulic resistance. This relationship holds for any channel geometry and is known as the Hagen-Poiseuille law. It is mathematically identical to Ohm's law, $\Delta V = RI$ which connects the electrical current I through a conductive wire to the electrical resistance R and the voltage drop across the length of the wire ΔV . Recalling the power dissipated as Joule heating by an electric current, $\mathcal{P} = I\Delta V$, we can obtain the viscous dissipation of energy in steady-state Poiseuille flow

$$\mathcal{P} = Q\Delta p \quad (2.118)$$

2.17 Compliance

We have seen that the hydraulic resistance plays the same role for fluid flow as the electrical resistance has for the flow of electrical currents. There is also an analogue quantity for the capacitance. Electrical capacitance is given by $C = dq/dV$

where q is the electric charge. We identify the charge q with fluid volume \mathcal{V} , electrical current I with flow rate Q and potential difference ΔV with pressure difference δp , motivating the introduction of hydraulic capacitance (or compliance) as:

$$C_{\text{hydr}} = -\frac{d\mathcal{V}}{dp} \quad (2.119)$$

For an incompressible fluid, compliance exists as real channels are not completely rigid.

Table 2.2: Summary of the equivalence between Hagen-Poiseuille law and Ohm's law.

	Ohm's law	Hagen-Poiseuille law
Current	Electrical current I	Volumetric flow rate Q
Transported quantity	Charge q	Fluid volume \mathcal{V}
Driving force	Potential difference ΔV	Pressure difference Δp
Resistance	Electrical resistance $R = \frac{\Delta V}{I}$	Hydraulic resistance $R_{\text{hydr}} = \frac{\Delta p}{Q}$
Capacitance	$C = \frac{dq}{dV}$	Hydraulic capacitance $C_{\text{hydr}} = -\frac{d\mathcal{V}}{dp}$

Chapter 3

Viscoelasticity and Brownian motion

3.1 Basic concepts in elasticity

3.1.1 Strain

In this chapter, we will be exploring the deformation of elastic and visco-elastic bodies in response to applied forces. We first start by summarising results from linear elasticity for solid bodies; these will then be combined with the description of fluids from chapter 2 to progress towards a general description of visco-elasticity. The position of any point in the undeformed body is given by its position vector \vec{x} ; when the body is deformed, the point \vec{x} will be displaced to \vec{x}' . The displacement vector is given by:

$$\vec{u} := \vec{x}' - \vec{x} \quad (3.1)$$

and determines fully the deformation of the body. The displacement vector will in general be different for all points in the body and therefore both the coordinates x'_i and the displacement vector u_i will be functions of the original coordinate of the point x_i . The manner in which the displacement vector changes with the position x_i , i.e. the derivatives $\partial_i u_k$, contains information about the strain.

When a body is deformed, the distances between points within it change. Let us consider two points \vec{x}_1 and \vec{x}_2 separated by a small distance $d\vec{x} := \vec{x}_2 - \vec{x}_1$ in the undeformed state. In the deformed state, the separation of the points will be $d\vec{x}' := \vec{x}'_2 - \vec{x}'_1 = \vec{x}_2 + \vec{u}(\vec{x}_2) - \vec{x}_1 - \vec{u}(\vec{x}_1) = d\vec{u} + d\vec{x}$, where $d\vec{u} := \vec{u}(\vec{x}_2) - \vec{u}(\vec{x}_1)$. For small deformations the distortion $d\vec{u}$ due to strain can be written as:

$$du_i = \epsilon_{ik} dx_k \quad (3.2)$$

or

$$d\vec{u} = \underline{\underline{\epsilon}} d\vec{x} \quad (3.3)$$

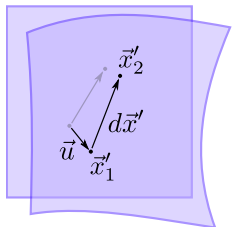
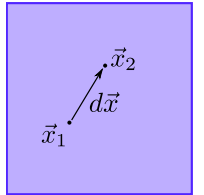


Figure 3.1:
Deformation.

in vector notation, an expression which defines the strain tensor ϵ_{ik} . To compute the strain tensor we examine the distance between the points 1 and 2 prior to and after deformation. The distance between the two points prior to deformation is

$$dl = \sqrt{dx_i^2} \quad (3.4)$$

and after deformation

$$dl' = \sqrt{dx'_i^2} \quad (3.5)$$

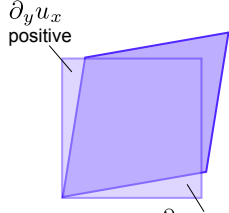
The later expression is equal to:

$$dl'^2 = \langle d\vec{x}', d\vec{x}' \rangle = \langle (1 + \underline{\epsilon})d\vec{x}, (1 + \underline{\epsilon})d\vec{x} \rangle = dl^2 + 2\epsilon_{ik}dx_idx_k + \mathcal{O}(\epsilon^2) \quad (3.6)$$

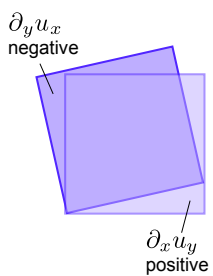
Using the chain rule, du_i can also be written as $du_i = (\partial_k u_i)dx_k$. We can then evaluate dl' :

$$dl'^2 = (dx_i + du_i)^2 = dl^2 + 2\partial_k u_i dx_i dx_k + \partial_k u_i \partial_l u_i dx_k dx_l \quad (3.7)$$

(i) Shear deformation



(ii) Rotation



For small deformations, $\partial_k u_i \ll 1$, and therefore we neglect the second order term in Eq. (3.7) $\partial_k u_i \partial_l u_i$ in front of the first order terms. Moreover, since the summation is taken over both the indices i and k , the second term on the right hand side of Eq. (3.7) can be written in a symmetric form as $(\partial_k u_i + \partial_i u_k)dx_i dx_k$. Finally, we can write the distance between two points after deformation as $dl'^2 = dl^2 + 2\epsilon_{ik}dx_i dx_k$ where by comparison with Eq. (3.6) we can identify the strain tensor as

$$\epsilon_{ik} = \frac{1}{2}(\partial_k u_i + \partial_i u_k) \equiv \frac{1}{2} \left(\frac{\partial u_i}{\partial x_k} + \frac{\partial u_k}{\partial x_i} \right). \quad (3.8)$$

We can qualitatively understand the symmetric form of the stress tensor in Eq. (3.8) by considering as an example the symmetric and anti-symmetric combinations $\partial_x u_y \pm \partial_y u_x$. As can be seen from Fig. Figure 3.2, for a pure shear deformation in the x, y plane, the quantity $\partial_x u_y + \partial_y u_x$ gives a measure of the deformation and $\partial_x u_y - \partial_y u_x$ vanishes, while in the case of a rotation, $\partial_x u_y - \partial_y u_x$ measures the amount of rotation (it is the z -component of $\vec{\nabla} \times \vec{u}$).

The strain tensor can be diagonalised at any point \vec{x} to yield

$$\epsilon_{i,j} = \begin{pmatrix} \epsilon_{11} & 0 & 0 \\ 0 & \epsilon_{22} & 0 \\ 0 & 0 & \epsilon_{33} \end{pmatrix} \quad (3.9)$$

resulting in a simple expressions for the length vector $d\vec{x}'$ after displacement in the eigenvector basis

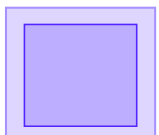
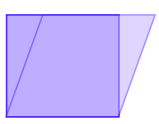
$$dx'_1 = (1 + \epsilon_{11})dx_1 \quad (3.10)$$

$$dx'_2 = (1 + \epsilon_{22})dx_2 \quad (3.11)$$

$$dx'_3 = (1 + \epsilon_{33})dx_3 \quad (3.12)$$

Figure 3.2: Shear versus rotation.

Table 3.1: Examples of deformation

Deformation	Strain	Schema
Unilateral compression	$\begin{pmatrix} \epsilon & 0 & 0 \\ 0 & 0 & 0 \\ 0 & 0 & 0 \end{pmatrix}$	
Hydrostatic compression (preserves shape)	$\begin{pmatrix} \epsilon & 0 & 0 \\ 0 & \epsilon & 0 \\ 0 & 0 & \epsilon \end{pmatrix}$	
Shear (preserves volume $\text{div}\epsilon = 0$)	$\begin{pmatrix} 0 & \epsilon/2 & 0 \\ \epsilon/2 & 0 & 0 \\ 0 & 0 & 0 \end{pmatrix}$	

The volume of the body is $dV = dx_1 dx_2 dx_3$ and after deformation

$$dV' = dx'_1 dx'_2 dx'_3 = dV \Pi_{i=1}^3 (1 + \epsilon_{ii}) \approx dV(1 + \epsilon_{ii}) \quad (3.13)$$

where in the latest approximate equality we have neglected terms higher than linear order in ϵ . And hence the relative volume change

$$\frac{dV' - dV}{dV} = \text{Tr } \underline{\epsilon} = \text{div } \vec{u} \quad (3.14)$$

is given as the trace of the strain tensor.

3.1.2 Stress

Before the body is deformed it is in mechanical equilibrium. In other words, the resulting forces on any portion of the body vanishes. When a deformation occurs, internal stress forces arise which tend to return the body to equilibrium. These are quantified by the stress which is defined as the force $d\vec{F}$ per unit area dS transmitted across the surface element dS :

$$dF_i = \sigma_{ik} dS_k \quad (3.15)$$

where σ_{ik} is the stress tensor. For example, σ_{xy} is the force per unit area in the x -direction transmitted across the plane with the normal vector in the y -direction (Figure 3.3).

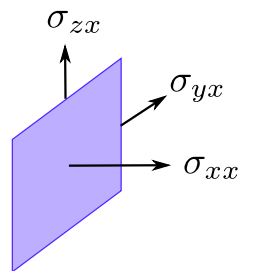


Figure 3.3: Forces on a surface element dS_x with normal in the x -direction are given by the components of the stress tensor $\sigma_{\dot{x}}$.

3.2 Linear elasticity and Hooke's law

The connection between strain and stress is the subject of the rest of this chapter. In many cases, for small strains, a linear relationship, Hooke's law, is observed between the stress and the strain:

$$\sigma_{ij} = C_{ijkl}\epsilon_{kl} \quad (3.16)$$

where C_{ijkl} is the (fourth order) stiffness tensor. Since $\underline{\underline{\sigma}}$ and $\underline{\underline{\epsilon}}$ are symmetric, each one has six independent matrix elements; as such, the stiffness tensor could in principle have 36 elements connecting the independent matrix elements of $\underline{\underline{\sigma}}$ and $\underline{\underline{\epsilon}}$. It turns out that similarly to the stress and strain tensors, the stiffness tensor is symmetric, leaving 21 independent elements, of which furthermore 3 are related to the orientation of the body in space. Finally, therefore, to describe the elastic behaviour of an anisotropic material, there are up to 18 independent tensor elements to consider; this is the case for instance for the description of the response of triclinic crystals. In order to simplify the situation and focus on the essential physical features, we will largely consider isotropic materials. We will see later that for this class of materials, the stiffness tensor only has two independent elements.

We consider a general isotropic linear elastic medium¹. For such a material, all directions behave in the same way and there are no specified internal directions; as such the right hand side of Eq. (3.16) can only have elements proportional to the strain tensor itself, or the only scalar combination $\sum_k \epsilon_{kk}$ of the matrix elements of the strain tensor as any other combination of the matrix elements of the strain tensor would not result in behaviour which is identical in all spatial directions.

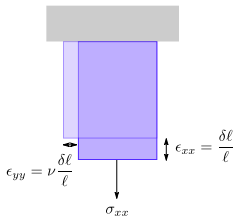


Figure 3.4: A cube of size ℓ of an isotropic material under tension in the x -direction.

3.2.1 Poisson's ratio

When a stress σ_{xx} is applied for instance along the x -axis of an elastic material, it stretches along this direction as described by the strain $\epsilon_{xx} > 0$. The stress and strain are linearly proportional

$$\sigma_{xx} = E\epsilon_{xx} \quad (3.17)$$

where E is the Young's modulus. The Young's modulus has units of pressure, and its values can span from kPa to TPa range. Soft materials are typically in the kPa-MPa range, or for small structures up to GPa.

In addition to stretching along the direction where the stress is applied, however, materials will also typically contract in directions transverse to the direction

¹This section is a recapitulation from the Dynamics course in Physics B in 1B

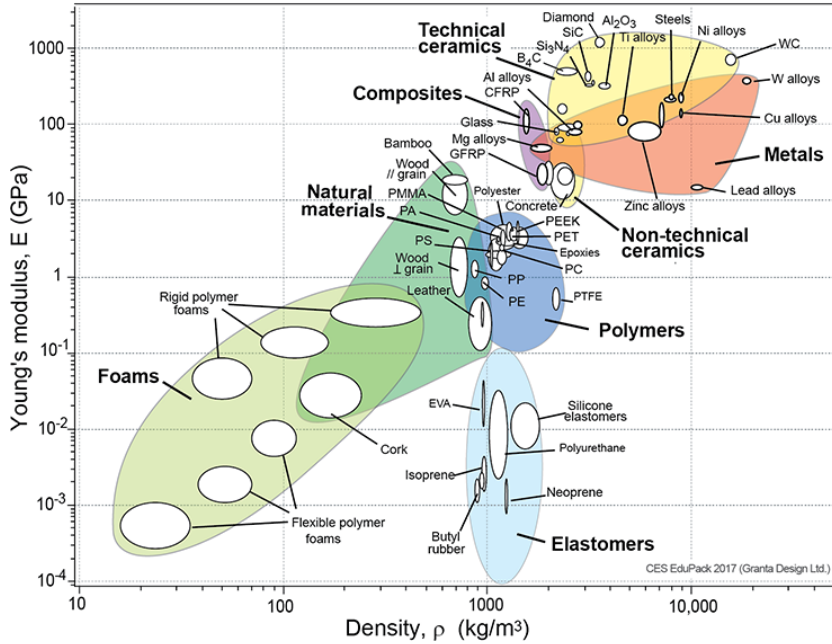


Figure 3.5: Examples of Young's moduli of different materials.

of extension, $\epsilon_{yy} = \epsilon_{zz} < 0$. The stretching in the direction of the load can be understood as a consequence of microscopic elastic (e.g. atomic) bonds within the material being stretched, while the contraction in the transverse direction originates from the fact that in an isotropic material there are bonds in all directions, and when bonds that are neither purely longitudinal nor purely transverse are stretched, they create a transverse tension which is relieved through contraction in this direction. This behaviour is quantified by Poisson's ratio

$$\nu := -\frac{\epsilon_{yy}}{\epsilon_{xx}}. \quad (3.18)$$

The strain tensor for this situation is therefore

$$\epsilon = \begin{pmatrix} \epsilon_{xx} & 0 & 0 \\ 0 & -\nu\epsilon_{xx} & 0 \\ 0 & 0 & -\nu\epsilon_{xx} \end{pmatrix} \quad (3.19)$$

and the strains are given by:

$$E\epsilon_{xx} = \sigma_{xx} \quad (3.20)$$

$$E\epsilon_{yy} = -\nu\sigma_{xx} \quad (3.21)$$

$$E\epsilon_{zz} = -\nu\sigma_{xx} \quad (3.22)$$

Since the material is isotropic, it responds in a similar manner to stresses σ_{yy} and σ_{zz} in the y and z directions. Moreover, the strains are additive, and therefore the combined action of stresses in all three directions gives:

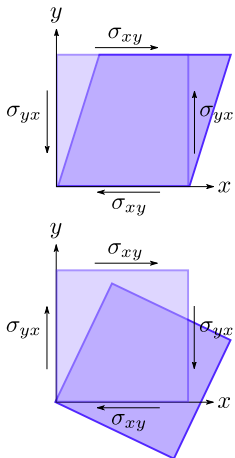
$$E\epsilon_{xx} = \sigma_{xx} - \nu\sigma_{yy} - \nu\sigma_{zz} \quad (3.23)$$

$$E\epsilon_{yy} = -\nu\sigma_{xx} + \sigma_{yy} - \nu\sigma_{zz} \quad (3.24)$$

$$E\epsilon_{zz} = -\nu\sigma_{xx} - \nu\sigma_{yy} + \sigma_{zz} \quad (3.25)$$

This linear system of equations can be solved for σ_{ii} yielding:

$$\sigma_{xx} = \frac{E}{(1+\nu)(1-2\nu)} [(1-\nu)\epsilon_{xx} + \nu\epsilon_{yy} + \nu\epsilon_{zz}] \quad (3.26)$$



and analogous expressions obtained through cyclic permutations for σ_{yy} and σ_{zz} . This equation is Eq. (3.16) for an isotropic material. We see that there are only two parameters required to describe the elastic response of such a material, the Young's modulus E and Poisson's ratio ν . In the next section, we briefly discuss a series of practical scenarios of deformations and show how it can be convenient to introduce the bulk modulus and the shear modulus.

3.2.2 Bulk modulus

Figure 3.6: Shear stresses have to be symmetric $\sigma_{xy} = \sigma_{yx}$ as there should not be a net couple at equilibrium. Indeed, if the couples don't cancel out, as would be the case for instance for $\sigma_{xy} = -\sigma_{yx}$, the body would rotate.

A simple case is that of a body exposed to an isotropic pressure p . In this case $\sigma_{xx} = \sigma_{yy} = \sigma_{zz} = -p$. For this case, Eqs. (3.23) reads

$$E\epsilon_{xx} = \sigma_{xx} - \nu\sigma_{yy} - \nu\sigma_{zz} = -p(1-2\nu) \quad (3.27)$$

and cyclic permutations for $E\epsilon_{yy}$ and $E\epsilon_{zz}$. Hence the strain is given as

$$\epsilon_{xx} = \epsilon_{yy} = \epsilon_{zz} = -\frac{p(1-2\nu)}{E} \quad (3.28)$$

The body therefore contracts uniformly. The change in volume is $\Delta V/V = \text{Tr } \underline{\epsilon} = -3p(1-2\nu)/E$. We can introduce the bulk modulus B through the relationship

$$p = -B \frac{\Delta V}{V} \quad (3.29)$$

with

$$B := \frac{E}{3(1-2\nu)} \quad (3.30)$$

3.2.3 Shear deformation

For shear deformations, it is convenient to introduce the shear modulus G which is the coefficient of proportionality between shear stress σ_{xy} and shear strain ϵ_{xy}

$$\sigma_{xy} = 2G\epsilon_{xy} \quad (3.31)$$

In order to connect the shear modulus to the Young's modulus and Poisson's ratio, we note, as shown in Figure 3.7 that a shear deformation can be obtained through a combination of tensile and compressive stresses.

We first consider a cube with linear dimension ℓ which is deformed under the action of shear stresses in the x, y plane $\sigma_{xy} = F_S/\ell^2$. From the definition of the shear modulus Eq. (3.31), we have $G = \sigma_{xy}/(2\epsilon_{xy})$. From Eq. (3.2), we have $\epsilon_{xy} = du_x/dx_y$. The solid is slanted by a small angle α , so $du_x \approx \alpha dx_y$. Therefore for this deformation, the strain tensor is:

$$\epsilon = \begin{pmatrix} 0 & 0 & \frac{\alpha}{2} \\ 0 & 0 & 0 \\ \frac{\alpha}{2} & 0 & 0 \end{pmatrix}$$

² and hence $G = \sigma_{xy}/\alpha$, and

$$\alpha = F_S/(\ell^2 G). \quad (3.32)$$

We can obtain this same deformation by applying a tensile stress along one diagonal and a compressive stress along another diagonal of the face of the cube. To this effect, we imagine the cube embedded at a 45° angle inside a bigger cube with dimension $\sqrt{2}\ell$ and subjected to the stresses $\sigma_{xx} = -\sigma_{yy} = F/(\sqrt{2}\ell^2)$, $\sigma_{zz} = 0$ as shown in Figure 3.7. The lateral distortion is $\ell \tan \alpha \approx \ell\alpha$. The diagonal of the face of the cube, d , has the length $\sqrt{2}\ell$ in the undeformed state and $d \approx \sqrt{\ell^2 + (\ell + \alpha\ell)^2} = \sqrt{2}\ell + \ell\alpha/\sqrt{2} + \mathcal{O}(\alpha^2)$ after deformation. The extension along the diagonal is therefore $\Delta d = \ell\alpha/\sqrt{2}$ and the strain along this direction is $\epsilon_{xx} = \Delta d/d = \alpha\ell/(\sqrt{2}\ell\sqrt{2}) = \alpha/2$. Using Eqs.(3.23) we can write in the direction of the diagonal of the smaller cube $E\alpha/2 = E\epsilon_{xx} = \sigma_{xx} - \nu\sigma_{yy} = F/(\sqrt{2}\ell^2) \cdot (1 + \nu)$ and hence

$$\alpha = \frac{\sqrt{2}F}{E\ell^2}(1 + \nu) \quad (3.33)$$

²Note: this form is the result of our definition of the strain tensor and is known as the *tensorial shear strain*. Slightly awkwardly, the matrix elements in the tensorial shear strain for pure shear deformations are equal to *half* the total angle change. For this reason, it is also common to use the "engineering shear strain" which is double that of the tensorial shear strain.

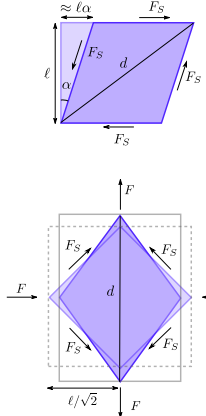


Figure 3.7: Shear stress can be achieved through a combination of tensile and compressive stresses.

Balance of forces implies $F = 2F_S/\sqrt{2} = \sqrt{2}F_S$. Equating the two expressions for the shear angle Eqs.(3.32) and (3.33) yields the expression for the shear modulus as a function of the Young's modulus and Poisson's ratio's:

$$G = \frac{E}{2(1+\nu)} \quad (3.34)$$

3.2.4 Physical constraints

We have shown above that of the potentially 18 free parameters required to describe the linear response of a material Eq. (3.16), only two independent ones are required to describe the elastic behaviour of an isotropic material. These are commonly expressed as combinations of the four commonly used material constants Young's modulus, shear modulus, Poisson's ratio and Bulk modulus of which only any two are required for a complete description of the elastic response. A convenient form of Eqs. (3.26) is

$$\underline{\underline{\sigma}} = \lambda \text{Tr}(\underline{\underline{\epsilon}}) \underline{\underline{1}} + 2G\underline{\underline{\epsilon}} \quad (3.35)$$

where $\lambda = E\nu/(1+\nu)(1-2\nu)) = B - 2/3G$ is (one of) Lamé coefficient(s). This expression can be written as a function of the bulk modulus and the shear modulus to give:

$$\underline{\underline{\sigma}} = (B - \frac{2}{3}G)\text{Tr}(\underline{\underline{\epsilon}}) \underline{\underline{1}} + 2G\underline{\underline{\epsilon}} \quad (3.36)$$

or in index notation

$$\sigma_{ik} = (B - \frac{2}{3}G)\epsilon_{mm}\delta_{ik} + 2G\epsilon_{ik} \quad (3.37)$$

There are physical constraints on the values that the material constants can take. In particular, the bulk modulus cannot be negative; a material with a negative bulk modulus would be unstable and when in a vessel e.g. together with a normal fluid, would expand, causing an increase in pressure, leading to further expansion and further increase in pressure, and hence a material unstable against infinite expansion. Since $B = E/(3(1-2\nu))$, $B > 0$ implies $\nu < 1/2$. The Poisson's ratio for a perfectly incompressible material can be obtained from setting $\text{Tr}(\underline{\underline{\epsilon}}) = 0$ in Eq. (3.19) to yield $\epsilon_{xx}(1-2\nu) = 0$ and thus $\nu = 1/2$. For such a perfectly incompressible material $G/B = 0$ which is the case for fluids. In principle ν can be smaller than 0; such auxetic materials when pulled expand rather than contract laterally. While most natural materials have $\nu > 0$, it is possible to construct artificial materials with suitable microstructure (e.g. by miniaturising an umbrella type mechanism) that expand laterally when subjected to longitudinal stress. Moreover, the shear modulus also has to be positive $G > 0$ otherwise materials would pull away from a shearing force instead of yielding to it. These conditions imply that the Young's modulus also has to be positive $E > 0$.

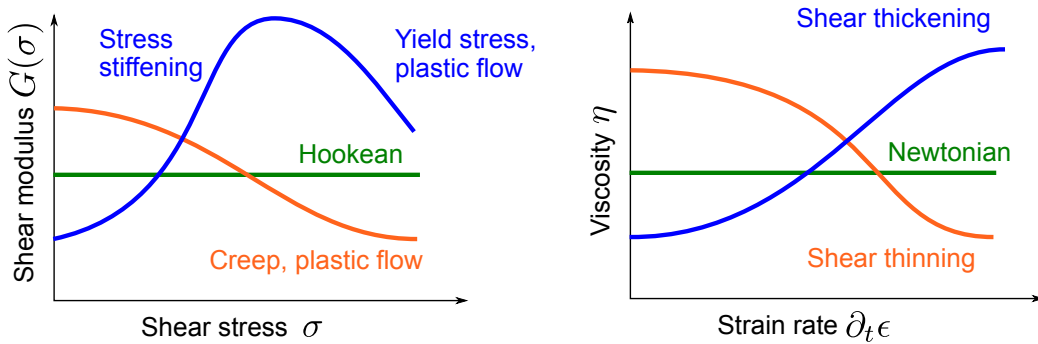


Figure 3.8: Examples of viscoelastic behaviour.

3.3 Viscoelasticity

So far we have seen two different types of simple material behaviour:

Newtonian liquids covered in chapter 2 which don't have a shear modulus but resist flow through their viscosity. The viscosity was assumed to be constant and independent of the flow rate.

Hookean solids covered in section 3.2 which respond immediately to a stress and change their shapes and don't dissipate energy.

Many real materials have more complex behaviour intermediate between an idealised (Newtonian) liquid and an idealised (Hookean) solid. These are viscoelastic materials which as their name indicates, show a combination of viscous and elastic effects and will be discussed in this chapter. We will focus on incompressible materials, $\text{Tr}(\underline{\epsilon}) = 0$ and therefore deformations will be shear deformations. The elastic aspect leads to energy storage. Its contribution to a shape change is lost once the stress is removed. The viscous aspect leads to energy dissipation, and irreversible shape changes associated with the flow.

Different scenarios of visco-elastic behaviour are shown in Fig. Figure 3.8 and contrasted with the ideal Hookean and Newtonian behaviour for solids and liquids, respectively. For example, viscosity can depend on the speed of deformation or flow. It is possible for η to increase (shear thickening) or decrease (shear thinning) when the strain rate $\partial_t \epsilon$ is increased. Examples are many household materials such as ketchup (shear thinning), shampoo (shear thickening), as well as many technologically important polymer solutions and melts, and many biological materials such as the cellular cytoplasm.

3.4 Linear viscoelastic materials

Linear rheology describes a systems whose responses are linearly proportional to the applied stresses. Therefore, the shear modulus is independent of strain. In particular, for such cases, the response to different perturbations is additive. In this lecture, we restrict our analysis to such linear rheological systems. Even non-linear systems close to thermodynamic equilibrium will exhibit linear responses for small enough stresses and strains. Moreover, analysis of the linear dynamic response of a system can be used to relate macroscopic measurements to its microscopic properties.

Since the response of a visco-elastic materials is time dependent, there are different possibilities for protocols to probe the stress strain response in the time domain:

Creep experiment where a constant stress σ_0 is applied rapidly, and the strain ϵ is measured as a function of time. At short times, the resulting strain is given by the immediate elastic response, while for longer times there is a delayed elastic response which originates a slow reorganisation of the microscopic structure of the material. This process is commonly monitored by tracking the compliance $\Gamma(t) = G^{-1}(t)$ of the system which relates the strain to the stress: $\epsilon(t) = \Gamma(t)\sigma_0$

Stress relaxation experiment where a rapid strain ϵ_0 is applied and maintained, and the decay of the stress is measured as a function of time. For a linear-response material, this decay is governed by the relaxation modulus $G(t)$, with $\sigma(t) = G(t)\epsilon_0$

Oscillatory measurements where an oscillating strain (or stress) is applied to a material and the other quantity is measured.

In linear viscoelastic materials, and in an ideal experiment where the time or frequency ranges are infinitely wide, any of the three experimental protocols completely characterises the material.

3.5 Time translation invariance

In a linear visco-elastic system with material properties which are independent of time, we can add together incremental stresses accumulated as a function of the history of the material. Specifically, we consider a material subjected to a series of increments in strain $d\epsilon(t')$ applied at a time $t' < t$. Each of these strain increments will trigger a time-dependent increment in stress $d\sigma(t) = G(t - t')d\epsilon(t')$. The

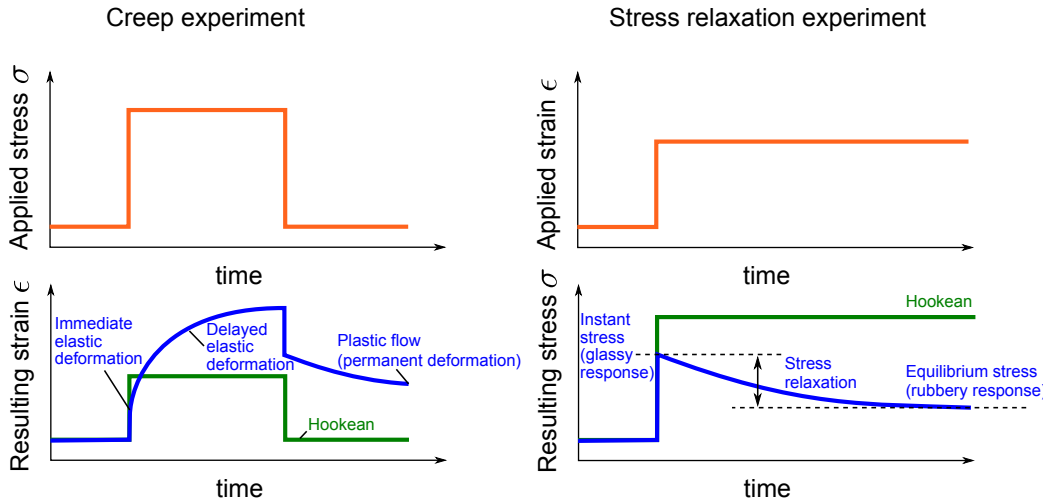


Figure 3.9: Common rheological experiments: creep experiment and stress relaxation experiment.

overall stress will be the linear superposition of the all the contributions from $d\sigma(t)$

$$\sigma(t) = \int d\sigma(t) = \int G(t - t')d\epsilon(t') = \int_{-\infty}^t G(t - t') \frac{d\epsilon(t')}{dt'} dt' \quad (3.38)$$

This is a "retarded" linear response: the stress at time t is a sum over the whole history of the system.

We consider briefly the behaviour in the limit of a Hookean solid. For such a system the shear modulus is constant in time $G(t' - t) = G_0$. Eq. (3.38) then becomes $\sigma(t) = G_0 \int_{-\infty}^t \frac{d\epsilon}{dt'} dt' = G_0 \epsilon(t)$. We therefore recover the instantaneous relationship between stress and strain characteristic of the ideal Hookean solid.

In the limit of a purely viscous system, the shear modulus vanishes for $t' > t$. When $t = t'$ and the strain is applied, a contribution to the stress proportional to strain rate and to the viscosity is present. For an infinitely fast strain increment we can write $G(t - t') = \eta \delta(t - t')$. For this system, Eq. (3.38) becomes $\sigma(t) = \eta \int_{-\infty}^t \delta(t - t') \frac{d\epsilon}{dt'} dt' = \eta \partial_t \epsilon(t)$ and we recover the viscous stress relationship for a Newtonian fluid.

In the case of complex viscoelastic fluids, we can define the shear viscosity as the ratio of steady state shear stress $\lim_{t \rightarrow \infty} \sigma(t)$ to a constant shear rate $\dot{\epsilon}$. In this situation, the constant shear rate can be pulled out of the superposition integral to yield

$$\sigma(t) = \int_{-\infty}^t \dot{\epsilon} G(t - t') dt' = \dot{\epsilon} \int_0^\infty G(\tau) d\tau \quad (3.39)$$

and hence the viscosity becomes

$$\eta = \int_0^\infty G(t)dt \quad (3.40)$$

The stress at long times in a steady shear experiment is thus constant and proportional to the shear rate.

3.6 Complex modulus

We consider the response of a linear viscoelastic material to an applied oscillating strain

$$\epsilon(t) = \epsilon_0 e^{i\omega t}. \quad (3.41)$$

Substituting this time dependent strain into the general response function of a viscoelastic material in Eq. (3.38) yields the time-dependent stress

$$\sigma(t) = \int_{-\infty}^t G(t-t') \frac{d\epsilon(t')}{dt'} dt' = \int_{-\infty}^t G(t-t') i\omega \epsilon_0 e^{i\omega t'} dt' \quad (3.42)$$

$$= \int_{-\infty}^t G(t-t') i\omega \epsilon_0 e^{i\omega t} e^{-i\omega(t-t')} dt' \quad (3.43)$$

$$= \epsilon_0 e^{i\omega t} i\omega \int_0^\infty G(\tau) e^{-i\omega\tau} d\tau = G^*(\omega) \epsilon_0 e^{i\omega t} \quad (3.44)$$

where we have introduced the complex modulus

$$G^*(\omega) := i\omega \int_0^\infty G(\tau) e^{-i\omega\tau} d\tau \quad (3.45)$$

For an ideal solid $G(\tau) = G_0$ and

$$G^*(\omega) = i\omega \int_0^\infty G_0 e^{-i\omega\tau} d\tau = G_0 \quad (3.46)$$

For this situation G^* is real and this relationship describes material stress which evolves perfectly in phase with the applied strain.

By contrast, for Newtonian fluid $G(\tau) = \delta(\tau)\eta$ and

$$G^*(\omega) = i\omega \int_0^\infty \delta(\tau) \eta e^{-i\omega\tau} d\tau = i\omega \eta \quad (3.47)$$

In this situation, G^* is purely imaginary, and the stress is out of phase with the applied shear.

For a general visco-elastic material $G^* =: G' + iG''$ has both a real part G' and an imaginary part G'' . Here G' describes the in-phase response originating from the elastic contribution while G'' describes the out-of phase response from the viscous dissipative contributions. Equivalently we can define a complex viscosity η^* as $G^*(\omega) = i\omega \eta^*(\omega)$.

3.7 Simple models of viscoelastic materials

In the following section, we discuss briefly some models of viscoelastic materials of practical importance.

3.7.1 Maxwell fluid

A material exhibiting a single relaxation time scale τ is known as the Maxwell fluid:

$$G(t) = G_0 e^{-t/\tau} \quad (3.48)$$

This can be represented as a purely viscous damper connected in series with a purely elastic spring. The spring models instantaneous deformation of bonds within the material while the viscous contribution coarse-grains inter-molecular friction.

For this scenario, the stress on the viscous damper σ_D and elastic spring σ_S is the same $\sigma = \sigma_S = \sigma_D$ while the total strain is the sum of the strains on both elements $\epsilon = \epsilon_S + \epsilon_D$. For a Hookean solid we have $\sigma_S = G_0\epsilon$ and for a Newtonian fluid $\sigma_D = \eta\partial_t\epsilon$. We consider a stress-relaxation experiment with a constant strain ϵ_0 with $0 = \dot{\epsilon} = \dot{\epsilon}_S + \dot{\epsilon}_D = \dot{\sigma}/G_0 + \sigma/\eta$. Therefore we have $\dot{\sigma} = -\sigma G_0/\eta$, which can be solved to yield $\sigma(t) = \sigma_0 e^{-t/\tau}$ with the relaxation time $\tau = \eta/G_0$, or $\sigma(t) = \epsilon_0 G(t)$ with $G(t) = e^{-t/\tau}\sigma_0/\epsilon_0$.

Thus for short times $t \ll \tau$ the Maxwell fluid behaves like a solid with a shear modulus G_0 , while for long times $t \gg \tau$ $G \rightarrow 0$ the shear modulus vanishes and we recover the behaviour of a Newtonian fluid. There are a number of cases of complex fluids that have a single dominant relaxation scale and thus their behaviour is approximately described by the Maxwell model. Two examples are:

Emulsions. Emulsions are discussed in more detail in a later chapter and consist of small droplets of a dispersed phase within an immiscible continuous phase. The material can store energy as the droplet deform since the surface tension will tend to restore their spherical shapes. When the droplets are of a uniform size, the system will have a single dominant relaxation time.

Surfactants. Surfactants (discussed in chapter 5) can self-assemble into rod-like micelles which are able to break and re-assemble. The characteristic relaxation time of such systems corresponds to the breakage time scale.

For an oscillating deformation, the relationship $\dot{\epsilon} = \dot{\sigma}/G_0 + \sigma/\eta$ becomes

$$i\omega\epsilon = \frac{i\omega\sigma}{G_0} + \frac{\sigma}{\eta} \quad (3.49)$$

yielding

$$\sigma(\omega) = \frac{i\omega G_0 \eta}{G_0 + i\omega \eta} \epsilon(\omega) \quad (3.50)$$

and hence for the Maxwell model

$$G^*(\omega) = \frac{i\omega G_0 \eta}{G_0 + i\omega \eta} \quad (3.51)$$

The Maxwell model is, however, not useful for studying creep since for long times it flows like a Newtonian fluid.

3.7.2 Kelvin-Voigt solid

An elementary model which exhibits viscoelastic creep can be obtained by connecting the viscous and elastic components in parallel, rather than in series as in the Maxwell model: this is the Kelvin-Voigt model. In this case the strain of the elastic element ϵ_D and of the viscous element ϵ_D are equal $\epsilon = \epsilon_S = \epsilon_D$ while the total stress is the sum of the contributions from both elements $\sigma = \sigma_S + \sigma_D$. When this material is loaded with a constant stress σ_0 , we have $0 = \dot{\sigma} = \eta \dot{\epsilon} + G \dot{\epsilon}$ which can be solved with the boundary conditions $\epsilon \rightarrow 0, t \rightarrow 0$ and $\epsilon \rightarrow \sigma_0/G_0, t \rightarrow \infty$ to yield $\epsilon(t) = (\sigma_0/G_0)(1 - e^{-t/\tau})$ with $\tau = \eta/G_0$. In contrast to the Maxwell fluid, this model doesn't exhibit stress relaxation.

3.7.3 Zener standard linear solid

A simple model which describes both stress relaxation and visco-elastic creep is the Zener model which is composed of the Maxwell model connected in parallel with an ideal solid. We consider the behaviour of the Zener solid under an oscillating deformation. The stress is given by the sum of the stresses from the elastic part with modulus G_1 and the Maxwell solid from Eq. (3.50) with the elastic contribution having a modulus G_2 :

$$\sigma(\omega) = \sigma_S(\omega) + \sigma_M(\omega) = G_1 \epsilon(\omega) + \frac{i\omega G_2 \eta}{G_2 + i\omega \eta} \epsilon(\omega) \quad (3.52)$$

$$= G_1 \frac{1 + i\omega(\frac{\eta}{G_1} + \frac{\eta}{G_2})}{1 + i\omega \frac{\eta}{G_2}} \epsilon(\omega) = G_1 \frac{1 + i\omega \tau_\epsilon}{1 + i\omega \tau_\sigma} \epsilon(\omega) \quad (3.53)$$

where the two time scales $\tau_\sigma = \eta/G_2$ and $\tau_\epsilon = \eta(G_1 + G_2)/(G_1 G_2)$ describe the relaxation of stress and strain, respectively.

From Eq. (3.53), we find the complex modulus as:

$$G^*(\omega) = G_1 \frac{1 + i\omega \tau_\epsilon}{1 + i\omega \tau_\sigma} \quad (3.54)$$

and the real part is

$$G'(\omega) = G_1 \frac{1 + \omega^2 \tau_\sigma \tau_\epsilon}{1 + \omega^2 \tau_\sigma^2} \quad (3.55)$$

For $\omega \ll \tau_\sigma^{-1}$, $G' \rightarrow G_1$ and for $\omega \gg \tau_\sigma^{-1}$, $G' \rightarrow G_1 + G_2$.

3.8 Stochastic forces and Brownian motion

3.9 Brownian motion

In soft materials, the thermal energy $k_B T$ is sufficient to induce deformations and motion. The simplest example is that of a particle undergoing random motion suspended in a solution. Its motion is induced by the multiple collisions of the solvent molecules with the particle, giving rise to Brownian motion³.

The characteristic lengthscales of structures that are able to undergo thermal motion are on the nano to micro scale. For larger particles, thermal energy is typically not enough to induce motion. For instance, let us consider a suspension of solid particles of one phase within an immiscible continuous liquid phase. In this scenario, the particles are only able to undergo Brownian motion if the thermal energy is enough to overcome the gravitational acceleration g . Very large particles will tend to sediment and will not move under thermal forces. The probability of finding a particle with mass m and radius r at a height h within a vessel is given by the Boltzmann factor:

$$P(h) = P_0 \exp\left(-\frac{m_b gh}{k_B T}\right) \quad (3.56)$$

where $m_b = 4\pi r^3(\rho - \rho_s)/3$ is the buoyant mass of the particle, and ρ and ρ_s are the densities of the particle and the solvent, respectively. The average height $\langle h \rangle = \int h P(h) dh / (\int P(h) dh) = k_B T / (m_b g)$. If $\langle h \rangle < r$, the particles have sedimented to the bottom of the container. As such, the condition for the particles to be suspended is $\langle h \rangle > r$ or $k_B T / (m_b g) > r$ and $3k_B T / [4\pi r^4(\rho - \rho_s)] > 1$. For particles with a density difference of 1g/cm^3 , this condition implies $r < 1.3\text{ }\mu\text{m}$, at room temperature, i.e. a micron sized object.

³The botanist Robert Brown observed in 1828 that small micron scale pollen grains suspended are constantly in motion. He also observed similar behaviour for non-biological particles, showing that the origin of the motion was physical in nature. In 1905 Einstein showed that this motion originated from the particle being moved by collisions with individual water molecules. This molecular explanation of Brownian motion led to some of the first experimentally testable predictions of the atomic and molecular nature of matter.

3.10 Langevin equation

For a particle suspended in a solvent and undergoing motion through molecular collisions from the solvent, there are fast degrees of freedom associated with the motion of the solvent, and slower degrees of freedom associated with the overall motion of the particle. The slow dynamics of the particle is described by Newton's equation with viscous drag

$$m \frac{d\vec{v}}{dt} = -\gamma \vec{v}, \quad (3.57)$$

where $\vec{v}(t)$ is the velocity of the particle at time t , m is its mass, γ is the drag (or damping) coefficient. If we approximate the particle as a spherical object with radius r , then from Eq. (2.67) $\gamma = 6\pi\eta r$ where η is the viscosity of the solvent.

To describe the effect of the solvent, we note that over two successive time intervals τ , which are longer than the inverse of the characteristic of rate of collisions from the solvent $\tau^{-1} \sim 10^{13} \text{ s}^{-1}$, the motion of the particle is uncorrelated between the two successive time steps. Over such time scales, we can therefore describe the motion the particle with Newton's laws (3.57), but with an additional random force field $\xi(t)$ which describes the molecular collisions:

$$m \frac{d\vec{v}}{dt} = -\gamma \vec{v} + \vec{\xi}(t) \quad (3.58)$$

This is the Langevin equation, which was historically one of the first examples of a stochastic differential equation. Indeed, $\vec{\xi}(t)$ is a random variable, and for each realisation of ξ , there is a different trajectory $\vec{v}(t)$; as such, the physically interesting quantities will be averages $\langle \cdot \rangle$ over different realizations of the random process $\xi(t)$.

3.10.1 White noise

In order to describe the physics predicted by the stochastic differential equation (3.58), we need to specify the statistical properties of the noise term $\vec{\xi}(t)$. In an isotropic fluid, molecular collisions with the solvent do not have a preferential direction. Thus, we have $\langle \vec{\xi}(t) \rangle = 0$. Moreover, due to the random uncorrelated nature of the noise force field, $\vec{\xi}(t)$ and $\vec{\xi}(t')$ must be uncorrelated when $t \neq t'$, i.e. $\langle \vec{\xi}(t) \cdot \vec{\xi}(t') \rangle = \langle \vec{\xi}(t) \rangle \langle \vec{\xi}(t') \rangle = 0$ for $t \neq t'$. The properties of $\vec{\xi}$ can therefore be summarised as:

$$\langle \vec{\xi}(t) \rangle = 0 \quad (3.59)$$

$$\langle \vec{\xi}(t) \cdot \vec{\xi}(t') \rangle = c \delta(t - t') \quad (3.60)$$

This is the definition of white noise. The value of the constant c will be discussed below.

3.10.2 Solution of the Langevin equation and the fluctuation-dissipation theorem

How can we solve the stochastic differential equation (3.58)? A simple strategy for solving linear stochastic differential equations such as (3.58) consists in re-writing the process $\vec{v}(t)$ as $\vec{v}(t) = \vec{w}(t)e^{-\frac{\gamma}{m}t}$. The transformed process $\vec{w}(t)$ satisfies the simpler stochastic differential equation

$$\frac{d\vec{w}}{dt} = \frac{\vec{\xi}(t)}{m} e^{\frac{\gamma}{m}t}. \quad (3.61)$$

The solution is thus

$$\vec{w}(t) = \vec{v}_0 + \int_0^t \frac{\vec{\xi}(t')}{m} e^{\frac{\gamma}{m}t'} dt'. \quad (3.62)$$

Note that the integral in this equation is a stochastic integral, i.e. it takes a different value for each realization of the stochastic process $\vec{\xi}(t)$. Finally, transforming back to the original process $\vec{v}(t)$, we find that the Langevin equation has the formal solution:

$$\vec{v}(t) = \vec{v}_0 e^{-\frac{\gamma}{m}t} + \int_0^t e^{-\frac{\gamma}{m}(t-t')} \frac{\vec{\xi}(t')}{m} dt'. \quad (3.63)$$

This is still a stochastic equation, and we thus examine the averages over different realisations of $\vec{\xi}$. Since $\langle \vec{\xi}(t) \rangle = 0$, we must have

$$\langle \vec{v}(t) \rangle = \vec{v}_0 e^{-\frac{\gamma}{m}t} + \int_0^t e^{-\frac{\gamma}{m}(t-t')} \underbrace{\frac{\langle \vec{\xi}(t') \rangle}{m}}_{=0} dt' = \vec{v}_0 e^{-\frac{\gamma}{m}t}. \quad (3.64)$$

Thus, $\langle \vec{v}(t) \rangle$ corresponds to the solution of the deterministic Newton equation (3.57). We next evaluate the mean square velocity $\langle \vec{v}(t)^2 \rangle$. To do this, we use the relationship $\langle \vec{\xi}(t) \cdot \vec{\xi}(t') \rangle = c \delta(t - t')$ and find

$$\begin{aligned} \langle \vec{v}(t) \cdot \vec{v}(t) \rangle &= \vec{v}_0^2 e^{-2\frac{\gamma}{m}t} + \frac{2}{m} \int_0^t e^{-\frac{\gamma}{m}(2t-t')} \vec{v}_0 \cdot \underbrace{\langle \vec{\xi}(t') \rangle}_{=0} dt' \\ &\quad + \frac{1}{m^2} \int_0^t dt' \int_0^t dt'' e^{-\frac{\gamma}{m}(2t-t'-t'')} \underbrace{\langle \vec{\xi}(t') \cdot \vec{\xi}(t'') \rangle}_{=c \delta(t'-t'')} \\ &= \vec{v}_0^2 e^{-2\frac{\gamma}{m}t} + \frac{c}{2m\gamma} \left(1 - e^{-2\frac{\gamma}{m}t} \right). \end{aligned} \quad (3.65)$$

Note that the solution has a characteristic time scale m/γ , which describes the time of relaxation of the initial condition. In other words, for times t much larger

than m/γ , the system has forgotten about its initial state. In this long time limit, $t \rightarrow \infty$, we find therefore

$$\langle \vec{v}(t)^2 \rangle = \frac{c}{2m\gamma}. \quad (3.66)$$

The equipartition theorem fixes the $t \rightarrow \infty$ value of $\langle \vec{v}^2 \rangle \rightarrow 3k_B T/m$ ($k_B T/2$ per degree of freedom). This constraint therefore determines the value of the constant in Eq. (3.60) $c = 6\gamma k_B T$ and thus

$$\langle \vec{\xi}(t) \cdot \vec{\xi}(t') \rangle = 6k_B T \gamma \delta(t - t') \quad (3.67)$$

This result is known as the fluctuation dissipation theorem; Eq. (3.67) relates the amplitude of the fluctuations of a particle induced by a random force to the dissipative drag γ that the same particle experiences when it is actively moved through a fluid.

3.10.3 Mean square displacement and the diffusion equation

We can compute explicitly the mean square displacement of the particle as a function of time by integrating Eq. (3.63) to give

$$\vec{x}(t) = \vec{v}_0 \frac{m}{\gamma} \left(1 - e^{-\frac{\gamma}{m}t}\right) + \int_0^t dt' \int_0^{t'} dt'' e^{-\frac{\gamma}{m}(t'-t'')} \frac{\vec{\xi}(t'')}{m} \quad (3.68)$$

where we have used the initial condition $\vec{x}(t = 0) = 0$. As expected, for long times, $\vec{x}/t \rightarrow 0$ and the random forces don't result in any overall drift. However, the mean square displacement $\langle \vec{x}^2 \rangle$ increases as the particle explores an increasing volume though random motion as a function of time. This effect can be quantified by taking the square of the integral on both sides of Eq. (3.63), averaging over the random force field ξ and then using the fluctuation-dissipation theorem Eq. (3.67) to evaluate the averages $\langle \xi^2 \rangle$ to give

$$\langle \vec{x}(t)^2 \rangle = \frac{m^2 \vec{v}_0^2}{\gamma^2} \left(1 - e^{-\frac{\gamma}{m}t}\right)^2 + \frac{3mk_B T}{\gamma^2} \left(2\frac{\gamma}{m}t - 3 + 4e^{-\frac{\gamma}{m}t} - e^{-2\frac{\gamma}{m}t}\right) \quad (3.69)$$

For long times $t \gg m/\gamma$ we find

$$\langle \vec{x}(t)^2 \rangle = \underbrace{\frac{6k_B T}{\gamma} t}_{:=6D} \quad (3.70)$$

a value which increases linearly with time, the characteristic of diffusion and random walks. We can write the right hand side of Eq. (3.70) as a function of a diffusion coefficient D by identifying

$$D = \frac{k_B T}{\gamma} \quad (3.71)$$

Eq. (3.71) is known as the Einstein relation. Using the result for the stokes drag for a sphere from Eq. (2.67) in Eq. (3.71) yields the Stokes-Einstein relation

$$D = \frac{k_B T}{6\pi\eta r} \quad (3.72)$$

In particular this result implies that the time scale τ_r for a colloidal particle to diffuse its own diameter is

$$\tau_r = r^2/D = \frac{6\pi\eta r^3}{k_B T} \quad (3.73)$$

We can connect this result to the diffusion equation by considering the probability distribution of a particle undergoing a random walk. We first consider a discrete 1D scheme of random uncorrelated steps with transition probability $w_{\pm} = 1/2$. The probability $\mathbb{P}(k, N+1)$ for the particle to be on site k after $N+1$ steps is

$$\mathbb{P}(k, N+1) = w_+ \mathbb{P}(k-1, N) + w_- \mathbb{P}(k+1, N) \quad (3.74)$$

and depends on the probability distribution at the previous step $\mathbb{P}(\cdot, N)$ but not on any of the previous steps. A process of this type where the future probabilities are determined by its most recent values is known as a Markov process. We can rewrite Eq. (3.74) as a difference between subsequent steps by subtracting from both sides of the equation $\mathbb{P}(k, N)$ and using the fact that $w_{\pm} = 1/2$

$$\mathbb{P}(k, N+1) - \mathbb{P}(k, N) = 1/2 \mathbb{P}(k-1, N) + 1/2 \mathbb{P}(k+1, N) - \mathbb{P}(k, N) \quad (3.75)$$

Dividing by a time scale Δt for taking a step gives

$$\frac{\mathbb{P}(k, t + \Delta t) - \mathbb{P}(k, t)}{\Delta t} = \frac{1}{2\Delta t} [\mathbb{P}(k-1, N) + \mathbb{P}(k+1, N) - 2\mathbb{P}(k, N)] \quad (3.76)$$

Finally, we denote the step size with a and hence the change in the position is $\Delta x = a\Delta k$ and Eq. (3.75) reads

$$\frac{\mathbb{P}(k, t + \Delta t) - \mathbb{P}(k, t)}{\Delta t} = \underbrace{\frac{a^2}{2\Delta t}}_{=D} \frac{\mathbb{P}(x - \Delta x, t) + \mathbb{P}(x + \Delta x, t) - 2\mathbb{P}(x, t)}{\Delta x^2} \quad (3.77)$$

The left hand side of this equation is a discrete first derivative with respect to t and the right hand side is a discrete second derivative with respect to x and hence in the continuum limit we have the partial differential equation

$$\frac{\partial \mathbb{P}(x, t)}{\partial t} = D \frac{\partial^2 \mathbb{P}(x, t)}{\partial x^2} \quad (3.78)$$

The probability $\mathbb{P}(t, x)$ of finding a particle at a given position x is proportional to the concentration $c(t, x)$ of (non-interacting) particles and hence Eq. (3.78) can be written in terms of the concentration to yield the diffusion equation

$$\partial_t c(x, t) = D \partial_x^2 c(x, t) \quad (3.79)$$

This equation has as solutions $c(x, t) = c_0 / \sqrt{4\pi Dt} e^{-\frac{x^2}{4Dt}}$ which satisfy $\sigma^2 = \langle x^2 \rangle = 2Dt$ (6Dt in 3 dimensions) in agreement with Eq. (3.70) and in 3D we have

$$\partial_t c(\vec{x}, t) = D \vec{\nabla}^2 c(\vec{x}, t) \quad (3.80)$$

3.10.4 Particle flux

Since the number of particles is conserved, the continuity equation

$$\partial_t c(\vec{x}, t) = -\vec{\nabla} \cdot \vec{J}(\vec{x}, t) \quad (3.81)$$

applies, where \vec{J} is the particle flux current density. To recover Eq. (3.80), $J(\vec{x}, t)$ has to be given by

$$\vec{J}(\vec{x}, t) = -D \vec{\nabla} c(\vec{x}, t) \quad (3.82)$$

which is Fick's law and has the interpretation that the particle flux is from regions of high concentration towards regions of low concentration.

3.10.5 Diffusion controlled processes

Diffusion may limit and often controls a range of different processes that take place in solution, such as the growth of regions of different composition in phase separation, including the growth of crystals and colloidal aggregates.

As an example, we consider spherically symmetric growth at steady state $\partial_t c = 0$. This situation corresponds for instance to particles or molecules attaching together when they meet a reference particle of radius a located at $r = 0$ and thus form clusters. For this situation, Eq. (3.80) reads

$$0 = \frac{1}{r^2} \frac{d}{dr} \left(r^2 \frac{dc}{dr} \right) = \frac{1}{r} \frac{d^2}{dr^2} [rc(r)] \quad (3.83)$$

with the boundary condition $c(r = a) = 0$ since the particles attach upon contact with the reference particle at $r = a$ and thus the concentration of free particles in this location vanishes. Moreover, we assume that the concentration of particles at infinity is constant $c(r \rightarrow \infty) \rightarrow c_\infty$. The solution to Eq. (3.83) is

$$c(r) = c_\infty \left(1 - \frac{a}{r} \right) \quad (3.84)$$

For this situation, the particle current density Eq. (3.82) is purely radial and has the form

$$J(r) = -D \frac{dc}{dr} = -\frac{Dc_\infty a}{r^2} \quad (3.85)$$

In particular, the $1/r^2$ dependence implies that the total flux of particles crossing any spherical shell is constant and independent of the distance from the central particle. We evaluate the total flux at $r = a$ to yield

$$\frac{dN}{dt} = -J(a)4\pi a^2 = 4\pi Dc_\infty a \quad (3.86)$$

For a growing cluster the number of particles N in the aggregate scales with the volume $\sim a^3$ and hence

$$\frac{dN(a)}{dt} \sim \frac{da^3}{dt} = 3a^2 \frac{da}{dt} \sim 4\pi Dc_\infty a \quad (3.87)$$

Hence the cluster grows as a function of time as

$$a(t) \sim t^{1/2} \quad (3.88)$$

In a real system, once a significant number of particles have aggregated into clusters, the assumption that c_∞ is a constant is no longer accurate and the growth slows. Finally, once most of the particles have been used up to form clusters, further growth proceeds through the growth of larger clusters at the expense of the shrinkage of smaller clusters (Ostwald ripening).

If instead of considering aggregation of particles, we apply this analysis to the reaction between two species in solution, the result Eq. (3.86) can be written as a rate law $dN/dt = kc$ with a rate constant

$$k = 4\pi Da \quad (3.89)$$

This is the fastest process that can happen in solution since every encounter between reaction partners leads to a reaction. This rate is known as the Smoluchowski rate.

3.10.6 Velocity relaxation

We can compute from Eq. (3.63) the autocorrelation of the velocity

$$\langle \vec{v}(0) \cdot \vec{v}(t) \rangle = \vec{v}_0^2 e^{-\frac{\gamma}{m}t} \quad (3.90)$$

This results shows that the memory of the original velocity \vec{v}_0 is lost over a time scale

$$\tau_v := \frac{m}{\gamma} \quad (3.91)$$

which is the velocity relaxation time and has a value of the order of the order of $10^{-10} - 10^{-8}$ s for particles in the size range 10nm to 1μm in water.

3.10.7 Overdamped limit

If observations are made on time scales which are much larger than the velocity relaxation time $\tau_v = m/\gamma$, then the particle effectively has no acceleration or inertia. The Langevin equation Eq. (3.58) therefore becomes:

$$0 = -\gamma \vec{v} + \vec{\xi}(t) \quad (3.92)$$

or which is known as the Smoluchowski or overdamped limit. Eq. (3.92) can be integrated to yield an expression for the particle position in the overdamped limit

$$\vec{x}(t) = \vec{x}_0 + \frac{1}{\gamma} \int_0^t \vec{\xi}(t') dt' \quad (3.93)$$

where x_0 is the initial position of the particle.

3.10.8 Confined Brownian motion

We next consider how thermal noise affects a system with a potential energy, using the example of a particle in a harmonic potential $V(\vec{x}) = k\vec{x}^2/2$. To do so, we consider first the deterministic equation of motion in the overdamped regime

$$\gamma \frac{d\vec{x}}{dt} = -\vec{\nabla}V(x) = -k\vec{x}(t). \quad (3.94)$$

To describe the stochastic dynamics associated with thermal noise, we extend Eq. (3.94) to a stochastic differential equation by adding a random white noise term $\vec{\xi}$ with $\langle \vec{\xi}(t) \rangle = 0$ and $\langle \vec{\xi}(t)\vec{\xi}(t') \rangle = 6k_B T \gamma \delta(t - t')$. The overdamped Langevin Equation for times $t \gg m/\gamma$ thus reads

$$\gamma \frac{d\vec{x}}{dt} = -k\vec{x}(t) + \vec{\xi}(t). \quad (3.95)$$

The formal solution to this equation with the initial condition $\vec{x}(t = 0) = \vec{x}_0$ is obtained using the same approach as in Section 3.10.2

$$\vec{x}(t) = \vec{x}_0 e^{-\frac{k}{\gamma}t} + \int_0^t e^{\frac{k}{\gamma}(t-t')} \frac{1}{\gamma} \vec{\xi}(t') dt' \quad (3.96)$$

As expected, $\langle \vec{x}(t) \rangle = \vec{x}_0 e^{-\frac{k}{\gamma}t} \rightarrow 0$, when $t \rightarrow \infty$ and the mean square deviation can be computed as in Section 3.10.3 to yield

$$\langle \vec{x}(t)^2 \rangle = \vec{x}_0^2 e^{-2\frac{k}{\gamma}t} + \frac{3k_B T}{k} \left(1 - e^{-2\frac{k}{\gamma}t} \right). \quad (3.97)$$

There is a new timescale $\tau_x := \gamma/k$, which governs the rate of the loss of the memory of the initial position and how rapidly the particle adopts the equilibrium distribution. For times $t \gg \tau_x$ we have

$$\langle \vec{x}(t)^2 \rangle = \frac{3k_B T}{k} \quad (3.98)$$

as expected from the equipartition theorem.

3.10.9 Diffusion in external potentials

We now extend the result from 3.10.3 to the presence of potentials $U(x)$ that exert deterministic external forces $\vec{F} = -\vec{\nabla}U$ on the particle during in addition to the stochastic force $\vec{\xi}(t)$. For this situation in Eq. (3.74) the transition probabilities in both directions are no longer the same as they are for a random walk in the absence of an external potential, but rather there is an average drift

$$w_{\pm} = \frac{1}{2} \pm \epsilon \quad (3.99)$$

and Eq. (3.75) becomes

$$\mathbb{P}(k, N+1) - \mathbb{P}(k, N) = w_- \mathbb{P}(k-1, N) + w_+ \mathbb{P}(k+1, N) - \underbrace{[w_- + w_+]}_{=1} \mathbb{P}(k, N) \quad (3.100)$$

Similarly as before, we can divide both sides of the equation by a small time increment Δt and take the continuum limit to obtain

$$\partial_t \mathbb{P}(x, t) = \underbrace{\frac{a^2}{2\Delta t}}_D \partial_x^2 \mathbb{P}(x, t) - \underbrace{\frac{2a\epsilon}{\Delta t}}_{=v_d=F/\gamma} \partial_x \mathbb{P}(x, t) \quad (3.101)$$

where v_d is the drift velocity which was assumed to be constant in the above derivation. More generally, this result suggests that diffusion in a potential energy $U(\vec{x})$ can be written as a modified diffusion equation

$$\partial_t \mathbb{P}(\vec{x}, t) = \vec{\nabla} \cdot \left[D \vec{\nabla} \mathbb{P}(\vec{x}, t) + \frac{1}{\gamma} \vec{\nabla} U(\vec{x}) \mathbb{P}(\vec{x}, t) \right] \quad (3.102)$$

or for the concentration

$$\partial_t c(\vec{x}, t) = \vec{\nabla} \cdot \left[D \vec{\nabla} c(\vec{x}, t) + \frac{1}{\gamma} \vec{\nabla} U(\vec{x}) c(\vec{x}, t) \right] \quad (3.103)$$

which takes the form of a continuity equation $\partial_t c = -\vec{\nabla} \cdot \vec{J}$ the right hand side of which represents the divergence of the particle current flux density

$$\vec{J}(\vec{x}) = -D\vec{\nabla}c(\vec{x}, t) - \frac{1}{\gamma}\vec{\nabla}U(\vec{x})c(\vec{x}, t) \quad (3.104)$$

This current can be seen to be composed of a contribution from drift down the potential gradient $\frac{1}{\gamma}\vec{\nabla}U(\vec{x})c(\vec{x}, t)$ and a diffusion contribution originating from the concentration gradient.

Thus the motion of a thermally excited particle subjected to a stochastic force can be described by two equivalent approaches: the Langevin equation Eq. (3.58) which describes the motion of an individual particle, and Eq. (3.102) which gives the time evolution of the probability density. The latter approach is known in the general case as the Fokker-Planck equation corresponding to a given Langevin equation; in the case of overdamped motion, the Fokker Planck equation is known as the Smoluchowski equation.

3.11 Escape over a potential barrier

A case of particular practical relevance is the escape of a system from a metastable local minimum through thermally activated motion. We consider a system in a metastable state at $x = A$ with energy $U(x = A) = 0$ separated by a barrier with height U^\ddagger from reaching its thermodynamic equilibrium at $x = B$ and wish to know the rate at which the system can escape this state and relax to the global minimum (Kramers problem). Using Eq. (3.71), the steady state probability current density can be written as

$$J = -D\partial_x\mathbb{P}(x) - \frac{\partial_x U(x)}{\gamma}\mathbb{P}(x) = -De^{-\beta U(x)}\partial_x [e^{\beta U(x)}\mathbb{P}(x)] \quad (3.105)$$

where $\beta = 1/(k_B T)$, and hence

$$Je^{\beta U(x)} = -D\partial_x [e^{\beta U(x)}\mathbb{P}(x)] \quad (3.106)$$

Rearranging and integrating both sides between $x = A$, the metastable minimum, and $x = B$, the global minimum yields

$$J \int_A^B e^{\beta U(x)}dx = -D [e^{\beta U(x)}\mathbb{P}(x)]_A^B \quad (3.107)$$

Here we assume steady state so that $\dot{\rho} = \partial_x J = 0$. If the potential well at $x = B$ is deep, then the right hand side can be approximated as $-D [e^{\beta U(x)}\mathbb{P}(x)]_A^B \approx$

$-D\mathbb{P}(A)$. For carrying out the integral, we note that the major contribution will arise from the point where $U(x)$ is largest, i.e. in the vicinity of the barrier. In this region, we expand the potential to second order to give $U(x) \approx U^\ddagger - \frac{1}{2}\kappa^\ddagger(x - x^\ddagger)^2$. We can then evaluate the integral as

$$J \int_A^B e^{\beta U(x)} dx \approx J e^{\beta U^\ddagger} \int_{-\infty}^{\infty} e^{-\beta \frac{1}{2}\kappa^\ddagger(x - x^\ddagger)^2} dx = J e^{\beta U^\ddagger} \sqrt{\frac{2\pi k_B T}{\kappa^\ddagger}} = D\mathbb{P}(A) \quad (3.108)$$

We have therefore found the steady-state flux from the metastable state A to the equilibrium at B as

$$J = D e^{-\beta U^\ddagger} \sqrt{\frac{\kappa^\ddagger}{2\pi k_B T}} \mathbb{P}(A) \quad (3.109)$$

The rate of escape $r = J/N_A$ is the ratio of this flux to the number of particles N_A in A which can be evaluated at thermal equilibrium as

$$N_A = \int_A \mathbb{P}(A) e^{-\beta U(x)} dx \approx \mathbb{P}(A) \int_{-\infty}^{\infty} e^{-\beta \frac{1}{2}\kappa_A x^2} dx = \mathbb{P}(A) \sqrt{\frac{2\pi k_B T}{\kappa_A}} \quad (3.110)$$

Therefore the escape rate is

$$r = D \frac{\sqrt{\kappa_A \kappa^\ddagger}}{2\pi k_B T} e^{-\beta U^\ddagger} \quad (3.111)$$

This result shows that the escape rate is proportional to the Boltzmann factor of the barrier. This type of exponential behaviour was discovered empirically to apply for many chemical reactions by Arrhenius.

3.11.1 Reaction controlled processes

When the interaction potential between particles is purely attractive, their aggregation is only limited by diffusion. This is the scenario discussed in 3.10.5. However, when the interaction potential $U(r)$ exhibits an intermediate repulsive barrier that the particles (or reactants in a chemical reaction) have to cross, the aggregation is slowed down. Qualitatively, this effect originates from the fact that multiple barrier crossing attempts are required for a successful reactive event. To evaluate quantitatively the rate of such processes, we extend the treatment in 3.10.5 from pure diffusion to the diffusion in the presence of a potential corresponding to the Smoluchowski equation. From Eq. (3.71) and (3.104), the radial current is given as

$$J(r) = -D \left(\frac{d}{dr} \frac{U(r)}{k_B T} + \frac{d}{dr} \right) c(r) \quad (3.112)$$

At steady state the divergence of the current vanishes, $J(r) \sim r^{-2}$ and the flux of particles $\dot{N} = 4\pi r^2 J(r)$ is the same across any spherical shell. We introduce a field $\Phi(r)$ by setting $c(r) = \Phi(r)e^{-\beta U(r)}$ which transforms Eq. (3.112) into the simple form

$$J(r) = \frac{\dot{N}}{4\pi r^2} = -D \left(\frac{d}{dr} \frac{U(r)}{k_B T} + \frac{d}{dr} \right) \Phi(r) e^{-\beta U(r)} = D e^{-\beta U(r)} \frac{d\Phi(r)}{dr} \quad (3.113)$$

Integrating both sides of the equation leads to

$$\underbrace{\Phi(\infty)}_{=c_\infty} - \underbrace{\Phi(a)}_{c(a)e^{\beta U(a)}} = \frac{\dot{N}}{4\pi D} \int_a^\infty \frac{e^{\beta U(r)}}{r^2} dr \quad (3.114)$$

The remaining integral has units of length⁻¹ and we define a lengthscale λ that characterises any barriers that may hinder inward diffusion

$$\lambda^{-1} := \int_a^\infty \frac{e^{\beta U(r)}}{r^2} dr \quad (3.115)$$

Similarly to the case treated earlier of pure diffusion, we introduce a rate constant k connecting the concentration c_∞ to the reaction rate

$$\dot{N} = kc_\infty \quad (3.116)$$

resulting in

$$c(a) = c_\infty e^{-\beta U(a)} \left(1 - \frac{k}{4\pi D \lambda} \right) \quad (3.117)$$

For purely diffusion controlled processes $U(a) = 0$, $\lambda = a$ and we recover the result $c(a) = 0$ from 3.10.5. However, when $U(a) > 0$, $c(a) > 0$. The concentration at the surface $c(a)$ governs the reactive step, and we can write $\dot{N} = kc_\infty = k^* c(a)$ with a rate constant k^* . We can now solve for the overall rate constant k to yield

$$k = \frac{4\pi D \lambda}{1 + \frac{4\pi D \lambda}{k^* e^{-\beta U(a)}}} = \frac{k_{\text{diff}} k_{\text{reac}}}{k_{\text{diff}} + k_{\text{reac}}} \quad (3.118)$$

The factor $k_{\text{diff}} := 4\pi D \lambda$ is the Smoluchowski rate for diffusion coontrolled reactions and $k_{\text{reac}} := k^* e^{-\beta U(a)}$ controls the processes on the surface of the reference particle.

When the rate of the surface processes is large, $k_{\text{reac}} \gg k_{\text{diff}}$ we recover the rate for diffusion limited reactions $k = k_{\text{diff}}$ while in the opposite limit the reaction does not depend on the diffusion coefficient anymore and $k = k_{\text{reac}}$. The latter case is known as a reaction controlled process.

3.11.2 Microrheology

Rheology (from the Greek “rhéō” : to flow) is the study of the deformation and flow properties of matter in response to external stresses. At the beginning of this chapter, we have seen that, depending on how force is applied, materials can behave more like liquids or like a spring. In the first case, viscous forces dominate the response of the system; in the second case, elastic forces dominate the system behavior. For this reason, rheology generally describes materials in terms of combined viscous and elastic properties.

Microrheology is a technique to measure the viscoelastic properties of a material by monitoring the trajectories of an ensemble of small and inert tracer particles embedded in it. There are two main ways of performing microrheological measurements: passive and active microrheology. In passive microrheology, the trajectories of the particles are measured under the effect of thermal fluctuations alone. In active rheology, an external force, generated for instance using magnetic fields or optical tweezers, is used to generate the random motion of particles. The rheological properties of the system are then extracted from the mean-square displacement $\langle \vec{x}(t)^2 \rangle$ which is obtained by averaging the trajectories of a sufficient number of tracer particles. An important advantage of microrheology compared to conventional rheological measurements (e.g. with a rheometer), is that microrheology can be used to measure viscoelastic properties of materials in very small volumes. For this reason, microrheology is particularly useful for biophysical studies e.g. in cells.

Determination of viscous properties

If the tracer particle is embedded in a purely viscous fluid of viscosity η , then it performs a Brownian motion due to random collisions with the solvent. In Section 3.10.3, we have seen that the mean-square displacement $\langle \vec{x}(t)^2 \rangle$ increases linearly with time

$$\langle \vec{x}(t)^2 \rangle = 6Dt = \frac{k_B T}{\pi \eta r} t. \quad (3.119)$$

Hence, if the size of the tracer particle r and the temperature T are known, from a measurement of $\langle \vec{x}(t)^2 \rangle$ over time it is possible to determine the viscosity of the fluid.

Determination of elastic properties

If the tracer particle is placed in a purely elastic medium with spring constant k , rather than a viscous fluid, then, as discussed in Section 3.10.8, the particle will

perform a motion characterized by a constant mean-square displacement

$$\langle \vec{x}(t)^2 \rangle = \frac{3k_B T}{k}. \quad (3.120)$$

Thus, over time each tracer particle has forgotten about its initial state and has $3k_B T/2$ of energy ($k_B T/2$ per degree of freedom).

Generalized Einstein relation

Many materials are more complex than a simple viscous fluid or a purely elastic material and microrheological measurements of tracer particle trajectories will show more complex time dependencies for the mean-square displacement of the form

$$\langle \vec{x}(t)^2 \rangle \sim t^\alpha. \quad (3.121)$$

α is called the diffusive exponent and the associated movement is known as “anomalous diffusion”. The case of $\alpha = 1$ corresponds to pure diffusion and $\alpha = 0$ corresponds to the situation when tracer particles are locally trapped in a solid. Certain systems may exhibit diffusive exponents $\alpha > 1$ corresponding to super-diffusion, while others can exhibit diffusive exponents $0 < \alpha < 1$ corresponding to sub-diffusion. This behaviour occurs when the viscosity of the fluid is not constant but rather is a function of time. In the following, we discuss how the viscoelastic behaviour of materials with time-dependent viscosity can be probed by monitoring the diffusion of an inert tracer particle in such systems. This can be achieved by means of a generalized Einstein relation.

The stochastic system dynamics can be described by means of a generalized Langevin equation

$$m \frac{d\vec{v}}{dt} = - \int_0^t \gamma(t-\tau) \vec{v}(\tau) d\tau + \vec{\xi}(t), \quad (3.122)$$

where $\vec{\xi}(t)$ is the random Brownian force and the integral term describes the damping of the fluid with where the time-dependent viscous damping coefficient $\gamma(t) = 6\pi R\eta(t)$ acts as a memory function and $\eta(t)$ is the (time-dependent) viscosity and R the hydrodynamic radius of the tracer particle. This generalized Langevin equation can be solved most conveniently by introducing the Laplace transform \mathcal{L}

$$\mathcal{L}[f] = \hat{f}(s) = \int_0^\infty f(t) e^{-st} dt. \quad (3.123)$$

Using the convolution theorem for the Laplace transform, i.e. that the Laplace transform of the convolution of two functions equals the product of the Laplace

transforms of the individual functions, we find that the generalized Langevin equation (3.122) reads in Laplace space as follows

$$ms\hat{\vec{v}}(s) - m\vec{v}(0) = -\hat{\gamma}(s)\hat{\vec{v}}(s) + \hat{\vec{\xi}}(s). \quad (3.124)$$

The main advantage of introducing the Laplace transform is that we have transformed the stochastic differential equation (3.122) into a simple algebraic equation for $\hat{\vec{v}}(s)$. Solving this equation for $\hat{\vec{v}}(s)$ yields

$$\hat{\vec{v}}(s) = \frac{\hat{\vec{\xi}}(s) + m\vec{v}(0)}{ms + \hat{\gamma}(s)}. \quad (3.125)$$

Next, we take the scalar product of this expression with $\vec{v}(0)$ and perform the ensemble average $\langle \cdot \cdot \cdot \rangle$. Using $\langle \hat{\vec{\xi}}(s)\vec{v}(0) \rangle = 0$, we find

$$\langle \hat{\vec{v}}(s)\vec{v}(0) \rangle = \frac{m\langle \vec{v}(0)^2 \rangle}{ms + \hat{\gamma}(s)}. \quad (3.126)$$

Finally, the equipartition theorem requires $m\langle \vec{v}(0)^2 \rangle / 2 = 3k_B T / 2$, and so we arrive at the expression

$$\langle \hat{\vec{v}}(s)\vec{v}(0) \rangle = \frac{3k_B T}{ms + \hat{\gamma}(s)}. \quad (3.127)$$

We next relate the velocity correlation function $\langle \hat{\vec{v}}(s)\vec{v}(0) \rangle$ to the mean-square displacement. To this effect, we note that

$$\vec{x}(t)^2 = \int_0^t dt_1 \int_0^t dt_2 \vec{v}(t_1) \vec{v}(t_2) = 2 \int_0^t dt_1 \int_0^{t_1} dt_2 \vec{v}(t_1) \vec{v}(t_2) \quad (3.128)$$

$$= 2 \int_0^t dt_1 \int_0^{t_1} d\tau \vec{v}(t_1) \vec{v}(t_1 - \tau) \quad (3.129)$$

with the integration variable $\tau = t_1 - t_2$. Taking the average on both sides of the equation yields:

$$\langle \vec{x}(t)^2 \rangle = 2 \int_0^t dt_1 \int_0^{t_1} d\tau \langle \vec{v}(t_1) \vec{v}(t_1 - \tau) \rangle = 2 \int_0^t dt_1 \int_0^{t_1} d\tau \langle \vec{v}(\tau) \vec{v}(0) \rangle \quad (3.130)$$

Differentiating both sides of the equation twice yields:

$$\frac{d^2}{dt^2} \langle \vec{x}(t)^2 \rangle = 2 \langle \vec{v}(0) \vec{v}(t) \rangle \quad (3.131)$$

Recalling the form of the Laplace transform of a second derivative

$$\mathcal{L} \left[\frac{d^2 f(t)}{dt^2} \right] = s^2 \mathcal{L}[f] - sf(0) - \frac{d}{dt} f(0) \quad (3.132)$$

and using $f(t) = \langle x(t)^2 \rangle$ then yields:

$$\mathcal{L} \left[\frac{d^2}{dt^2} \langle x(t)^2 \rangle \right] = s^2 \mathcal{L}[\langle \vec{x}(t)^2 \rangle] - s \underbrace{\langle \vec{x}^2(0) \rangle}_{=0} - \underbrace{\frac{d}{dt} \langle \vec{x}(t)^2 \rangle|_{t=0}}_{=\langle \vec{x}(0) \vec{v}(0) \rangle = 0} \quad (3.133)$$

Finally, using Eqs. (3.127) and (3.131) yields:

$$\mathcal{L} [\langle \vec{x}(t)^2 \rangle] = \frac{6k_B T}{s^2 [ms + \hat{\gamma}(s)]}. \quad (3.134)$$

Except at very high frequencies, the inertial term ms is negligible compared to the memory term $\hat{\gamma}(s)$, so that Eq. (3.134) can be simplified to

$$\mathcal{L} [\langle \vec{x}(t)^2 \rangle] = \frac{6k_B T}{s^2 \hat{\gamma}(s)}. \quad (3.135)$$

Equation (3.135) is known as generalized Einstein relation and is a key result for applications of microrheology since it provides a means of determining the Laplace transform of the time-dependent viscous damping coefficient $\gamma(t)$ from the Laplace transform of measured mean square displacements of tracer particles.

Chapter 4

Polymers

4.1 Definitions and examples

Polymers are large molecules (macromolecules) having dimensions on the nanoscale. They consist of linear or branched chains of monomer units linked together most commonly through covalent bonds. Polymers represent a major class of soft materials which exhibit viscoelasticity. Moreover, polymers are technologically crucial materials, with the worldwide production of polyethylene exceeding 80 million tonnes per year, and polymers underpinning technological applications ranging from medical devices to aircraft construction. Polymer physics is also a key element in biological physics and is the tool to describe a wide range of molecular phenomena in nature, including protein folding, misfolding, aggregation.

Homopolymers consist of N identical monomers. The number of monomer units in a polymer is its degree of polymerisation N . Therefore the molar mass M of a polymer is given by its degree of polymerisation and the molar mass of the monomer:

$$M = NM_{\text{mono}} \quad (4.1)$$

Heteropolymers consist of chemically distinct monomers assembled into a single macromolecule. A special case of the latter class is given by block-copolymers, which are composed of two or more covalently linked homopolymer chains.

A number of key biological macromolecules are polymers. Examples include proteins which form the machinery of the cell, nucleic acids which store genetic information, lipids which form membranes that delimit biological compartments and polysaccharides which are used extensively by plants as structural materials.

The nature of the chain chemistry is crucial for explaining certain features of the chains, in particular their chemical reactivity. However, many universal aspects of polymer behaviour emerge in the limit of $N \gg 1$ and we review a few key results in this chapter.

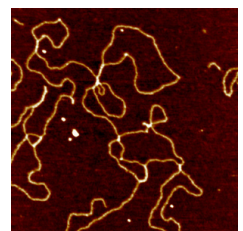


Figure 4.1: AFM image of a polymer (DNA) on an atomically flat mica substrate (JPK instruments).

Common name	Repeating unit	Use
polyethylene polythene (IUPAC)	$\text{--CH}_2\text{--CH}_2\text{--}$	Rigid plastic
polyethylene glycol (PEG) polyethylene oxide (PEO) polyoxyethylene (POE)	$\text{H--CH}_2\text{--CH}_2\text{--O--CH}_2\text{--CH}_2\text{--OH}$	Inert biocompatible hydrophilic polymer, prevention of protein adsorption
polystyrene poly(1-phenylethene-1,2-diyil))	$\text{--CH}_2\text{--C}_6\text{H}_5\text{--}$	Thermoplastic
polydimethylsiloxane (PDMS)	$\text{H}_3\text{Si--CH}_2\text{--O--SiH}_2\text{--CH}_2\text{--O--SiH}_3$	Silicone oil, elastomer

Figure 4.2: Examples of common synthetic polymers

4.2 Polydispersity

Polymers can be synthesized by condensation reactions which release as by-products small molecules such as water or ethanol or by addition reactions, commonly free-radical addition. These processes produce polydisperse polymers with a distribution of N values. Natural biopolymers, including proteins and nucleic acids can be monodisperse and their synthesis exploits enzymatic catalysis to achieve a level of control which exceeds that of synthetic polymer chemistry.

The polydispersity of a sample is described by the molar mass distribution $n(M)$. The full length distribution is often challenging to determine experimentally, and average values are commonly introduced (which can be measured by various techniques): the number average

$$\langle M \rangle_n = \frac{\int Mn(M)dM}{\int n(M)dM} \quad (4.2)$$

and the mass average

$$\langle M \rangle_w = \frac{\int M^2 n(M)dM}{\int Mn(M)dM} \quad (4.3)$$

It is always the case that $\langle M \rangle_n \leq \langle M \rangle_w$, and $M_w/M_n = 1$ is satisfied only for fully monodisperse system which in practice is only achieved by biological systems. Special synthetic techniques can yield $M_w/M_n \sim 1.03$, and more commonly $M_w/M_n > 2$ for industrial polymers such as polyethylene.

4.3 The ideal chain

We first consider the conformation of polymer chains with no interactions between the monomer units that are distant along the polymer chain, even if the chain folds on itself and the monomers overlap in space. These types of chains are known as ideal chains. Despite its simplicity, the ideal chain is a useful model of many aspects of polymer behaviour. However, in a real polymer chain, the finite volume of the monomers, as well as either repulsive or attractive interactions between them modify this behaviour, and we will turn to this aspect in 4.9. Typically, at high temperature, the repulsive interactions dominate, and polymer chains tend to swell; by contrast at low temperatures, attractive interactions dominate, and chains can collapse. At a specific intermediate temperature (θ) temperature, these two opposing tendencies cancel, and even a real chain behaves to a good approximation like an ideal chain.

There are a number of specific models which describe the ideal chain. In all cases, when the chain is long enough, the ideal chain size, as measured by the average end-to-end distance between the beginning and the end of the polymer chain $\langle R^2 \rangle$ has a simple scaling form

$$\langle R^2 \rangle = \text{const } a^2 N \quad (4.4)$$

This is a consequence of the fact that if there are no interactions between polymer segments, the chain behaves like a random walk in space, with the polymer chain length taking the role of time.

4.4 Lattice polymer and freely jointed chain

We consider first a simple idealisation of a flexible polymer where the segments of the polymer are restricted to positions on a three dimensional cubic lattice. Although this model is very simple, the behaviour that emerges from the study of this system is consistent with that of realistic atomic polymers in a range of length scales; indeed although there are typically no lattice restrictions for structures of real polymers, the statistical properties of both lattice polymers and realistic atomistic models are in essence defined by the random nature of the orientation of adjacent segments within a polymer. We will see that this behaviour leads to Gaussian chain statistics which is a defining feature of the ideal chain.

The lattice model consists of a linear polymer of $N + 1$ segments labelled with the index i with $0 \leq i \leq N$ and with positions r_i . Therefore there are N bonds connecting the segments and we number these from 0 to $N - 1$. The bond vectors are given as:

$$\vec{u}_i = \vec{r}_{i+1} - \vec{r}_i \quad (4.5)$$

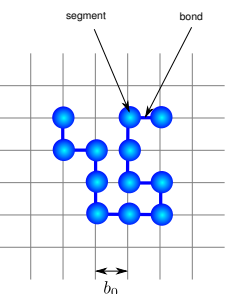


Figure 4.3: Definition of the parameters for the lattice model of polymers. Note the (initially potentially confusing) convention in polymer science of calling the vertices segments.

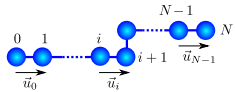


Figure 4.4: Conventional numbering of the segments from 1 to \$N\$ and the bonds from 1 to \$N - 1\$.

The bond vectors are assumed to be statistically independent of each other, implying that the position of the \$i + 1\$th segment can be any of the 6 nearest neighbour lattice sites of the segment \$i\$ in a cubic lattice. Note that in this description two segments can occupy the same lattice site! i.e. there is no excluded volume. This effect will be considered below.

The polymer can adopt many conformations and it is informative to consider average properties. One of the main measures of the spatial extension of a polymer chain is the distance between the first and last segments of the chain, given as the end-to-end vector \$\vec{R}\$:

$$\vec{R} = \vec{r}_N - \vec{r}_0 \quad (4.6)$$

and the root mean square of the end-to-end vector is known as the end-to-end distance \$\sqrt{\langle \vec{R}^2 \rangle}\$. Note that the average of \$\langle \vec{R} \rangle = 0\$ and is therefore not a suitable quantity to describe the size of a polymer. The end-to-end distance can be evaluated:

$$\langle \vec{R}^2 \rangle = \langle (\vec{r}_0 - \vec{r}_N)^2 \rangle = \langle (\vec{r}_1 - \vec{r}_0 + \vec{r}_2 - \vec{r}_1 + \cdots + \vec{r}_N - \vec{r}_{N-1})^2 \rangle \quad (4.7)$$

$$= \left\langle \left(\sum_{i=0}^{N-1} \vec{u}_i \right)^2 \right\rangle = \sum_{i=0}^{N-1} \langle \vec{u}_i^2 \rangle + \sum_{i=0}^{N-1} \sum_{j \neq i} \underbrace{\langle \vec{u}_i \cdot \vec{u}_j \rangle}_{=0} = Nb_0^2 \quad (4.8)$$

with \$b_0\$ the length of a bond. Therefore the average end-to-end distance of an ideal chain is proportional to the square root of the number of bonds:

$$\sqrt{\langle \vec{R}^2 \rangle} = N^{1/2} b_0 \quad (4.9)$$

The exponent \$\nu = 1/2\$ in Eq. (4.9) is known as the scaling exponent of the chain.

The analysis above required the bond length \$b_0\$ to be constant but is not reliant on the segments being on a lattice. If this constraint is relaxed and we consider a chain of segments of equal length where each segment can point in any direction in space, we also obtain the result Eq. (4.9). This latter model is known as the “freely jointed chain”.

Similarly, one can consider the root mean square of the distance of every segment of the chain to its centre of gravity; this is known as the radius of gyration \$R_G\$. One can show that for the ideal chain \$R_G^2 = \frac{1}{6} \langle \vec{R}^2 \rangle = Nb_0^2/6\$. Thus both measures of the size of the polymer possess the same scaling exponent.

4.5 Freely rotating chain

In many polymer systems, the bond angles between segments are fixed by the geometry of the chemical bonds that hold them together. However, the bonds can

commonly rotate¹. For such a fixed valence bond angle model, the end-to-end distance becomes

$$\langle R^2 \rangle = \sum_{i,j=0}^{N-1} \langle \vec{u}_i \cdot \vec{u}_j \rangle = \sum_{i=0}^{N-1} \langle \vec{u}_i^2 \rangle + 2 \sum_{i=0}^{N-1} \sum_{j=i+1}^{N-1} \langle \vec{u}_i \cdot \vec{u}_j \rangle \quad (4.10)$$

Contrarily to the lattice polymer or the freely jointed chain, the term $\langle \vec{u}_i \cdot \vec{u}_j \rangle$ doesn't vanish since the bond orientations are not uncorrelated due to the fixed bond angle θ between two adjacent segments. We can evaluate $\langle \vec{u}_i \cdot \vec{u}_j \rangle$ by first considering two adjacent segments \vec{u}_i and \vec{u}_{i+1} and write \vec{u}_i as a sum of the projection parallel and perpendicular to \vec{u}_{i+1} as

$$\vec{u}_i = \frac{\vec{u}_i \cdot \vec{u}_{i+1}}{b_0^2} \vec{u}_{i+1} + \vec{u}_{i,\perp} = \cos \theta \vec{u}_{i+1} + \vec{u}_{i,\perp} \quad (4.11)$$

Now for the correlation between segments separated by two links we have

$$\begin{aligned} \langle \vec{u}_i \cdot \vec{u}_{i+2} \rangle &= \underbrace{\langle \cos \theta \vec{u}_{i+1} \cdot \vec{u}_{i+2} \rangle}_{=\cos \theta \langle \vec{u}_{i+1} \cdot \vec{u}_{i+2} \rangle} + \underbrace{\langle \vec{u}_{i,\perp} \cdot \vec{u}_{i+2} \rangle}_{=0} = b_0^2 (\cos \theta)^2 \\ &= b_0^2 \cos \theta \end{aligned} \quad (4.12)$$

Due to the free rotation of the bond, the term $\langle \vec{u}_{i,\perp} \cdot \vec{u}_{i+2} \rangle$ vanishes. Recursion yields $\langle \vec{u}_i \cdot \vec{u}_{i+3} \rangle = b_0^2 (\cos \theta)^3$ and finally

$$\langle \vec{u}_i \cdot \vec{u}_j \rangle = b_0^2 (\cos \theta)^{|j-i|} \quad (4.13)$$

We can evaluate the end to end distance for $N \gg 1$ as

$$\begin{aligned} \langle R^2 \rangle &= Nb_0^2 + 2b_0^2 \sum_{i=0}^{N-1} \sum_{j=i+1}^{N-1} (\cos \theta)^{j-i} = b_0^2 \left[N + 2 \sum_{i=0}^N \underbrace{\sum_{k=1}^{N-1} (\cos \theta)^k}_{\approx \sum_{k=1}^{\infty} (\cos \theta)^k = \frac{\cos \theta}{1-\cos \theta}} \right] \\ &\quad (4.14) \end{aligned}$$

$$= Nb_0^2 \left[1 + 2 \frac{\cos \theta}{1 - \cos \theta} \right] = Nb_0^2 \frac{1 + \cos \theta}{1 - \cos \theta} \quad (4.15)$$

Hence we recover the scaling $R^2 \sim N$ of the ideal chain $\langle R^2 \rangle = \tilde{b}_0^2 N$ but with an effective segment length $\tilde{b}_0 = b_0 \sqrt{(1 + \cos \theta) / (1 - \cos \theta)}$

¹This is for instance the case for polyethylene, but also more complex polymers such as polypeptide chains. In most cases, the bonds are in reality not completely free to rotate, but are subject to a radial potential which depends on the specific chemical composition of the polymer. In the case of polypeptide chains, certain regions in the space of the torsion angles (the Ramachandran plot) are more readily populated, leading to the major secondary structure elements of proteins. We consider here, however, the model approximate case where all torsional angles are equally likely.

4.5.1 Bead spring model and Gaussian statistics

We can also describe an ideal chain as a series of $N+1$ beads $i = 0 \dots N$ connected linearly by springs with spring constant κ , leading to an energy of the form $U = \frac{\kappa}{2}(\vec{r}_{i+1} - \vec{r}_i)^2$. The partition function for such a system for a given fixed end-to-end distance is

$$Z(R) = \int d\vec{r}_1^3 \int d\vec{r}_2^3 \cdots \int d\vec{r}_{N-1}^3 e^{-\frac{\kappa}{2k_B T}(\vec{r}_0 - \vec{r}_1)^2 - \frac{\kappa}{2k_B T}(\vec{r}_1 - \vec{r}_2)^2 \cdots - \frac{\kappa}{2k_B T}(\vec{r}_{N-1} - \vec{r}_N)^2} \quad (4.16)$$

For Gaussian integrals $\int d\vec{r}_1 e^{-\alpha(\vec{r}_0 - \vec{r}_1)^2 - \alpha(\vec{r}_1 - \vec{r}_2)^2} = \sqrt{\pi/(2\alpha)}e^{-\alpha/2(\vec{r}_0 - \vec{r}_2)^2}$. As such, after $N - 1$ integrations, the partition function becomes

$$Z(R) = \text{const } e^{\frac{-\kappa}{2k_B T} \frac{(r_N - r_0)^2}{N}} = \text{const } e^{-\frac{\kappa R^2}{2k_B T N}} \quad (4.17)$$

The end-to-end distance can then be evaluated as

$$\langle R^2 \rangle = \frac{\int Z(R) R^2 d^3 R}{\int Z(R) d^3 R} = \underbrace{\frac{3k_B T}{\kappa}}_{=b_0^2} N \quad (4.18)$$

4.5.2 Segment correlation function in the ideal Gaussian chain

In section 4.5.1 we have shown that the end-to-end distance of the ideal chain follows Gaussian statistics

$$P(\vec{R}) = G(\vec{R}, N) = \left(\frac{3}{2\pi N b_0^2} \right)^{\frac{3}{2}} e^{-\frac{3(\vec{r}_0 - \vec{r}_N)^2}{2N b_0^2}} \quad (4.19)$$

and that this relationship is also true for two arbitrary segments within the polymer:

$$G(\vec{r}_m - \vec{r}_n, m - n) = \left(\frac{3}{2\pi |m - n| b_0^2} \right)^{\frac{3}{2}} e^{-\frac{3(\vec{r}_0 - \vec{r}_N)^2}{2|m - n| b_0^2}} \quad (4.20)$$

where $G(\vec{r}_m - \vec{r}_n, m - n)$ is the probability density for \vec{r}_n for a fixed \vec{r}_m , i.e. the correlation function. Using the convolution property of Gaussians we can show

$$\int G(\vec{r}_m - \vec{r}_k, m - k) G(\vec{r}_k - \vec{r}_n, k - n) d\vec{r}_k^3 = G(\vec{r}_m - \vec{r}_n, m - n) \quad (4.21)$$

This property shows that a Gaussian chain of $m - k$ segments and another Gaussian chain of $k - n$ segments can be joined together to form a Gaussian chain of $m - k + k - n = m - n$ segments. The form of $G(\vec{r} - \vec{r}', m)$ is identical to the

kernels of the heat equation, and the correlation function is a solution of a heat or diffusion equation

$$\left(\partial_n - \frac{b_0^2}{6} \vec{\nabla}^2 \right) G(\vec{r} - \vec{r}', m) = \delta(\vec{r} - \vec{r}') \delta m \quad (4.22)$$

with the segments number n or arc length in the continuous formulation taking the role of time in the usual diffusion equation, and $b_0^2/6$ being an effective diffusion coefficient.

Simple proof of the convolution property of Gaussians. Without loss of generality, let us assume that $m > k > n$. The product of the two Gaussian probability density functions $G(\vec{r}_m - \vec{r}_k)$ and $G(\vec{r}_k - \vec{r}_n)$ reads

$$G(\vec{r}_m - \vec{r}_k)G(\vec{r}_k - \vec{r}_n) = \left(\frac{9}{4\pi^2(m-k)(k-n)b_0^4} \right)^{\frac{3}{2}} e^{-\frac{3(\vec{r}_m - \vec{r}_k)^2}{2(m-k)b_0^2} - \frac{3(\vec{r}_k - \vec{r}_n)^2}{2(k-n)b_0^2}}. \quad (4.23)$$

Through simple algebraic manipulations, the argument of the exponential function can be re-written as follows:

$$\begin{aligned} \frac{3(\vec{r}_m - \vec{r}_k)^2}{2(m-k)b_0^2} + \frac{3(\vec{r}_k - \vec{r}_n)^2}{2(k-n)b_0^2} &= \frac{3}{2b_0^2} \left[\frac{\vec{r}_m^2 - 2\vec{r}_m \vec{r}_k + \vec{r}_k^2}{m-k} + \frac{\vec{r}_k^2 - 2\vec{r}_k \vec{r}_n + \vec{r}_n^2}{k-n} \right] \\ &= \frac{3}{2b_0^2} \left[\frac{\vec{r}_k^2 - 2\frac{(k-n)\vec{r}_m + (m-k)\vec{r}_n}{m-n}\vec{r}_k + \frac{(k-n)\vec{r}_m^2 + (m-k)\vec{r}_n^2}{m-n}}{\frac{(m-k)(k-n)}{m-n}} \right] \end{aligned}$$

Note that, in this form, the argument of the exponential is a quadratic form in \vec{r}_k , hence $G(\vec{r}_m - \vec{r}_k)G(\vec{r}_k - \vec{r}_n)$ is a Gaussian in \vec{r}_k . To perform the integration over \vec{r}_k , we note that

$$\frac{\vec{r}_k^2 - 2\frac{(k-n)\vec{r}_m + (m-k)\vec{r}_n}{m-n}\vec{r}_k + \frac{(k-n)\vec{r}_m^2 + (m-k)\vec{r}_n^2}{m-n}}{\frac{(m-k)(k-n)}{m-n}} = \frac{\left[\vec{r}_k - 2\frac{(k-n)\vec{r}_m + (m-k)\vec{r}_n}{m-n} \right]^2}{\frac{(m-k)(k-n)}{m-n}} + \frac{(\vec{r}_m - \vec{r}_n)^2}{m-n}.$$

The integration over \vec{r}_k thus yields $\left(\frac{2\pi(m-k)(k-n)b_0^2}{3(m-n)} \right)^{3/2}$. We thus arrive at the result in (4.21).

4.6 Kuhn length

We have seen that the different models of the ideal chain give the same scaling behaviour at large N . We can thus construct an equivalent freely jointed chain with the same end-to-end distance and the same contour length as the actual polymer by considering a polymer formed N effective ‘‘Kuhn segments’’, each one with an effective bond length \tilde{b}_0 .

4.7 Semi-flexible polymers

We saw that for the freely jointed chain, the Kuhn length can be much larger than the true segment size: the chain retains some memory of its orientation over a

Table 4.1: Kuhn length for different ideal chain models

Model	Kuhn length
Random walk	b_0
Freely rotating chain	$b_0 \sqrt{\frac{1+\cos\theta}{1-\cos\theta}}$
Beads and springs	$\sqrt{\frac{3k_B T}{\kappa}}$

significant length. We can quantify this effect by considering the mean value of the projection of the end-to-end distance on the first segment:

$$\langle h \rangle = \left\langle \vec{R} \cdot \frac{\vec{u}_0}{b_0} \right\rangle = \frac{1}{b_0} \left\langle \sum_{i=0}^{N-1} \vec{u}_i \cdot \vec{u}_0 \right\rangle = b_0 \sum_{i=0}^{N-1} (\cos \theta)^i \approx b_0 \frac{1}{1 - \cos \theta} \approx \frac{2b_0}{\theta^2} =: l_p \quad (4.24)$$

The quantity l_p is known as the persistence length, and for the freely jointed chain Eq. (4.24) shows that it is equal to half the Kuhn segment.

For large persistence lengths θ is small and it is useful to consider the continuum limit. In this case for $\theta \ll 1$ and $m \gg 1$

$$(\cos \theta)^m \approx (1 - \theta^2/2)^m \approx e^{-m\theta^2/2} = e^{-mb_0/l_p} \quad (4.25)$$

And therefore the cosine of the angle between segments decays exponentially with increasing separation $|s_1 - s_2|$

$$\langle \cos(\theta(s_1) - \theta(s_2)) \rangle = e^{-\frac{|s_1 - s_2|}{l_p}} \quad (4.26)$$

This relationship can also be written as a function of the tangent vector field to the polymer chain $\vec{t}(s)$

$$\langle \vec{t}(s_1) \cdot \vec{t}(s_2) \rangle = e^{-\frac{|s_1 - s_2|}{l_p}} \quad (4.27)$$

The freely jointed chain for small values of θ is a special case of a semi flexible (or Kratky-Porod or worm like chain) polymer for which the memory of the initial orientation decays slowly along the polymer arc length. This type of behaviour is commonly found for biopolymers such as DNA and protein filaments including actin and tubulin which compose the cytoskeleton of the cell. For such biopolymers, the molecular origin of the persistence length is commonly a finite bending rigidity rather than free rotation of bonds. For this scenario we can define an energetic cost for bending as

$$U = C_B \frac{1}{2} \int_0^L [\partial_s \theta(s)]^2 ds \quad (4.28)$$

where C_B is the bending rigidity of the chain. For a short polymer $L \ll l_p$ we can work with the average $d\theta/ds \approx \theta/b_0$. In this case the equipartition theorem yields

$$\left\langle \left(\frac{d\theta(s)}{ds} \right)^2 \right\rangle = \frac{2k_B T}{C_B b_0} \quad (4.29)$$

Since $\partial_s \theta = \theta/b_0$ and $\theta^2 = 2b_0/l_p$ we have

$$l_p = \frac{C_B}{k_B T} \quad (4.30)$$

which relates the mechanical bending rigidity of the polymer to its persistence length.

We finally examine the end-to-end distance for semiflexible chains. For chains long compared to the segment lengths, we can approximate the mean end-to-end distance R with an integral of the tangent vectors along the length of the polymer: $\langle \vec{R} \rangle = \langle \int_0^L \vec{t}(r) dr \rangle$, where L is the contour length, or the length of the polymer chain if it were fully stretched. This expression evaluates of course to zero, as the tangent vectors are randomly distributed so that the mean $\langle \vec{t} \rangle$ over the polymer is $\vec{0}$.

The mean square end-to-end distance, in contrast, gives

$$\langle R^2 \rangle = \langle \vec{R} \cdot \vec{R} \rangle = \left\langle \left(\int_0^L \vec{t}(r) dr \right) \cdot \left(\int_0^L \vec{t}(r) dr \right) \right\rangle \quad (4.31)$$

Introducing the dummy variable r' allows us to collect the integrals into a double integral: $\langle R^2 \rangle = \int_0^L dr \int_0^L dr' \langle \vec{t}(r') \cdot \vec{t}(r) \rangle = \int_0^L dr \int_0^L dr' \exp(-|r - r'|/l_p)$. Now $|r - r'| = r - r'$ iff $r \geq r'$, and by symmetry of dummy variable exchange, $\int_0^L dr \int_0^L dr' = 2 \int_0^L dr \int_0^r dr'$ (you can convince yourself of this by sketching out the integration area as a square in (r, r') space and realising it is made of two triangles separated by the line $r' = r$, which marks the boundary of the absolute value domain). Hence $\langle R^2 \rangle = 2 \int_0^L dr \int_0^r dr' \exp[-(r - r')/l_p] = 2l_p^2 [\exp(-L/l_p) - 1 + L/l_p]$.

The contour length L and the mean end-to-end distance $\langle R^2 \rangle$ are related to the persistence length l_p by:

$$\langle R^2 \rangle = 2l_p^2 [\exp(-L/l_p) - 1 + L/l_p]. \quad (4.32)$$

If $L \gg l_p$ we obtain $\langle R^2 \rangle = 2l_p L$, i.e. the same scaling as for the ideal chain but with an effective segment length of $2l_p$ and an effective number of segments $N = L/(2l_p)$; $2l_p$ is known as the Kuhn length. By contrast for $L \ll l_p$ we obtain $\langle R^2 \rangle = L^2$, i.e. the chain is fully stretched. Examples of rigid polymers

include DNA which has a persistence length of approximately 45 nm. Another class of polymers with a persistence length significantly larger than the size of the monomer is that of polyelectrolytes. These are charged polymers and the repulsion between the charges can cause the chain to extend leading to a persistence length defined mainly by electrostatic effects.

4.8 Entropy of an ideal chain

For an ideal Gaussian chain Eq. (4.17) shows that the probability of observing an end to end distance \vec{R} for a chain with N segments is

$$\mathbb{P}(\vec{R}, N) = \left(\frac{3}{2\pi Nb_0^2} \right)^{\frac{3}{2}} e^{-\frac{3\vec{R}^2}{2Nb_0^2}} \quad (4.33)$$

With this information at hand, we can explore the Helmholtz free energy of the ideal chain. The Helmholtz free energy $F = U - TS$ is given by its internal energy U minus the product of the absolute temperature T and the entropy. The ideal chain has no internal energy since the segments do not interact, and the entropy can be computed from $S = k_B \ln(\mathbb{P}(\vec{R}, N))$; therefore we obtain the free energy as:

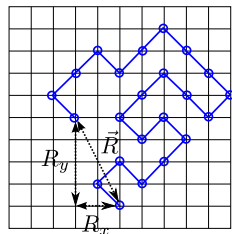
$$F(\vec{R}, N) = k_B T \frac{3}{2} \frac{\vec{R}^2}{Nb_0^2} + F(0) \quad (4.34)$$

since

$$S(\vec{R}, N) = -k_B \frac{3}{2} \frac{\vec{R}^2}{Nb_0^2} + S(0) \quad (4.35)$$

where $F(0)$ and $S(0)$ represent the constants that do not depend on R .

Figure 4.5: A conformation of a polymer chain represented as a random walk on a two dimensional square lattice. Every step results in a change in both the x and y coordinates by $\pm b_0/\sqrt{2}$ ($\pm b_0/\sqrt{3}$ in 3D). Note this lattice is rotated by 45° relative to the lattice used to define the polymer model in Figure 4.3 such that every step results in a change in x and y coordinates.



We note that this same result can be obtained for the lattice polymer. The average polymer conformation can be described by the average end-to-end distance. More information, however, is contained in the distribution of the end-to-end distance which reports on how probable it is to observe an individual chain with a given value of the end-to end distance. Clearly the maximal end-to-end distance occurs when the chain is stretched $\vec{R}_{\max}^2 = (Nb_0)^2$; there is only one (up to rotations and translations) possible conformation of the chain that has this maximal end-to-end distance, namely the case where all the bonds are aligned. We therefore expect this conformation to be very unlikely since its entropy is low.

The probability $P(\vec{R})$ for a chain to be in a conformation that results in an end-to-end vector $\vec{R} = (R_x, R_y, R_z)$ can be written as:

$$P(\vec{R}) d\vec{R} = P_{1D}(R_x) P_{1D}(R_y) P_{1D}(R_z) dR_x dR_y dR_z \quad (4.36)$$

since all directions in space are equally likely for the bond orientations. We now need an expression for the probability $P_{1D}(R_x)$ that the x-coordinate of the end-to-end vector has the value R_x . When we follow the polymer chain in a given conformation from one end to the other, we are undertaking a random walk in three dimensions; P_{1D} corresponds therefore to a random walk in one dimension. If there are a large number of paths of N steps that start at 0 and end at the same value of $x = R_x$, this will correspond to an R_x value with a higher probability relative to cases where there are only few paths. We now need to work out the number of such paths $W(N, n)$ where N is the number of steps, and $n = R_x/(b_0/\sqrt{3})$ is the number of steps away from the origin at the end of the random walk. For instance after one step, the random walk can lead to either $n = 1$ or $n = -1$, and therefore $W(N = 1, n = \pm 1) = 1$, but there is not a possibility to be at the origin $W(N = 1, n = 0) = 0$.

The general expression for $W(N, n)$ can be worked out using combinatorics. Let N_+ be the number of steps to the right and N_- the number of steps to the left. The total number of steps clearly still has to be $N = N_+ + N_-$ and the end position will be the difference in the number of steps to the right and to the left $n = N_+ - N_-$ and therefore $N_\pm = (N \pm n)/2$. The total number of trajectories is the number of ways that we can chose N_+ steps to the right out of a total number of steps N ; this is simply the binomial coefficient:

$$W(N, n) = \binom{N}{N_+} = \binom{N}{\frac{N+n}{2}} = \frac{N!}{[(N+n)/2]![(N-n)/2]!} \quad (4.37)$$

since the binomial coefficient is given as $\binom{N}{k} = \frac{N!}{(N-k)!k!}$ where $N! = 1 \cdot 2 \dots N$ is the factorial of N . This is an exact expression for $W(N, n)$ but it is inconvenient to handle since it is cumbersome to manipulate the factorials of large numbers ($100!$ is approximately 9 followed by 157 zeros!). Let us instead consider the logarithm of $W(N, n)$ and simplify it using the properties of the logarithm $\ln(a \cdot b) = \ln(a) + \ln(b)$ and $\ln(a/b) = \ln(a) - \ln(b)$:

$$\ln(W(N, n)) = \ln(N!) - \ln\left(\left[\frac{N+n}{2}\right]!\right) - \ln\left(\left[\frac{N-n}{2}\right]!\right) \quad (4.38)$$

This expression can be simplified further using Stirling's approximation $\ln(N!) \approx N \ln(N) - N \approx N \ln(N)$ for $N \gg 1$:

$$\ln(W(N, n)) \approx N \ln(N) - \frac{N+n}{2} \ln\left(\frac{N+n}{2}\right) - \frac{N-n}{2} \ln\left(\frac{N-n}{2}\right) \quad (4.39)$$

Since when $N \gg 1$ most walks don't reach to the maximal extension possible, $N \gg n$, and we can use the Taylor expansion of $\ln(1+x) = x - x^2/2 \dots$ to write

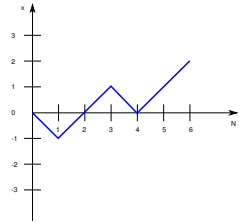


Figure 4.6: One-dimensional random walk.

Stirling's approximation originates from the observation that $\ln(N!) = \ln(1) + \ln(2) + \dots + \ln(N)$ a sum which can be approximated as the integral:

$$\int_1^N \ln(x) dx = N \ln(N) - N + 1 \approx N \ln(N) - N$$

$\ln((N \pm n)/2) = \ln(N/2) + \ln(1 \pm n/N) \approx \ln(N/2) \pm n/N - n^2/(2N^2)$ and obtain the simple result:

$$\ln(W(N, n)) \approx N \ln(2) - \frac{n^2}{2N} \quad (4.40)$$

Since the probability of observing an end-to-end distance R is proportional to the number of trajectories that satisfy this constraint, we obtain:

$$P_{1D}(N, x) dn = \sqrt{\frac{1}{2\pi N}} e^{-\frac{n^2}{2N}} dn = \sqrt{\frac{3}{2\pi Nb_0^2}} e^{-\frac{3x^2}{2Nb_0^2}} dx \quad (4.41)$$

where the distribution has been normalised $\int_{-\infty}^{\infty} P_{1D}(x) dx = 1$ as it describes a probability distribution and the total probability should be 1. Finally, the full 3D probability is given as the product from Eq. (4.36):

$$\mathbb{P}(\vec{R}, N) = \left(\frac{3}{2\pi Nb_0^2} \right)^{3/2} e^{-\frac{3\vec{R}^2}{2Nb_0^2}} \quad (4.42)$$

This expression is a Gaussian in R in agreement with Eq. (4.17); note that the only aspect of the lattice nature of the polymer model that remains in this expression is the length-scale b_0 .

4.9 Real chains: excluded volume

We saw in section 4.3 that the ideal chain is characterised by an end-to-end distance that varies with the square root of the number of bonds (scaling exponent 1/2). The size of a chain in solution can be measured experimentally by recording the light that is scattered by the polymer solution as a function of the angle between the incident and the scattered light. These experiments show that real polymer chains are typically much larger than the ideal chain, and the experimental values for the exponent are closer to $\nu \approx 3/5$ rather than the value for the ideal chain of 1/2; real chains are “swollen” compared to the ideal chain. Why is this?

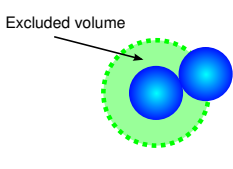


Figure 4.7: The finite volume of a segment excludes the presence of another segment in the same location in space.

This feature was first explained by Flory² by using a simple but powerful argument which we will consider here. We start with a real chain that is swollen $R > R_0 = b_0 N^{1/2}$. The monomers in the polymers are assumed to be distributed uniformly within the volume $V = 4\pi R^3/3$ and hence are present at the effective concentration c :

$$c = \frac{N}{V} = \frac{3N}{4\pi R^3} \quad (4.43)$$

²Paul Flory, 1910-1985, American Chemist, Nobel Laureate 1974

Because of the finite volume of the segments in a real polymer, two segments cannot be in the same location in space at the same time (excluded volume). This effect leads to a decrease in the number of configurations that are available to the polymer and a decrease in its entropy. A simple scheme to estimate this entropy is based on a lattice calculation. We consider a lattice where each cell has the same volume as the solutes, v . There are then V/v positions in the lattice where the solute can be placed, and $W_{\text{id}} = (V/v)^N/N!$ ways of placing N indistinguishable solutes. Therefore, if the solutes do not interact, the entropy of the system is:

$$S_{\text{id}} = k_B \ln(W_{\text{id}}) = k_B \ln [(V/v)^N/N!] = k_B [N \ln(V/v) - \ln(N!)] . \quad (4.44)$$

To simplify the last term, we employ Stirling's approximation $\ln(N!) \approx N \ln(N) - N$, such that

$$S_{\text{id}} = k_B [N \ln(V/v) - N \ln(N) + N] . \quad (4.45)$$

However, if we assume that the particles cannot overlap, the number of ways in which the solutes can be arranged in the lattice is $W_{\text{ex}} = \binom{V/v}{N} = (V/v)!/[N!(V/v - N)!]$ since we need to chose N sites from a total of V/v . In computing the entropy of the system

$$S_{\text{ex}} = k_B \ln(W_{\text{ex}}) = k_B [\ln(V/v)! - \ln(N!) - \ln(V/v - N)!] , \quad (4.46)$$

we can use again Stirling's formula and obtain

$$S_{\text{ex}} = k_B [(V/v) \ln(V/v) - N \ln(N) - (V/v - N) \ln(V/v - N)] . \quad (4.47)$$

The formula can be simplified further by employing a series expansion of the logarithm $\log(1 + x) \approx x$ for small values of $x \ll 1$. In particular, the third term in the equation above can be written as $\ln(V/v - N) = \ln(V/v) + \ln(1 - Nv/V)$; using the fact that $N \ll V/v$, we find $\ln(V/v - N) \approx \ln(V/v) - Nv/V$. Hence, using Eq. (4.47), we find

$$S_{\text{ex}} = k_B \left[N \ln(V/v) - N \ln(N) + N - \frac{N^2 v}{V} \right] . \quad (4.48)$$

Recognizing that the first three terms in the equation equals the entropy of the ideal chain, we arrive at the final result

$$S_{\text{ex}} = S_{\text{id}} - k_B \frac{N^2 v}{V} . \quad (4.49)$$

We see that we have obtained an additional term $N^2 v/V$ compared to the non-interacting system. This term results in an additional Helmholtz free energy of

$F = -TS = k_B T \frac{N^2 v}{V}$. Per unit volume V , the Helmholtz free energy has increased by a factor proportional to the concentration $c = N/V$ squared: $F/V = k_B T v c^2$. Finally, the excess Helmholtz free energy reads:

$$F_{\text{excl}} = \frac{3k_B T v N^2}{4\pi R^3} \quad (4.50)$$

This excluded volume interaction leads to a driving force to swell the polymer. There is, however, also an opposing force from the spring constant of the polymer Eq. (4.34) that we discussed in the previous section, $F_{\text{spring}} = k_B T \frac{3R^2}{2Nb_0^2}$. Adding both contributions together yields the total free energy for the polymer with excluded volume:

$$F = k_B T \frac{3vN^2}{4\pi R^3} + k_B T \frac{3R^2}{2Nb_0^2} \quad (4.51)$$

The equilibrium size R of the polymer is given by the condition that it must result in the minimum in the Helmholtz free energy. This minimum is found by setting the derivative of the free energy $dF/dR = 0$ to be zero:

$$-\frac{3vN^2}{4\pi R^4} + \frac{R}{Nb_0^2} = 0 \quad (4.52)$$

and therefore the size of the polymer coil is given as:

$$R = \left(\frac{3vb_0^2}{4\pi} \right)^{1/5} N^{3/5} \quad (4.53)$$

We see that the scaling exponent has changed compared to the ideal chain. Note that, in a lattice model with perfectly exclusive interactions, v is the volume occupied by one segment of the chain, so that $v = b_0^3$. Hence the prefactor in Eq. (4.53) depends on b_0^5 , thereby explaining the exponent of $1/5$.

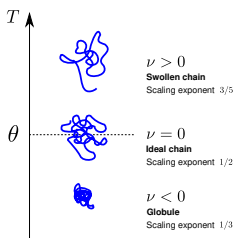


Figure 4.8: Coil-globule transition.

4.10 Coil-globule transition

When the excluded volume parameter v is positive, swelling of the chains occurs in solution and the end-to-end-distance scales with the power $3/5$. It turns out, however, that the excluded volume parameter can also be negative, and this leads to very different behaviour.

To shed light on this phenomenon, we examine the effect of an attractive pairwise potential between two segments

$$U = \frac{1}{2} \sum_{i,j} \Phi(\vec{r}_i - \vec{r}_j) \quad (4.54)$$

By introducing the local density $n(\vec{r}) = \sum_i \delta(\vec{r} - \vec{r}_i)$ the energy can be written as

$$U = \frac{1}{2} \int d\vec{r}^3 d\vec{r}'^3 n(\vec{r})n(\vec{r}')\Phi(\vec{r} - \vec{r}') \quad (4.55)$$

With this interaction term, the probability distribution of the chain can no longer be computed exactly. We make progress within a mean field picture and assume that the segment concentration $n(\vec{r}) = n \approx N/R^3$ is constant within the polymer coil of volume $V \sim R^3$. The energy then becomes

$$U = \frac{1}{2} \left(\frac{N}{R^3} \right)^2 \int d\vec{r}^3 d\vec{r}'^3 \Phi(\vec{r} - \vec{r}') = \frac{1}{2} \left(\frac{N}{R^3} \right)^2 \int d\vec{r}^3 dw^3 \Phi(\vec{w}) = -Van^2 \quad (4.56)$$

where a is a parameter with units of energy \times volume that determines the strength of the attractive interaction.³ Therefore this term combines with that from the previous section to yield a temperature-dependent interaction between the segments in the chain:

$$\frac{F_{\text{int}}}{V} = k_B T v(T) n^2 \quad (4.57)$$

with

$$v(T) = v_0 - \frac{a}{k_B T} = v_0 \left(1 - \frac{a}{v_0 k_B T} \right) \quad (4.58)$$

It is customary to introduce the Flory parameter $\chi(T) = \frac{1}{2}(1 - v(T)/v_0)$ and then $v(T) = v_0(1 - 2\chi(T))$. In particular, there is a temperature at which the excluded volume interaction vanishes: this is known as the θ temperature and is given by $\theta = a/(v_0 k_B)$ or $\chi(\theta) = 1/2$. Note that with θ defined, we can now rewrite $v(T) = v_0(1 - \frac{\theta}{T})$ and $\chi(T) = \frac{\theta}{2T}$. For real systems, a (and v_0) can in principle be temperature dependent; it is found, however, that the scaling $\chi \sim T^{-1}$ is typically the observed behaviour and it emerges from the simple arguments presented here.

At the θ temperature, a real chain behaves therefore like an ideal chain. When the temperature is significantly below this value, the interactions between the segments become strongly attractive, and the chain collapses into a compact globule. This is the coil to globule transition.

Therefore when $v(T) > 0$ (or $\chi(T) < 1/2$) the polymer chain is swollen and is said to be in a good solvent; conversely for $v(T) < 0$ (or $\chi(T) > 1/2$) corresponds to a bad solvent and the polymer is collapsed. Typically, the transition from coil

³The interaction term a is related to the second virial coefficient: $U = k_B T B_2(T) V n^2$. This can be seen by recalling the statistical mechanical form of the second virial coefficient $B_2 = \frac{1}{2} \int d\vec{r}^3 (1 - e^{-\beta\Phi(\vec{r})}) \approx \frac{1}{2} \beta \int d\vec{r}^3 \Phi(\vec{r})$. As such, a term in the energy that depends on the square of the concentration is proportional to B_2 and contains information on the pairwise interactions between particles and vanishes for an ideal gas.

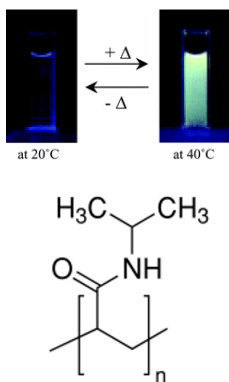


Figure 4.9: Coil to globule transition in p-NIPAAm. (J. Mater. Chem., 2005, 15, 2796)

4.11 Flory Huggins free energy

To understand the physical origin of the χ parameter, we examine in more detail the behaviour of polymers in solution. We first consider regular solutions which are mixtures of low molecular weight species A with solvent molecules B . We work with a lattice model with $M = N_A + N_B$ lattice sites which can be occupied either by a solvent molecule or by a solute. The number of solute molecules is N_A and that of solvent molecules is N_B . The entropy of the system is $S = k_B \ln(\Omega)$ where

$$\Omega = \frac{M!}{N_A! N_B!} \quad (4.59)$$

is the number of microstates (the ways to arrange the molecules of solute and solvent on the lattice). Using Stirling's approximation $\ln(M!) \approx M \ln M - M$ for $M \gg 1$ yields the entropy of mixing for the solution

$$\Delta S = k_B \ln \left(\frac{(N_A + N_B)!}{N_A! N_B!} \right) = k_B [\ln(N_A + N_B)! - \ln(N_A!) - \ln(N_B!)] \quad (4.60)$$

$$\approx -k_B \left[N_A \ln \left(\frac{N_A}{N_A + N_B} \right) + N_B \ln \left(\frac{N_B}{N_A + N_B} \right) \right] \quad (4.61)$$

or

$$\Delta S = -k_B M (\Phi_A \ln \Phi_A + \Phi_B \ln \Phi_B) \quad (4.62)$$

where $\Phi_{A,B} = N_{A,B}/M$ is the volume fraction.

This increase in the entropy when different molecules are mixed originates from the increase in the numbers of arrangements of the centres of mass of the molecules upon mixing (a pure substance in this lattice model has $\Omega = 1$), and provides the thermodynamic driving force favouring mixing.

For a polymer solution, the solute is a macromolecule and occupies N lattice sites rather than a single one. Moreover, all N segments of a given polymer have

to occupy adjacent positions, and as such, the translational entropy of the polymer is reduced by a factor of N relative to the same volume concentration of small molecular solutes:

$$\begin{aligned}\Delta S &= -k_B M \left(\frac{\Phi_A}{N} \ln \Phi_A + \Phi_B \ln \Phi_B \right) \\ &= -k_B M \left[\frac{\Phi}{N} \ln \Phi + (1 - \Phi) \ln(1 - \Phi) \right]\end{aligned}\quad (4.63)$$

where $\Phi := \Phi_A$. This behaviour generally reduces the solubility of polymers relative to small molecules.

We now also allow for pairwise interactions between different lattice sites, with an energy contribution of ϵ_{pp} for the interaction between two polymer sites, ϵ_{ps} for the polymer/solvent interaction and ϵ_{ss} for solvent/solvent interactions. The interaction energy for such a system is

$$\begin{aligned}U &= \frac{1}{2} \sum_{\langle i,j \rangle} \sum_{\substack{K=\{A,B\} \\ K'=\{A,B\}}} \epsilon_{K,K'} \Phi_K(i) \Phi'_{K'}(j) \\ &\approx \frac{1}{2} M z [\Phi^2 \epsilon_{pp} + 2\epsilon_{ps} \Phi(1 - \Phi) + \epsilon_{ss}(1 - \Phi)^2]\end{aligned}\quad (4.64)$$

where $\langle i,j \rangle$ denotes summation over nearest neighbours, z is the coordination number (number of nearest lattice sites), and we have used a mean field approximation to evaluate the total energy by replacing the spatially dependent concentration $\Phi(i)$ for each site with its mean value Φ . In the unmixed state, obtained by partitioning the solute to one side of the lattice, the interaction energy is (neglecting the surface tension of the interface)

$$U_{\text{unmixed}} = \frac{1}{2} M z [\epsilon_{pp} \Phi + \epsilon_{ss}(1 - \Phi)] \quad (4.65)$$

And hence the energy change upon mixing is

$$\Delta U = \frac{zM}{2} [\epsilon_{pp} \Phi^2 + 2\epsilon_{ps} \Phi(1 - \Phi) + \epsilon_{ss}(1 - \Phi)^2 - \epsilon_{pp} \Phi - \epsilon_{ss}(1 - \Phi)] \quad (4.66)$$

$$= \frac{zM}{2} \Phi(1 - \Phi) [2\epsilon_{sp} - \epsilon_{ss} - \epsilon_{pp}] =: \chi M k_B T \Phi(1 - \Phi) \quad (4.67)$$

with the parameter

$$\chi := \frac{z}{2} \frac{2\epsilon_{sp} - \epsilon_{ss} - \epsilon_{pp}}{k_B T} \quad (4.68)$$

Taken together, we can express the free energy density $f = \Delta F/M = \Delta U/M - T\Delta S/M$ of mixing as

$$f_{\text{mix}} = k_B T \left[\frac{\Phi}{N} \ln \Phi + (1 - \Phi) \ln(1 - \Phi) + \chi \Phi(1 - \Phi) \right] \quad (4.69)$$

4.12 Osmotic pressure and chemical potential of polymer solutions

At low concentrations of polymer solute $\Phi \ll 1$, the energy density can be expanded in a power series in Φ by using $\ln(1 - \Phi) \approx -\Phi - \Phi^2/2 + \mathcal{O}(\Phi^3)$ giving

$$f = k_B T \left[\frac{\Phi}{N} \ln \Phi + (1 - \Phi) \left(-\Phi - \frac{\Phi^2}{2} \right) + \chi \Phi (1 - \Phi) \right] \quad (4.70)$$

$$= k_B T \left[\frac{\Phi}{N} \ln \Phi + \Phi(\chi - 1) + \frac{\Phi^2}{2}(1 - 2\chi) \right] \quad (4.71)$$

The osmotic pressure Π is the pressure exerted by molecules in solution against a membrane which is impenetrable to them but allows the flow of solvent molecules and can be obtained from the change in the free energy of the system as a function of volume with constant number of solutes N_A

$$\Pi = - \left. \frac{\partial \Delta F}{\partial V} \right|_{N_A} = - \frac{1}{b_0^3} \frac{\partial(M f)}{\partial M} = - \frac{1}{b_0^3} \left(f + M \frac{\partial f}{\partial M} \right) = \frac{1}{b_0^3} \left(-f + \Phi \frac{\partial f}{\partial \Phi} \right) \quad (4.72)$$

where $\Phi = N_A/M$ implies $d/d\Phi = -\Phi^{-1}Md/dM$. The chemical potential of the polymers is given as the rate of change in the free energy as a function of the number of polymers in solution

$$\mu = \frac{\partial \Delta F}{\partial N_A} = M \frac{\partial f}{\partial N_A} = M \underbrace{\frac{\partial \Phi}{\partial N_A}}_{=M^{-1}} \frac{\partial f}{\partial \Phi} = \frac{\partial f}{\partial \Phi} \quad (4.73)$$

and hence the osmotic pressure is

$$\Pi = \frac{-f + \Phi \mu}{b_0^3} \quad (4.74)$$

By using Eq. (4.72) we can evaluate the osmotic pressure as

$$\Pi = \frac{k_B T}{b_0^3} \left[\frac{\Phi}{N} - \Phi - \ln(1 - \Phi) - \chi \Phi^2 \right] \approx \frac{k_B T}{b_0^3} \left[\frac{\Phi}{N} + \frac{1}{2}(1 - 2\chi)\Phi^2 \right] \quad (4.75)$$

where we have used the approximation from Eq. (4.71). This is the virial expansion; the first term is the ideal gas law, and the second term which is quadratic in the concentration, is the first correction to the ideal gas law and contains information on the inter-particle interactions. The coefficient of the quadratic term $B_2 = (1 - 2\chi)/2$ is the second virial coefficient. If it is positive, there is a repulsive interaction, while negative values of B_2 describe an attractive interaction. As such, the term

$$v(T) = b_0^3(1 - 2\chi(T)) \quad (4.76)$$

can be recognised as the excluded volume parameter $v(T)$ introduced earlier. The solvent quality thus affects the excluded volume parameter and the coil to globule transition.

4.13 Polymer melt

We have so far examined dilute solutions of polymers in a low molecular weight solvent. What happens if we replace this solvent with a second polymer, with identical chemistry (and hence identical inter and intra polymer segment interactions) but with a polymerisation number $N_2 \neq N$? In such a polymer we can introduce into Eq. (4.63) the parameter N_2 which now reduces the translational entropy of the solvent to yield

$$\Delta S = -k_B M \left[\frac{\Phi}{N} \ln \Phi + \frac{1-\Phi}{N_2} \ln(1-\Phi) \right] \quad (4.77)$$

Repeating the analysis leading to the excluded volume parameter in Eq. (4.76) results in a modified form

$$v = b_0^3 \left(\frac{1}{N_2} - 2\chi \right) \quad (4.78)$$

Since the polymer solute and the polymer solvent have the same chemical composition, $\epsilon_{pp} = \epsilon_{ps} = \epsilon_{ss}$ and hence the Flory parameter vanishes $\chi = 0$, and we are for the polymer melt we are only left with a small entropic term $v = b_0^2/N_2 \rightarrow 0$ for $N_2 \gg 1$ which vanishes in the limit of long chains. As such in dense polymer melts $v = 0$ and chains adopt nearly ideal conformations. This surprising result was first discovered by Flory and physically this effect originates from the fact that each chain has difficulty distinguishing contacts with itself from contacts with surrounding chains, and interactions are thus screened. Thus polymer chains behave as ideal chains in the melt since the expanding tendency of polymers in dilute solution through excluded volume interactions is counterbalanced by the interactions with segments from other polymers which would lead to the compaction of the coil. Overall, these two tendencies cancel out and the chains behave as ideal chains.

4.14 Semi-dilute solutions

An intermediate scenario between a dilute solution and a dense polymer melt is a semi-dilute solution where the polymer coils start to overlap in solution. In solution polymer chains can interact with each other if the concentration is high

enough. In very dilute solutions, the volume enclosed by the polymer coil is mainly occupied by solvent molecules. However, the expanded nature of the polymer coil implies that the coils may start to overlap as the concentration increases. This happens in semi-dilute solutions. Under such conditions, the monomer units in one chain can make contact with the monomers in another polymer chain leading to a network with a mesh size smaller than the end-to end distance. The change from dilute to semi dilute concentration regimes is measured by the overlap concentration Φ^* . We expect this concentration to be comparable to the concentration of segments within one polymer:

$$\Phi^* \sim \frac{Nb_0^3}{(\sqrt{\langle R^2 \rangle})^3} \sim N^{-4/5} \quad (4.79)$$

since in a good solvent $\sqrt{\langle R^2 \rangle} \sim N^{3/5}$. The higher the molecular weight of the polymer, the lower the overlap concentration will be; this reflects the fractal nature of the chain where the dimensions grow faster than the mass of the polymer.

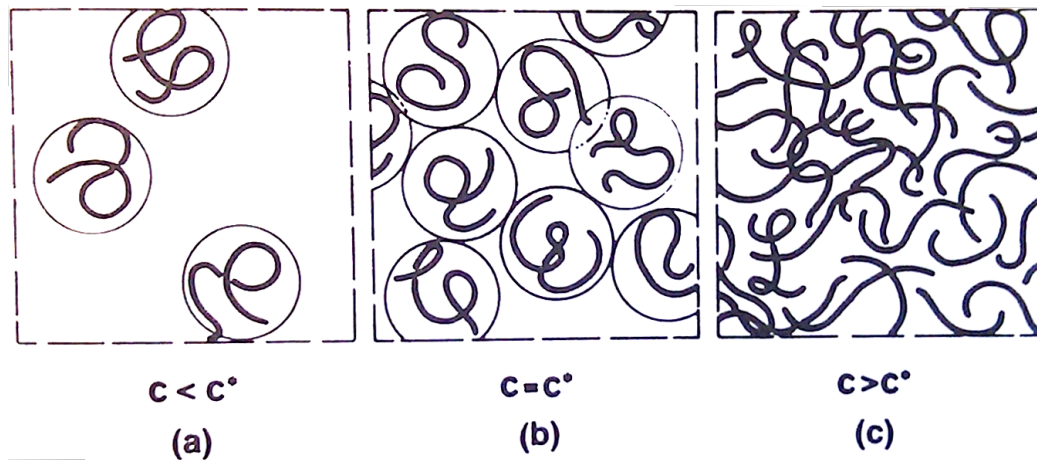


Figure 4.10: Polymer chains in dilute (a) and semi-dilute (c) solution; the onset of overlap is shown in (b). (From: Scaling concepts in Polymer Physics, de Gennes, Cornell University Press 1979)

4.15 Phase diagram for polymer solutions

We now investigate the stability of a polymer solution with respect to phase separation into two domains, one with concentration $\Phi' := \Phi + \delta\Phi$ and the other with concentration $\Phi'' := \Phi - \delta\Phi$. We work within the Flory Huggins model and consider a situation for the phase separated system where both domains consist of

half of the lattice $M/2$. The change in the free energy when changing from the homogeneous solution to the separated state is

$$\Delta F = M \left(\frac{f(\Phi + \delta\Phi, \chi) + f(\Phi - \delta\Phi, \chi)}{2} - f(\Phi, \chi) \right) \quad (4.80)$$

For a small change $\delta\Phi$ we expand this difference as a series to yield

$$\Delta F \approx \frac{M}{2} \frac{\partial^2 f(\Phi, \chi)}{\partial \Phi^2} \delta\Phi^2 \quad (4.81)$$

Since $\delta\Phi^2 > 0$ the condition for the stability of the homogeneous solution is $\partial_\Phi^2 f > 0$, i.e. the free energy must be convex with respect to composition changes. The spinodal curve delimiting the unstable situation $\partial_\Phi^2 f < 0$ from the stable (or metastable) system is given by $\partial_\Phi^2 f = 0$. Within the Flory Huggins model, this corresponds to

$$\begin{aligned} \partial_\Phi^2 f &= \frac{\partial}{\partial \Phi} \left[\ln \left(\frac{\Phi}{N} \right) \frac{1}{N} + \frac{1}{N} - \chi\Phi + \chi(1 - \Phi) - \ln(1 - \Phi) - 1 \right] \\ &= \frac{1}{\Phi N} + \frac{1}{1 - \Phi} - 2\chi = 0 \end{aligned} \quad (4.82)$$

giving the spinodal equation $\chi(\Phi)$ as

$$\chi(\Phi) = \frac{1}{2} \left(\frac{1}{\Phi N} + \frac{1}{1 - \Phi} \right) \quad (4.83)$$

4.15.1 The critical point

The spinodal point has a minimum in the (Φ, χ) plane corresponding to the values of the parameters when the instability of the homogeneous solution first emerges when χ is increased (corresponding to a decrease in temperature for the common case where $\chi \sim T^{-1}$). This is the critical point and is given by

$$\frac{d}{d\Phi} \chi(\Phi = \Phi_c) = \frac{1}{2} \left[\frac{1}{(1 - \Phi)^2} - \frac{1}{\Phi^2 N} \right]_{\Phi_c} = 0 \quad (4.84)$$

resulting in the critical point Φ_c

$$\Phi_c = \frac{1}{\sqrt{N} + 1} \quad (4.85)$$

and a critical interaction parameter close to $1/2$

$$\chi_c = \frac{1}{2} + \frac{1}{\sqrt{N}} + \frac{1}{2N} \approx \frac{1}{2} + \frac{1}{\sqrt{N}} \quad (4.86)$$

The interaction parameter is most readily varied experimentally through changing the system temperature, and phase diagrams are commonly shown in the temperature-composition plane. If $a > 0$, then χ decreases as the temperature is raised. The highest temperature of the two-phase region is the upper critical solution temperature T_c . When $T > T_c$ the homogeneous solution is stable. By contrast, if $a < 0$, then χ increases as the temperature is lowered. In the latter case, the homogeneous solution is stable below T_c which is known as the lower critical solution temperature in this case. The former case is more common, but there are systems which phase separate when the temperature is raised (e.g. PNIPAM).

4.16 Polymers at surfaces

Polymers may adsorb to surfaces spontaneously or through covalent coupling. Even for non-covalent coupling, and although the adsorption energy of each monomer unit in the chain is small, there may be many segments and hence the accumulated effect can become very large; indeed if $E_{\text{ads}} \gg k_B T$ adsorption will be irreversible. Chemical modification of surfaces through polymer adsorption has wide technological applications in areas ranging from lubrication to antifouling coatings, and living systems also make use of polymer coatings in lubrication of joints, and control of cell adhesion.

4.16.1 Grafting density

The grafting density is the number of chains per unit area on a surface

$$\sigma := \frac{1}{D^2} \quad (4.87)$$

where D is the distance between grafting points on the surface. When $D \gg R$, the grafted chains don't touch. This is the mushroom regime. By contrast, when $D < R$ the grafted chains overlap, and intersegment excluded volume repulsion leads to the chains being stretched to give a polymer brush. For chains at high density in a good solvent, we can apply the Flory argument to estimate the height of the polymer brush. The length scale in the entropic part of the free energy is the brush height h , leading to $F_1 = k_B T / (2b_0^2 N) h^2$ and the volume of the coil is confined to a cylinder with a volume of $V = hD^2 = h/\sigma$ leading to a contribution to the free energy from the excluded volume repulsion of $F_2 = \frac{1}{2} k_B T b_0^3 N^2 \sigma / h$. Minimisation of the free energy

$$F = k_B T \frac{h^2}{2b_0^2 N} + \frac{k_B T b_0^3 N^2 \sigma}{2h} \quad (4.88)$$

with respect to h yields the average brush height

$$\langle h \rangle = \left(\frac{1}{2} b_0^5 \sigma \right)^{\frac{1}{3}} N \quad (4.89)$$

and the brush height is directly proportional to the polymerisation number.

4.17 Rubber elasticity

Rubbers are cross linked polymer networks. Due to the cross linking, for long times, the material behaves like an elastic material and cannot flow like a liquid. However, polymer networks can deform up to several times their size, a characteristic which gives rubbers their unique properties. Here, we consider a simple model of polymer elasticity, the affine network model⁴. We assume that the relative deformation of each polymer strand in the network is the same as that of the overall network. We consider a rubber network with undeformed dimensions L_{x0}, L_{y0}, L_{z0} . We consider a polymer chain in the network with end to end distance \vec{R}_0 in the undeformed state and \vec{R} after deformation where \vec{R}_0 and \vec{R} are related by the linear transformation

$$R_x = \lambda_x R_{x0} \quad (4.90)$$

$$R_y = \lambda_y R_{y0} \quad (4.91)$$

$$R_z = \lambda_z R_{z0} \quad (4.92)$$

The free energy difference between the initial and stretched states is

$$\Delta F = F(N, \vec{R}) - F(N, \vec{R}_0) = \frac{3k_B T}{2Nb_0^2} (R_x^2 + R_y^2 + R_z^2) - \frac{3k_B T}{2Nb_0^2} (R_{x0}^2 + R_{y0}^2 + R_{z0}^2) \quad (4.93)$$

$$= \frac{3k_B T}{2Nb_0^2} [(\lambda_x^2 - 1)R_{x0}^2 + (\lambda_y^2 - 1)R_{y0}^2 + (\lambda_z^2 - 1)R_{z0}^2] \quad (4.94)$$

For n such strands we obtain

$$\Delta F = \frac{3k_B T}{2Nb_0^2} \left[(\lambda_x^2 - 1) \sum_{i=1}^n (R_{x0})_i^2 + (\lambda_y^2 - 1) \sum_{i=1}^n (R_{y0})_i^2 + (\lambda_z^2 - 1) \sum_{i=1}^n (R_{z0})_i^2 \right] \quad (4.95)$$

For a rubber that is made by crosslinking the chains in their ideal state in a polymer melt, the unstretched end-to-end distances obey the ideal chain scaling relationship

$$\langle R_{x0}^2 \rangle := \frac{1}{n} \sum_{i=1}^n (R_{x0})_i^2 = \frac{Nb_0^2}{3} \quad (4.96)$$

⁴This model was originally proposed by Flory

and therefore Eq. (4.94) becomes

$$\Delta F = n \frac{k_B T}{2} (\lambda_x^2 + \lambda_y^2 + \lambda_z^2 - 3) \quad (4.97)$$

For an incompressible network, the volume V is maintained over the deformation

$$V = L_{x0}L_{y0}L_{z0} = L_xL_yL_z = \lambda_x L_{x0} \lambda_y L_{y0} \lambda_z L_{z0} = \lambda_x \lambda_y \lambda_z V \quad (4.98)$$

and therefore $\lambda_x \lambda_y \lambda_z = 1$

For example, for a tensile elongation by λ_x along x in which y and z are left free, the conservation of volume Eq. (4.98) implies $\lambda_y = \lambda_z = 1/\sqrt{\lambda_x}$. Hence the free energy difference becomes

$$\Delta F = n \frac{k_B T}{2Nb_0^2} \left[\lambda_x^2 + \frac{2}{\lambda_x} - 3 \right] \quad (4.99)$$

with the shorthand notation $\lambda = \lambda_x$. The force required to achieve this deformation is

$$f_x = \frac{\partial \Delta F}{\partial L_x} = \frac{\partial \Delta F}{\partial (\lambda L_{x0})} = \frac{1}{L_{x0}} \frac{\partial \Delta F}{\partial \lambda} = n \frac{k_B T}{L_{x0}} \left(\lambda - \frac{1}{\lambda^2} \right) \quad (4.100)$$

The stress is then

$$\sigma_x = \frac{f_x}{L_y L_z} = \frac{n k_B T}{L_{x0} L_y L_z} \left(\lambda - \frac{1}{\lambda^2} \right) = \frac{n k_B T \lambda}{L_x L_y L_z} \left(\lambda - \frac{1}{\lambda^2} \right) = \frac{n k_B T}{V} \left(\lambda^2 - \frac{1}{\lambda} \right) \quad (4.101)$$

We can introduce the strain by setting $\lambda = 1 + \epsilon_x$ and then to linear order in ϵ_x , $\lambda^2 - \lambda^{-1} \approx 3\epsilon + \mathcal{O}(\epsilon_x^3)$. The strain and stress are therefore related by

$$\sigma_x = 3 \frac{n}{V} k_B T \epsilon_x = E \epsilon_x \quad (4.102)$$

and the Young's modulus for a rubber is

$$E = 3 \frac{n}{V} k_B T \quad (4.103)$$

is proportional to the density of strands (cross-link junctions) per volume and the temperature. For an incompressible material $G = E/3$ and hence the shear modulus of a rubber is

$$G = \frac{n}{V} k_B T \quad (4.104)$$

Rubbers therefore become stiffer with increasing temperature. This is the opposite behaviour to most other common materials, including metals, and originates from the fact that as we have seen, on a molecular level the elasticity of a rubber is entropic in nature, rather than enthalpic as in most other materials.

4.18 Dynamics

A simple model for the dynamics of polymers is to return to the bead spring Gaussian model. We assume that the spheres undergo Brownian motion as discussed in Chapter 3. The (overdamped) Langevin equation for the motion of the sphere n is then

$$\gamma \frac{d\vec{R}_n}{dt} = \kappa(\vec{R}_{n+1} + \vec{R}_{n-1} - 2\vec{R}_n) + \vec{\xi}(n, t) \quad (4.105)$$

where $\kappa = 3k_B T/b_0^2$ is the spring constant of the Gaussian chain, and the random noise satisfies the relation

$$\langle \xi_i(n, t) \xi_j(m, t') \rangle = 2\gamma k_B T \delta(m - n) \delta(t - t') \delta_{ij}. \quad (4.106)$$

Eq. (4.105) is known as the Rouse equation. In the continuum limit the equation reads

$$\gamma \frac{d\vec{R}(n)}{dt} = \kappa \frac{\partial^2 \vec{R}}{\partial n^2} + \vec{\xi}(n, t) \quad (4.107)$$

We decompose the motion of the chain into normal modes $\vec{X}(t)$

$$\vec{R}(n, t) = \vec{X}_0(t) + 2 \sum_{p=1}^{\infty} \vec{X}_p(t) \cos\left(\frac{p\pi n}{N}\right) \quad (4.108)$$

which are given as the Fourier transform of \vec{R}

$$\vec{X}_p(t) = \frac{1}{N} \int_0^N \vec{R}(n, t) \cos\left(\frac{p\pi n}{N}\right) dn \quad (4.109)$$

and the choice of the cosine mode originates from the boundary condition $\partial_n \vec{R} = 0$ for $n = 0$ and $n = N$. The modes are orthogonal for $p, p' \geq 1$

$$\frac{2}{N} \int_0^N \cos\left(\frac{p\pi n}{N}\right) \cos\left(\frac{p'\pi n}{N}\right) dn = \delta_{pp'} \quad (4.110)$$

Substituting Eq. (4.108) into Eq. (4.107) yields an equation of motion for each independent mode $p \geq 1$

$$2N\gamma \frac{d\vec{X}_p(t)}{dt} = -k_p \vec{X}_p + \vec{\xi}_p(t) \quad (4.111)$$

with the spring constant $k_p = 6k_B T \pi^2 p^2 / (Nb_0^2)$ while the centre of mass mode satisfies

$$N\gamma \frac{\partial \vec{X}_0}{\partial t} = \vec{\xi}_0(t) \quad (4.112)$$

with $\gamma_{\text{CM}} = N\gamma_0$

The centre of mass undergoes diffusion with a diffusion coefficient of $D_{\text{CM}} = k_B T / \gamma_0 = k_B T / (\gamma N)$.

According to the strategy explored in Chapter 3, the correlation function between the mode amplitudes can be computed

$$\langle X_{p;i}(t) X_{q;j}(t') \rangle = \frac{k_B T}{k_p} \delta_{pq} \delta_{ij} e^{-|t-t'|/\tau_p} \quad (4.113)$$

where the relaxation time is $\tau_p = \underbrace{N\gamma}_{\gamma_p} / k_p$. The higher modes relax faster, and the slowest relaxation time is

$$\tau_R := \tau_1 = \frac{\gamma N^2 b_0^2}{6\pi^2 k_B T} \quad (4.114)$$

and is known as the Rouse time. This is the time scale for the relaxation of the overall shape of the polymer molecule since it corresponds to the amplitude of the normal mode with a single nodal point.

4.18.1 Viscoelastic behaviour

The Rouse model discussed here doesn't include hydrodynamic interactions which are commonly important for polymer chains in dilute solutions⁵. By contrast, in a dense polymeric fluid, the chains can screen the hydrodynamic interactions and the Rouse model can qualitatively describe the behaviour of the fluid. To explore this aspect further, we compute the stress tensor for a dense polymeric fluid within the Rouse model. The stress tensor σ_{ij} gives the i th component of the force per unit area transmitted across a plane with its normal vector in the j th direction. We consider a cube with dimension L ; it contains $c/\tilde{N}L^3$ subchains of length \tilde{N} , where $c = \Phi/b_0^3$ is the concentration of segments. The probability that one subchain with an end-to-end vector \vec{R} cuts the j plane in the cube is $\mathbb{P}_j = R_j/L$. The i th component of the force transmitted by this chain cross the j plane is $F_i = 3k_B T R_i / (\tilde{N}b_0^2)$. Taken together, the contribution to the stress tensor σ_{ij} of this subchain is $\mathbb{P}_j F_i / L^2 = 3k_B T R_i R_j / (\tilde{N}b_0^2 L^3)$. For all subchains in the volume we obtain

$$\sigma_{ij} = \frac{3k_B T c}{\tilde{N}^2 b_0^2} \langle R_i R_j \rangle \quad (4.115)$$

In the continuum limit we can replace \vec{R}/\tilde{N} with $\partial \vec{R} / \partial n$ (for a small L and hence R) and thus the stress tensor becomes

$$\sigma_{ij} = \frac{3k_B T c}{b_0^2} \left\langle \frac{\partial R_i}{\partial n} \frac{\partial R_j}{\partial n} \right\rangle \quad (4.116)$$

⁵Hydrodynamic interactions are addressed by the Zimm model

This expression can be evaluated for the Rouse model to yield

$$\sigma_{ij} = \frac{c}{N} \sum_p k_p \langle X_{p;i} X_{p;j} \rangle \quad (4.117)$$

We consider a stress relaxation scenario, where we apply a step strain ϵ at $t = 0$ in the x-direction. After the strain has been applied, $X_{p;x}(t) = X_{p;x}(0) + \epsilon X_{p;y}(0)$. The stress after the strain jump is

$$\sigma_{xy} = \epsilon \frac{c}{N} \sum_p \underbrace{k_p \langle X_{p;y}(0) X_{p;y}(t) \rangle}_{=k_B T e^{-t/\tau_p}} \quad (4.118)$$

where we have used the result from Eq. (4.113). Each mode thus decays back to equilibrium with its own time constant $\tau_p = \tau_R/p^2$ giving the shear modulus as $G(t) = \sigma_{xy}/\epsilon$ as

$$G(t) = \frac{c k_B T}{N} \sum_p e^{-p^2 t / \tau_R} \quad (4.119)$$

This expression has the simple qualitative interpretation that each unrelaxed mode contributes $c k_B T$ to the modulus. Each one of the modes behaves like a Maxwell fluid. Moreover, the overall polymer system behaves as a Maxwell fluid for long times beyond the Rouse time where only the $k = 1$ mode contributes and hasn't yet relaxed. For shorter times, many modes contribute and we can approximate the sum with the integral $\int dp e^{-2p^2 t / \tau_R} \sim \sqrt{\tau_R/t}$ and hence $G(t) \sim t^{-1/2}$ has power law behaviour in this regime.

4.19 Helix to coil transition

Many biological polymers, including DNA, RNA and proteins can undergo a transition between an ordered helical state and a disordered random coil when temperature is increased. The ordering is commonly driven by the formation of hydrogen bonds in such systems. For simplicity we consider a two state transition and assume that each segment can either be in the helical or coil state. The transition can be cooperative: the tendency of each part of the chain to be in a given state depends on the state of its neighbours. We examine this cooperativity with different models below.

4.19.1 Non-cooperative model

If there is no cooperativity, the state of each segment in the chain is independent of all the others and the partition function for the system consisting of a chain with

N segments will be

$$Z = z_1^N = (e^{-\beta\epsilon} + 1)^N \quad (4.120)$$

where ϵ is the energy difference between the helix and coil state. The number of segments in the helical state is then

$$\langle i \rangle = Z^{-1} \sum_{i=0}^N i \binom{N}{i} e^{-\beta i \epsilon} \quad (4.121)$$

which can be computed easily by noting that this expression is nothing else than $-\frac{1}{Z} \frac{1}{\epsilon} \frac{\partial Z}{\partial \beta} = \frac{\partial \ln Z}{\partial \ln s}$ and therefore we obtain $\langle i \rangle = \frac{Ns}{1+s}$ where $s := e^{-\beta\epsilon}$. Therefore the fraction of helical segments is given as $f = \langle i \rangle / N$:

$$f = \frac{s}{1+s} \quad (4.122)$$

The helical fraction depends on the temperature through the T -dependence of s .

4.19.2 Fully cooperative model

For most real systems, the presence of helical neighbours increases the probability of a given segment to also be in the helical state. An extreme case is if the chain is either completely helical or completely coiled, representing a fully cooperative model. The partition function of the chain is then

$$Z = 1 + s^N \quad (4.123)$$

and hence the average number of helical segments is $\langle i \rangle = Ns^N / (1 + s^N)$. The fraction of helical segments is

$$f = \frac{s^N}{1 + s^N} \quad (4.124)$$

For large N , the transition becomes very sharp.

4.19.3 Nearest neighbour cooperative Zimm-Bragg model

An intermediate scenario is between the two cases studied above is one which contains nearest neighbour interactions. In such a scenario there are four statistical weights to consider: C with C neighbour, C with H neighbour, H with C neighbour and H with H neighbour. We take the relative statistical weight of C to be one, and that of H to be s except if a H follows a C or if the H is the first unit of the chain, in which case the statistical weight is σs . The latter condition introduces nearest

neighbour cooperativity, as we are more likely to find a H following another H (propagating the helix) than a H following a C (nucleating a helix).

The weights for one single segment can be written as the vector

$$\vec{q}_1 = \begin{pmatrix} 1 \\ \sigma s \end{pmatrix} \quad (4.125)$$

and the partition function is just $Z_1 = 1 + \sigma s$ which can be written as the product between the vectors

$$Z_1 = (1 \ 1) \begin{pmatrix} 1 \\ \sigma s \end{pmatrix} \quad (4.126)$$

For two segments, the weights of the second segment depend on those of the first:

$$\vec{q}_2 = \begin{pmatrix} \text{C after C} & \text{C after H} \\ \text{H after C} & \text{H after H} \end{pmatrix} \vec{q}_1 = \underbrace{\begin{pmatrix} 1 & 1 \\ \sigma s & s \end{pmatrix}}_{=:G} \vec{q}_1 \quad (4.127)$$

where G is known as the transfer matrix. The partition function can then be computed by adding together both elements in \vec{q}_2

$$Z_2 = (1 \ 1) \begin{pmatrix} 1 & 1 \\ \sigma s & s \end{pmatrix} \begin{pmatrix} 1 \\ \sigma s \end{pmatrix} \quad (4.128)$$

Applying this relationship iteratively, we get the partition function for the chain of N segments as

$$Z_N = (1 \ 1) \left(\begin{pmatrix} 1 & 1 \\ \sigma s & s \end{pmatrix}^{N-1} \begin{pmatrix} 1 \\ \sigma s \end{pmatrix} \right) \quad (4.129)$$

The partition function Q_N will thus be a linear combinations of the two eigenvalues $\lambda_{1,2}$ of G raised to the power of $N - 1$: $Q_N = a_1 \lambda_1^{N-1} + a_2 \lambda_2^{N-1}$ where

$$\lambda_{1,2} = \frac{1+s}{2} \pm \sqrt{\frac{(1-s)^2 + 4\sigma s}{4}} = \frac{1+s \pm \alpha}{2} \quad (4.130)$$

with $\alpha := \sqrt{(1-s)^2 + 4\sigma s}$. For large $N \gg 1$, the partition function will be dominated by the larger eigenvalue

$$Z_N \approx \alpha_1 \lambda_+^{N-1} \quad (4.131)$$

The fraction of helical segments can be found as before through

$$f = -\frac{1}{N} \frac{\partial \ln Z_N}{\partial \ln s} = \frac{1}{N} \frac{\partial \ln \lambda_+^{N-1}}{\partial \ln s} = \underbrace{\frac{N-1}{N}}_{\approx 1} \frac{s}{\lambda_+} \frac{\partial \lambda_+}{\partial s} = \frac{2s}{s+1+\alpha} \frac{\partial \lambda_+}{\partial s} = \frac{\alpha+s-1}{\alpha} \quad (4.132)$$

Substituting back the expression for α we therefore have

$$f = \frac{1}{2} \left(1 + \frac{s - 1}{\sqrt{(1-s)^2 + 4\sigma s}} \right) \quad (4.133)$$

For $\sigma = 1$ we recover the result $f = s/(1+s)$ from the non-cooperative model.

Chapter 5

Self-assembly: Part I molecular self-assembly

5.1 Self-assembly

Self-assembly is the generation of a functional material from its constituent parts in a spontaneous process, guided by the interactions between the components or by a specific rearrangement of them, that proceeds without any special external impetus. Self-organisation and supra-molecular assembly are key characteristics of biological systems. Although individual proteins stochastically move within a cell (Brownian motion), they eventually stick to a specific place as a properly positioned part of an ordered structure. The machinery which provides biological functionality to organisms is largely generated through self-assembly from protein molecules and results in structures as diverse as rotary motors, enzymes or structural filaments. The natural propensity of biomolecules towards self-assembly also leads increasingly to the exploitation of such species to synthesize artificial supra-molecular assemblies.

5.2 Driving forces for molecular self-assembly

5.2.1 Hydrogen bonding

In addition to the electrostatic contribution $A-H\cdots B$ from the attraction between the partial positive charge of a hydrogen bound to an electronegative atom A and another electronegative atom B with a partial negative charge, the delocalisation of the wave functions of A , B and H is an important factor in defining hydrogen bonds. Indeed, we can construct a molecular orbital $\psi_{HB} = c_1\psi_A + c_2\psi_H + c_3\psi_B$ from the atomic orbitals of A , B , and H where each supply one atomic orbital

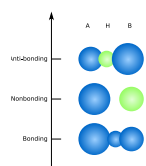


Figure 5.1: Molecular orbitals involved in hydrogen bonding $A-H\cdots B$ obtained as a linear superposition of the atomic orbitals of A , B and H .

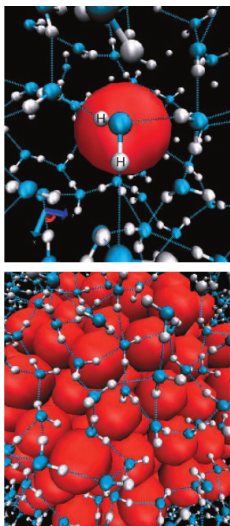


Figure 5.2: The solvation of a small hydrophobe (top) occurs without loss of hydrogen bonding but with a loss of microstates that allow the network to be maintained intact, leading to an entropic cost. By contrast, for large solutes, hydrogen bonds are broken close to the solute, and the cost of solvation is enthalpic (figure from Nature, 437, 29, 2005).

ψ_i . Three molecular orbitals can be formed, a bonding one where $\text{sign}(c_1) = \text{sign}(c_2) = \text{sign}(c_3)$, a non-bonding one with $\text{sign}(c_1) = -\text{sign}(c_3)$ and $c_2 = 0$ and an anti-bonding orbital with two nodes: $\text{sign}(c_1) = -\text{sign}(c_2) = \text{sign}(c_3)$. We consider the A–H bond to consist of a molecular orbital resulting from the overlap of an orbital on A, ψ_A , with the 1s orbital on H; the atom B possesses a lone pair which resides in the atomic orbital ψ_B . Four electrons need therefore to be accommodated into the MOs ψ_{HB} , two from the lone pair of B and two from the A–H bond. Hence the anti-bonding orbital remains empty and stabilisation results. Typically in biological systems A,B can be either O or N, and the observed bond strengths are of the order of 20 kJ/mol. Because the interaction depends on orbital overlap, a close contact and a specific orientation are required for the bond to form. Hence hydrogen bonds are important in defining structures and folds of protein and nucleic acid molecules.

5.2.2 Hydrophobic effect

Oil and water do not mix; contrary to many simple immiscible substances, however, the de-mixing is primarily driven by entropy for small solutes (see table Table 5.1). This finding might seem paradoxical since de-mixing is an order generating process and should in principle be entropically unfavourable.

Table 5.1: Gibbs free energy, enthalpy and entropy of transfer of hydrophobic substances into water at 25°.

Substance	ΔG (kJ/mol)	ΔH (kJ/mol)	$-T\Delta S$ (kJ/mol)
Benzene	19.4	2.08	17.3
Pentane	28.7	-2.0	30.7
Hexane	32.5	0.0	32.5

Indeed, although it might appear that water repels oil, in fact the de-mixing of oil and water under ambient conditions is not due to repulsion between water and oil molecules, but to strong favourable hydrogen bonding between water molecules; each water can participate in 4 hydrogen bonds, two as a donor and two as an acceptor. Due to this strong water-water interaction, the hydrogen bonds persist even in the presence of a small (less than 10 Å) hydrophobic entity and simply reorganises around the hydrophobe. The hydrogen bonding remains highly dynamic, but a reduction in the entropy of the water results from the smaller number of microstates available to the surrounding water molecules that preserve the hydrogen bonding network while avoiding the solute. Therefore, the cost of hydrating a small hydrophobic solute is largely entropic. For a large solute, however, the hydrogen bonding network is unable to reorganise to avoid the solute, and some hydrogen bonds are lost; therefore the cost of solvating large

hydrophobes is mainly enthalpic. The nature of hydrophobicity therefore changes as the size of the solute increases.

In this sense the term hydrophobicity (“water fearing”) is somewhat of a misnomer since it is more the water that “fears” the presence of the solutes rather than the solutes that fear the water.

Hydrophobicity is a major driving force in biological self-assembly in situations such as protein-folding and the formation of lipid bilayers.

5.2.3 Electrostatics

In the gas phase and non-conducting media, electrostatics is a long range interaction. In a solution with a high ionic strength, however, electrostatic interactions decay over nm length scales, and this behaviour is important for the assembly of molecular systems. We discuss below briefly where this difference in behaviour originates from.

In non-conducting media, two oppositely charged ions, q and q' , interact with each other with the Coulomb potential

$$U(r) = \frac{qq'}{4\pi\epsilon_0\epsilon_r r} \quad (5.1)$$

However, this simple behaviour changes dramatically when there are small mobile charges in solution, as is the case for most environments in which soft materials are found, and the decrease in the field strength deviates from the simple r^{-1} form. Let us compute the distribution of charges in the solvent around a central charge q . The potential $\psi(r)$ is given as the potential energy divided by the magnitude of q' :

$$\psi(r) = \frac{q}{4\pi\epsilon_0\epsilon_r r} \quad (5.2)$$

and since as usual $\vec{E} = -\vec{\nabla}\psi$ and $\vec{\nabla} \cdot \vec{E} = \rho/\epsilon$, $\psi(r)$ satisfies the Poisson equation

$$\vec{\nabla}^2\psi(r) = -\frac{\rho}{\epsilon} \quad (5.3)$$

which in spherical coordinates reads

$$\frac{1}{r^2} \frac{d}{dr} \left(r^2 \frac{d\psi}{dr} \right) = \frac{\rho}{\epsilon} \quad (5.4)$$

where $\rho(r)$ is the density of charges. Let $c(r)$ be the concentration of a type of ion in solution. We also know that the charge density around the central charge q is distributed according to the Boltzmann distribution: the probability to observe a charge in a given position is proportional to the exponential of the resulting

energy $\sim e^{-\beta U}$ where $\beta = 1/(k_B T)$ is the inverse temperature and $U = q'\psi(r)$ is the energy of a charge $q' = ze$ in the potential $\psi(r)$. Therefore we obtain the charge density of ions around the central ion as:

$$q'c(r) = q'c_0e^{-\beta q'\psi(r)} \approx q'c_0(1 - \beta q'\psi(r)) \quad (5.5)$$

if the energy $U = q'\psi(r)$ is small.

Up to this point we have considered only one species of ion with charge q' but there will be other species, minimally including a counter-ion with charge $-q'$ for monovalent ions. In general charge neutrality requires $\sum_i q'_i c_{0,i} = 0$ and therefore under summation the right hand side of Eq. (5.5) reduces to $\sum_i -q'^2_i c_0 \beta \psi(r)$. Finally by combining the equations (5.4) and (5.5) we obtain the Poisson-Boltzmann equation:

$$\frac{1}{r^2} \frac{d}{dr} \left(r^2 \frac{d\psi}{dr} \right) = \frac{1}{\epsilon} \sum_i c_{0,i} \beta q'^2_i \psi(r) = \frac{e^2 \beta \psi(r)}{\epsilon} \sum_i c_{0,i} z_i^2 \quad (5.6)$$

which has as a solution

$$\psi(r) = \frac{q}{4\pi\epsilon r} e^{-r/r_D} \quad (5.7)$$

where

$$r_D = \sqrt{\frac{\epsilon k_B T}{2000 N_A I e^2}} \quad (5.8)$$

where N_A is the Avogadro number, e the elementary charge and $I = 1/2 \sum_i c_i z_i^2$ is the ionic strength (note: c_i and therefore also I has units of $\frac{mol}{l}$ in this expression for r_D !).

Thus the radius of action of electrostatic potentials is dramatically reduced in solution due to the exponential screening over the Debye length r_D .

5.3 Free energy of monomers and clusters

Self-assembly can lead monomeric molecules to come together to form multimers or clusters. We consider here a solution of N_T molecules and assume that they can form clusters composed each of a number α of monomers. We denote with N_α the number of molecules belonging to clusters of size α and the number of clusters of size α is then

$$n_\alpha = \frac{N_\alpha}{\alpha} \quad (5.9)$$

with

$$\sum_{\alpha=1}^N N_\alpha = N_T \quad (5.10)$$

If the aggregates don't interact as is the case at low cluster concentration, the partition function of the system is

$$Z_{\text{id}} = \prod_{\alpha=1}^N \frac{1}{n_\alpha!} \left(\frac{V z_\alpha}{\Lambda_\alpha^3} \right)^{n_\alpha} \quad (5.11)$$

where V is the overall system volume, Λ_α^3 is the volume of an α cluster and z_α is the partition function of the internal degrees of freedom. The resulting free energy is

$$F = -k_B T \ln Z_{\text{id}} = \sum_{\alpha=1}^N \left[n_\alpha k_B T \left(\ln \left(\frac{n_\alpha \Lambda_\alpha^3}{V} \right) - 1 \right) + n_\alpha f_\alpha \right] \quad (5.12)$$

where $f_\alpha = -k_B T \ln z_\alpha$ is the internal free energy of each α cluster. The chemical potential of a surfactant molecule belonging to an α cluster is

$$\mu_\alpha = \left(\frac{\partial F}{\partial N_\alpha} \right)_{T,V} = \frac{1}{\alpha} \left(\frac{\partial F}{\partial n_\alpha} \right)_{T,V} = \frac{k_B T}{\alpha} \ln \left(\frac{n_\alpha \Lambda_\alpha^3}{V} \right) + \frac{f_\alpha}{\alpha} \quad (5.13)$$

where f_α/α is the internal free energy per monomer belonging to an aggregate with aggregation number α . We can write these results as a function of the (mass) concentration of clusters.

$$c_\alpha = \frac{N_\alpha}{V} = \frac{n_\alpha \alpha}{V} \quad (5.14)$$

Therefore the chemical potential becomes

$$\mu_\alpha = \frac{k_B T}{\alpha} \ln \left(\frac{c_\alpha}{\alpha} \right) + \epsilon_\alpha \quad (5.15)$$

where $\epsilon_\alpha = \frac{f_\alpha}{\alpha} + \frac{k_B T}{\alpha} \ln(\Lambda_\alpha^3)$. The first term in the chemical potential is the ideal chemical potential which originates from the translational entropy, and the second part is the excess chemical potential which takes into account the internal degrees of freedom.

5.4 Self-assembly of amphiphiles into micelles

A simple form of self-assembly is the organisation of surfactant molecules into micelles. Surfactants are asymmetric molecules composed of a hydrophobic (literally “water-fearing”) part connected to hydrophilic (literally “water-loving”) part. The combination of hydrophobic and hydrophilic parts within the same molecule is referred to as amphiphilic (i.e. both-loving) character. The hydrophobic parts of the amphiphilic molecules have a tendency to phase separate, but since the

hydrophilic parts have a strong driving force to remain in solution, microscopic rather than macroscopic phase separation occurs resulting in the formation of nano to micro scale structures such as micelles, bilayers and vesicles.

Through variations of the chemical nature of the head and tail groups, surfactants with a wide variety of characteristics can be synthesised for a diversity of applications in areas ranging from cosmetics to detergent products. Commonly, the hydrophilic head of a surfactant consists of a charged group; such surfactants are ionic surfactants. The charged head group can have either cationic or anionic character. Cationic surfactants are found in many disinfectant products whereas anionic surfactants are found in soaps and detergent products. Alternatively, the surfactant head can be an uncharged chemical group with an affinity for water, such as a polyether or a sugar. Such surfactants are called non-ionic surfactants are used as detergents or emulsifiers. In certain cases, known as zwitterionic surfactants, the hydrophilic head contains both positive and negative charges such as carboxylates (-), phosphates (-) or quaternary ammonium (+). Many natural products such as protein, lecithin, gelatin, and phosphatidylcholine are examples of zwitterionic surfactants.

Table 5.2: Examples of common surfactant head groups.

Category	Head group	Use
Anionic	$-\text{CO}_2^-\text{Na}^+$	Soaps
	$-\text{SO}_3^-\text{Na}^+$	Synthetic detergents
	$-\text{OSO}_3^-\text{Na}^+$	Detergents, toiletries
	$-\text{OPO}_3^-\text{Na}^+$	Emulsifiers, corrosion inhibitors
	$-(\text{OCH}_2\text{CH}_2)_n\text{OSO}_3^-\text{Na}^+$	Detergents, toiletries, emulsifiers
Cationic	$-\text{NMe}_3^-\text{Cl}^-$	Disinfectants
	$>\text{NMe}_3^-\text{Cl}^-$	Fabrics, hair conditioners
Non-ionic	$-(\text{OCH}_2\text{CH}_2)_n\text{OH}$	Detergents, emulsifiers
Zwitterionic	$-\text{NMe}_2^+\text{CH}_2\text{SO}_3^-$	Shampoos, cosmetics

The non-polar, hydrophobic tail is commonly composed of hydrocarbon chains. Most surfactants found in detergents and soaps have one hydrophobic chain attached to the polar head, but some can have two hydrophobic tails. Perhaps the best known example of such surfactant are phospholipids, which have fundamental functional roles in living systems as the major component of biological membranes.

We focus in more detail on micelle formation. At equilibrium the chemical potential of monomers either in solution or in a micelle of size α has to be equal

$$\mu_\alpha = \frac{k_B T}{\alpha} \ln \left(\frac{c_\alpha}{\alpha} \right) + \epsilon_\alpha = \mu_1 = k_B T \ln c_1 + \epsilon_1 \quad (5.16)$$

and hence we can solve for c_α

$$\ln\left(\frac{c_\alpha}{\alpha}\right) = \alpha \left(\ln(c_1) + \frac{\epsilon_1 - \epsilon_\alpha}{k_B T} \right) \quad (5.17)$$

and

$$c_\alpha = \alpha \left[c_1 e^{\frac{\epsilon_1 - \epsilon_\alpha}{k_B T}} \right]^\alpha \quad (5.18)$$

We see that if $\epsilon_\alpha > \epsilon_1$, the exponential term is negative, and no aggregates will form. By contrast, if $\epsilon_\alpha < \epsilon_1$ then most of the amphiphiles will be present as aggregates at high concentration. In practice, there is an optimum number α^* for the size of a micelle; indeed, micelles containing a smaller number of amphiphiles within them have a too large surface area to be covered by the available head groups, and conversely for micelles larger than the optimal size, there are hydrophilic head groups that are forced to reside within the hydrophobic core of the micelle. If each surfactant molecule has the volume v and head group has the area a_0 then within a micelle of radius R there are $\alpha^* = 4\pi R^3/(3v)$ surfactant molecules; the surface of the micelle is $S = 4\pi R^2 = \alpha^* a_0$ which has to be covered by α head-groups. Hence the optimal radius is $R = 3v/a_0$. If we call $\Delta\epsilon = \epsilon_\alpha^* - \epsilon_1$ the difference in the mean interaction energies of an amphiphile in solution and as part of a micelle of the optimum size α^* , then the concentration of micelles is given by:

$$c_{\alpha^*} = \alpha^* \left[c_1 e^{-\frac{\Delta\epsilon}{k_B T}} \right]^{\alpha^*} \quad (5.19)$$

This is a mass balance expression which describes the equilibrium between the monomer and the cluster of size α^* . If $c_1 < \exp(\Delta\epsilon/(k_B T))$, then the concentration of micelles is very small. The concentration C_{CMC} represents the critical micelle concentration. Above the critical micelle concentration, most new amphiphiles added to the system are integrated into micelles and below the critical concentration they stay in solution.

5.5 Micellar shape and packing parameter

We finally discuss how the properties of the surfactant monomers determine the shape of the micelle that is formed through surfactant self-assembly. As discussed above, for a spherical micelle composed of α surfactants with chain length l , equilibrium head group area a_0 and volume v , the volume of the micelle is $V = (4\pi/3)R^3 = \alpha v$ and its surface area is $A = 4\pi R^2 = \alpha a_0$. Dividing these two expressions, we find an equation for the radius of the micelle as a function of the parameters v and a_0 as $R = 3v/a_0$. If the core of the spherical micelle is

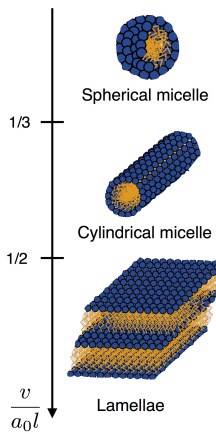


Figure 5.3: Dependence of aggregate shape on the surfactant packing parameter.

packed with no spaces, then the radius R must be smaller than the tail length l . This condition $R < l$, motivates the definition of the packing parameter p

$$p := \frac{v}{a_0 l} < \frac{1}{3} \text{ (spherical micelles).} \quad (5.20)$$

Hence, spherical micelles will be formed only if the packing parameter $p < 1/3$. According to this criterion, if the tails are too long then there will be a rather large micelle which will have a very large surface area, and there will not be enough head group area to cover it. Hence another micelle shapes must be formed.

We can apply very similar arguments to understand the condition for the formation of a cylindrical micelle or radius r and length L . In this case, the micellar volume is $V = \pi r^2 L = \alpha v$ and the surface area is $A = 2\pi r L = \alpha a_0$. Dividing the two expressions, we obtain a formula for the cylinder radius $R = 2v/a_0$. For the same reasons as in the case of spherical micelles, we require $R < l$, leading to the following condition

$$p = \frac{v}{a_0 l} < \frac{1}{2} \text{ (cylindrical micelles).} \quad (5.21)$$

Hence, cylindrical micelles will form if the packing parameter is $1/3 < p < 1/2$. When the value of the packing parameter is larger than $1/2$, bilayers will form. Finally, for $p > 1$, inverted micelles will form.

The table below summarizes the dependency on the surfactant shape apply for the various micelle shapes: spherical, cylindrical, lamella, etc.

Table 5.3: Examples of micellar shape depending upon the relative packing geometry of the surfactant head groups and tail groups.

Micellar shape	Condition
Spherical micelles	$v/(a_0 l) < 1/3$
Non-spherical/cylindrical micelles	$1/3 < v/(a_0 l) < 1/2$
Vesicles of bilayers	$1/2 < v/(a_0 l)$
Inverted micelles	$1 < v/(a_0 l)$

These considerations demonstrate the role of the surfactant molecular architecture in determining micellar shape. According to the criteria above, modulating these parameters offers a way to control and design micellar shape. One possibility is to change tail group size, for example by using di-chains vs monochains. Single chains will have lower values for the volume v than di-chains leading to lower values of the packing parameter; therefore, monochains will tend to aggregate into spherical or cylindrical micelles, whereas dichains will favor the formation of bilayers. This is for example the case with phospholipids. Another way of controlling micellar shape is to change the head group size, a_0 . In particular, bigger

head groups (i.e. large values of a_0) favor the formation of spherical micelles, whereas small a_0 will favor the formation of lamellae.

5.6 Self-assembly of protein filaments

In general, biological self-assembly is heteromolecular and gives rise to complex geometries. A particularly simple form of biological self-assembly is that of the polymerisation of identical protein molecules into linear filaments. Despite its elementary nature, this process is encountered often in biology. Examples are the formation of microtubules, actin fibrils and intermediate filaments that compose the cytoskeleton. Furthermore, aberrant homomolecular polymerisation of normally soluble proteins is involved in the molecular mechanisms underlying many pathologies, including sickle cell anemia which results from the polymerisation of sickle haemoglobin and the amyloid disorders which are characterised by the formation of filamentous aggregates from a variety of different peptides and proteins. For the cytoskeletal filaments, hydrophobicity and electrostatic interactions are driving assembly.

A simple model of linear protein self-assembly is that of linear polymerisation. In this picture, we assume chemical equilibrium for all the polymers with the same equilibrium constant K :



where m is the monomer and X_N is a protein filament composed of N monomers. By analogy to the CMC, a quantity of interest is the free monomer concentration at a given total protein concentration. This can be found as follows. The concentration of the dimer is $c_2 = K[c_1]^2$, the trimer $K^2 c_1^3$ and the i-mer $[c_i = K^{-1}(Kc_1)^i]$. Therefore the total concentration of protein is:

$$c_{\text{tot}} = \sum_{i=1}^{\infty} i c_i = K^{-1} \sum_{i=1}^{\infty} i (Kc_1)^i = \frac{c_1}{(1 - Kc_1)^2} \quad (5.26)$$

and we can solve for c_1 to give

$$c_1 = \frac{1 + 2Kc_{\text{tot}} - \sqrt{4Kc_{\text{tot}} + 1}}{2K^2 c_{\text{tot}}} \quad (5.27)$$

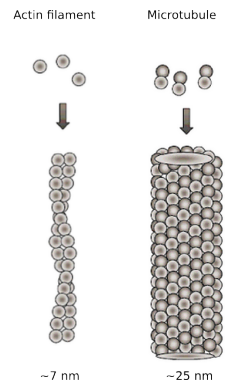


Figure 5.4: Biofilaments formed as the result of homomolecular protein self-assembly (From An introduction to Bionanotechnology, Ehud Gazit, Imperial College Press).

The identity $\sum_{j=0}^{\infty} j x^j = x/(1 - x)^2$ can be seen by noting that $(1 + x + x^2 + x^3 + \dots + x^n)(1 - x) = 1 - x^{n+1}$ and hence $\sum_{j=0}^{\infty} x^j = 1/(1 - x)$ if $x < 1$. Differentiating this expression with respect to x yields the identity.

We see therefore that this system exhibits behaviour which is in many ways similar to that of micelles. When c_{tot} is small $c_1 \approx c_{\text{tot}}$ and most new proteins added to the system remain as monomers. However, above $c_{\text{tot}} = K^{-1}$, the concentration of monomers remains approximately constant at $c_1 \approx c^*$ and most proteins in the system exist as filaments. Therefore the concentration $c^* = K^{-1}$ plays a role analogous to the CMC for micelles. The transition from soluble to aggregates material is, however, less abrupt than for micelles, due to the absence of the exponential in Eq. (5.27).

In addition to the natural role of cytoskeletal filaments in providing rigidity and motility to a cell, the principle of linear assembly has been used in a synthetic context for short peptides as well as non-natural organic molecules. Such nanostructures currently find applications as cell culture scaffolds and in the delivery of long lasting anti-cancer peptide drugs which are administered in the nanostructured form and released slowly through the dissolution of the nanostructures inside the body.

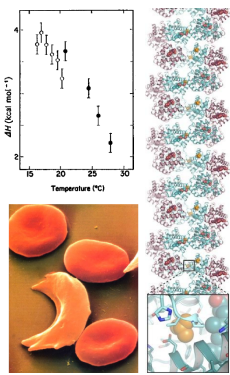


Figure 5.5: Sickle haemoglobin fibril formation is enthalpically unfavorable.

Linear polymerisation of normally soluble proteins is a process connected to nanomedicine through its involvement in a range of diseases. A well-known example is that of the aberrant polymerisation of haemoglobin to yield sickle haemoglobin fibres in sickle cell anemia. These are fibrils of approximately 20 nm in diameter and microns in length and their formation deforms erythrocytes in a manner which impedes their passage in capillaries, leading to blockages and thereby causing pathological effects. Wild-type haemoglobin is not prone to aggregation, but familial mutants in which a hydrophilic amino acid serine is replaced with a more hydrophobic amino acid valine display increased aggregation propensity. The physiological concentration of haemoglobin, up to 300 g/L, is significantly above the critical concentration c^* for the pathological mutant and therefore the pathological mutant haemoglobin is unstable in solution. Sickle haemoglobin fibril formation has been shown to be enthalpically unfavourable and is therefore driven purely by entropy, showing the role of hydrophobic interactions – as expected since the pathological mutation increases the hydrophobicity of the system.

Chapter 6

Problems

Q 1 The equation for the drag force on a sphere can be obtained (within a numerical factor of order of unity) from dimensional analysis, by considering only the parameters that are physically relevant. Discuss the approximations one needs to make to derive the expressions for the viscous drag at low Reynolds numbers, and the inertial drag at high Reynolds numbers. The result at low Reynolds numbers was obtained in the notes.

Q 2 A long flat plate of width b , inclined at an angle α to the horizontal, is covered by a liquid film of uniform thickness a which is flowing steadily downhill. Discuss the boundary conditions at the free surface of the liquid, and show that the volumetric flow rate is $Q = (a^3 b / 3\eta) \rho g \sin \alpha$.

Q 3 In a Couette viscometer the fluid is contained between concentric cylinders, each of length $L=150$ mm. The inner cylinder, with radius $r_1=95$ mm, rotates at an angular velocity of $\omega_1=5$ rad s $^{-1}$, while the outer one, with radius $r_2=100$ mm, is fixed. This is the geometry that is used in experiments. The viscometer is filled with an oil whose viscosity is 1 Pa s. What torque is measured on the outer cylinder?

Q 4 A pipeline transporting crude oil is a straight pipe of circular cross-section, of diameter 2m and length 100km. Estimate the minimal mean velocity of oil flow below which dissipation due to viscous friction will become significant. Take the density of crude oil to be $\rho = 800\text{kg/m}^3$ and the viscosity to be $\eta = 0.005\text{Pa s}$.

Q 5 A major river of the world can be approximated as a semi-circular trough of radius 20 m. Assuming the river uniformly drops 1 km over its 1000 km length, and assuming a laminar flow dominated by viscosity, calculate the terminal velocity of flow at the midpoint of its surface. What would be the river's maximum possible velocity, ignoring friction? Why are both these velocities unphysical?

Q 6 For a rectangular channel ($W \times H$), the dimensionless stokes equation is:

$$[\partial_{y'}^2 + \partial_{z'}^2]V(y', z') = 1 \quad (6.1)$$

with $y' = y/W$, $0 \leq y' \leq 1$, $z' = z/W$, $0 \leq z' \leq \beta$, and $\beta = H/W$. The boundary conditions are:

$$V(0, z') = V(1, z') = V(y', 0) = V(y', \beta) = 0 \quad (6.2)$$

- (a) What is the expression of the Poiseuille flow as a function of $V(y', z')$?
- (b) We can make the ansatz $V(y', z') = V_y(y')V_z(z')$. Show that this ansatz fails to easily separate the variables.
- (c) We can modify the original equation to try to go further. Use this ansatz to solve, with the same boundary conditions,

$$[\partial_{y'}^2 + \partial_{z'}^2]V(y', z') = 0 \quad (6.3)$$

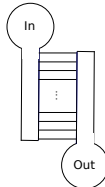
Do you run into any problems?

- (d) From what we learned, we make the following ansatz:

$$V(y', z') = \sum_{nm} A_{nm} \sin(n\pi y') \sin(m\pi z'/\beta) \quad (6.4)$$

What expression for A_{nm} solves the original equation?

Q 7 A microfluidic chip is designed as two parallel channels linked with small grooves.



- (a) If the hydraulic resistance of the channels is negligible and the resistance of the grooves is R_g , What is the resistance of the microfluidic chip between the inlet and the outlet for $N = 100$ grooves?
- (b) What about if there is a resistance R_c in the channels between two grooves? You can consider a recursive argument with increasing number of grooves.

Q 8 A hollow sphere, with inner radius R_1 and outer radius R_2 , is thin when compared to the radius. Knowing that the internal pressure p_1 is larger than the external pressure p_2 , what is the sphere radius variation?

The fact that the sphere is thin means you can take mean values over the thickness.

Q 9 Consider a torsional pendulum consisting of a cylindrical rod (length l , radius R) with an inertial disk (moment of inertia I) attached at the bottom end. The upper end is clamped firmly, whilst the bottom disk can rotate by an angle θ .

- (a) Show that for small angular rotations θ , the restoring torque is given by:

$$\text{torque} = \frac{G\pi R^4}{2l}\theta$$

where G is the shear modulus of the material of the cylinder.

- (b) Now consider experiments in which the rod is set in oscillatory motion at a frequency ω . $G(\omega) = G'(\omega) + iG''(\omega)$ is the complex modulus of the cylinder. Show that the solution to the equation of motion can be written in the form

$$\theta = \theta_0 \exp(-\Lambda t) \exp(i\Omega t).$$

Demonstrate that in the case of light damping Ω is independent of G'' .

Q 10

- (a) Calculate how long it would take a red blood cell to travel from the lungs to the tips of our fingers if it relied on diffusion. [Approximate the RBC as an 8 μm sphere, and take the viscosity of blood to be 0.01 Pa s. Ignore vessel wall effects.]
- (b) Some animals, in particular insects, largely rely on gas diffusion for respiration. During the Carboniferous geologic period, the first trees began to develop and rapidly conquered the entire earth. The oxygen content of the atmosphere thus rose to 35% compared to the current 20%. This enabled insects to grow to sizes which were much larger than today. Assuming the following:
- (a) Insects are cylinders.
 - (b) The wingspan is proportional to the weight.
 - (c) All the cells have the same oxygen need (They are sinks of oxygen).
 - (d) Steady state.

Give an estimate of how much wider the wingspan of a dragonfly was during this period.

- Q 11** For a particle moving in a harmonic potential $U(x) = \frac{1}{2}\kappa x^2$, and whose motion is described by a Langevin equation

$$\frac{dx}{dt} = -\frac{1}{\xi} \frac{\partial U}{\partial x} + g(t)$$

where $g(t)$ is a stochastic term representing thermal fluctuations, evaluate the time autocorrelation function of $x(t)$ and the equilibrium mean square displacement of the particle.

- Q 12** A Gaussian chain with fluorescent tag on one end and its quencher on the other end is dissolved in a non-quenching solvent. If there is no specific interaction between the two ends other than the fluorescence quenching, how does the fluorescence intensity change with the chain length? The fluorescence is quenched when the quencher is in close proximity.

Q 13

- (a) Go through the calculation in the lectures to make sure you can derive the end to end distance of a wormlike chain. Specifically, for a wormlike chain, the magnitude of the orientation function between two segments a distance s apart depends only on this distance. This means that we can write:

$$\langle \cos(\theta(s) - \theta(0)) \rangle = \exp(-s/L_p)$$

where L_p is the persistence length. Show that the mean end-to-end length of the chain is given by

$$\langle R^2 \rangle = 2L_p L \left[1 - \frac{L_p}{L} \left(1 - \exp\left(-\frac{L}{L_p}\right) \right) \right]$$

where L is the total contour length of the chain. Examine and discuss the limits of very stiff and very flexible chains.

- (b) The size of a typical cell is 10 μm . The bending rigidity is $C_B = E\pi r^4/2$. A cytoskeletal filament has to be straight on the lengthscale of the cell. Compute the minimal diameter of a cytoskeletal filament that can achieve this. You can assume a Young's modulus of 10 GPa.

Q 14 In a simple model for the entropic elasticity, the polymer molecule is treated as a one-dimensional freely jointed chain of N segments. Each segment can be described by a two state variable, which has a value of +1 if the segment points forward in the direction of the constant applied force f , and -1 if it points backward to oppose the force. Within this framework the total extension z can be written as: $z = a \sum_{i=1}^N \sigma_i$, where a is the length of a segment. Show that the relationship between $\langle z \rangle$, the total length of the chain L and the applied force f can be expressed by

$$\langle z \rangle = L \tanh\left(\frac{fa}{k_B T}\right).$$

Sketch the force-extension relation and examine the limits of low and high force.

Q 15 Obtain an expression for the stress along the x-direction for a rubber sheet when it is stretched biaxially by an amount $\lambda_x = \alpha_1$ along the x -direction, and $\lambda_y = \alpha_2$ along the y -direction.

Q 16 Compare the end-to-end distances of a single polymer chain with monomer size a and degree of polymerisation N , in the cases that the chain is in bulk solution, or when it is confined to a planar surface. In both cases assume good solvent conditions.

Q 17 Consider a solution of a polymer A, consisting of N monomers, in a mono-molecular solvent B. The effective interaction of A and B is characterised by the Flory interaction parameter χ . The volume fraction of the A component is $\phi = \phi_A = 1 - \phi_B$.

Write down an expression for the free energy of mixing within the Flory-Huggins theory and obtain the condition for stability against phase separation. What is the critical point χ_c and how does it vary with temperature and N ?

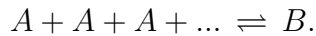
Now write down the free energy in the form of a series expansion for low polymer concentrations ($\phi \ll 1$) and discuss the chain conformation for good and poor solvent conditions. Define the “ θ -point” and describe the conformation of the chains at this point.

Q 18 Sketch the phase diagram for the polymer solution and discuss the different solubility regimes.

Calculate the overlap volume fraction, ϕ^* , for polystyrene with statistical segment length of $a = 6.7 \text{ \AA}$ and a degree of polymerisation of $N = 1000$ in cyclohexane at 34.5°C (a θ -solvent).

Q 19 A non-physical feature of the Gaussian chain is that it has a non-zero probability of having an end-to-end distance which is larger than the chain length. This probability, however, is very small. Evaluate it for $N = 100$ and $b_0 = 1 \text{ nm}$.

Q 20 Solute molecules self-assemble in solution to form clusters of aggregation number N per cluster. The equation between monomers (A) and aggregates (B) in solution can be expressed as



X_A and X_B are concentrations of A and B in mol fraction units. K is the equilibrium constant for the reaction and c is the total concentration of solute molecules. Obtain a relationship between K , N , c and X_A and then show that for $K \gg 1$ and $N \gg 1$ the concentration of monomers X_A can never exceed $(NK)^{-\frac{1}{N}}$.

Q 21 Actin is a cytoskeletal protein that can polymerize in solution to form linear filaments, by the addition of successive monomers. Show that if $\alpha k_B T$ is the free energy gain of binding a monomer to the aggregate, and X_N is the

concentration of molecules in aggregates of number N , then

$$X_N = N \left[X_1 \exp \left(\alpha \left(1 - \frac{1}{N} \right) \right) \right]^N.$$

Hence show that for a total concentration C of molecules, the peak in the distribution of N (for concentrations above the critical micelle concentration) is given by $N \simeq \sqrt{C \exp \alpha}$.